Nederland Maritiem Land

MIIP Project:

DEEP CORR ON SITE

Study of deep sea corrosion near hydrothermal vents.
Deployment of 5 x 37 construction materials for in-situ long-term exposure.

Project team:
Marc Lavaleye, NIOZ
Felipe Leon Morales, Endures
Gerard Duineveld, NIOZ
Stas Verichev, IHC
Arjen de Jong, TNO
Wiebe Boomsma, IHC
Offshore company
Marck Smit, NIOZ

Date: Dec 15, 2014
Project code: IC_B130214/038
NIOZ-report: 2014-5

Nederland Maritiem Land

Format eindrapportage MIIP		
Datum	:	15 Dec 2014
Projectcode	:	IC_B130214/038
Projectnaam	:	Deep Corr On Site
Kenmerk	:	IC_MIIP230913-216

Projectleider	:	Marck Smit
Organisatie	:	NIOZ
Adres	:	Landsdiep 4
Postcode + plaats	:	1797SZ 't Horntje
Telefoonnummer	:	0222369308
Emailadres	:	marck.smit@nioz.nl

Project

Aim of the project [Doelstelling project]:

Current economy dictates technological advances in exploring the ocean depths for the recovery of new types of raw materials necessary for society. For this reason there is an industrial and political interest for deep sea mining (DSM). DSM locations with seafloor massive sulfide (SMS) deposits are known for the presence of highly corrosive components such as sulfide, carbon dioxide and hydrogen. The latter additionally complicates the mining environment, decreases material resistance and fosters the corrosion rates. Active microbial metabolisms in the water column and sediments provoke extra corrosive effects. For adequate corrosion risk assessments at the DSM sites, the characteristics of the environment, corrosion mechanism, and its rates should be established. Processes involving the transformation of iron and sulfur, especially at close proximity to hydrothermal vents will be highly relevant to asses chemical and microbiologically influenced corrosion processes (MIC) affecting industrial materials in the deep sea.

This project is a follow-up of the first DeepCorr project successfully finished in 2012. The aim of the present DeepCorr- On-Site project is to perform actual deep-sea experiments to investigate the effects of especially SMS environment on the corrosion of a set of commercial metals, and furthermore to obtain insight into the microbial community mediating corrosion. The study site of this project is the Rainbow Vent site at the Mid-Atlantic Ridge which is being studied in the NWO-STW project TREASURE. Using the infrastructure of TREASURE (i.e. ship, moorings) as "platform", we propose to deploy various materials used in the construction of deep-sea mining instruments. The role of the industrial project partners (among others IHC) with respect to selection, supply and assessment of materials, safeguards the probability of the correct evaluation of the possible risks for deep-sea industry. Additionally TNO will analyse potential corrosive micro-organisms from the Rainbow site from sediment samples to be collected during the cruise.

The following activities have been carried out within the project [De volgende activiteiten zijn binnen het project uitgevoerd]:

Encounters of difficulties during the project and how these have been solved [Ondervonden knelpunten en daarop ondernomen acties]:

The original plan of installing the material samples for DeepCorr-on-site project in the "Lucky Strike" vent field was abandoned because of logistical reasons. The main reasons was to avoid interference with extensive monitoring equipment of French and Azorean research groups at Lucky Strike. Therefore the cruise efforts were at a late stage diverted to the Rainbow hydrothermal vent field located 100 nm SW of Lucky Strike. Though this site is less intensively monitored as Lucky Strike, there is a considerable amount of literature data available on Rainbow. Further it has a greater water depth (2200m against 1700m), which had an effect on sampling time. The positive site of it is that Rainbow produces the strongest plume of its kind known on the Mid-Atlantic Ridge. Overall the switch from Lucky Strike to Rainbow had no serious consequences for the goals of the project.

[Resultaten (projectinhoudelijk, maar ook m.b.t. rapporten, video's, presentaties, vervolgprojecten e.d.)]:

The Results follow the summary of activities given above.

1. **Define materials** (IHC - Wiebe Boomsma)

Mining the deep sea on an economical feasible requires a large and complex system. There are currently many concept available describing methods and equipment making this possible. For the Deep corrosion on site project, IHC has look at the possible concept and taken the material choices from the design lists and made assumptions for the unknowns. Not only the materials itself are tested but also the combinations of materials. In practice this means, Not only the construction steel is tested but also combined with anode materials, painted and welded. Furthermore possible aluminum alloys are tested ranging from medium strength alloys with good corrosion properties to ultra-high strength alloys which are not developed for use in a marine environment. Besides the metals, also synthetic materials and rubbers are tested. All of the materials tested are relevant for possible use in deep sea mining equipment.

2. Modelling corrosion- a literature study (ENDURES-TNO by C.F. Leon Morales)

INTRODUCTION

Assessing the corrosion risk in relatively deep seawater and seafloor is acquiring every time more relevance, especially with the expanding exploration and industrial activities including deep sea mining. All of these activities imply the use of degradable materials, especially metals and metal alloys. As in any other activity the maintenance cost of these assets is a primary concern. Potential sites with economic interest are located close to hydrothermal systems. Hydrothermal vents are a source of exploitable resources that accumulate on the seafloor. Hydrothermal fluids, however, can be extremely harsh environments for exposed infrastructure with extremes on corrosive chemicals, steep gradients of temperature, pH, etc.

Marine corrosion types and general seawater corrosion is a subject reviewed already abundantly in the literature and it will not be included here. Similarly the influence of high pressure, oxygen and temperature are also available. A review on Marine Corrosion within present project was done already by one of the industrial partners (see appendix A) and includes important information on potential corrosion types in deep sea environments.

This report collects available information on biogeochemistry of the site and puts it in the context of potential corrosion processes that could take place. It is not part of the focus to include general corrosion aspects but to concentrate on microbiological processes that could have an important impact, especially for MIC, which is an acute and unpredictable form of corrosion. Conclusions will be brought on the impact of these activities on corrosion processes at similar sites as the Rainbow vent site. This report also uses information from ENDURES report RPT14069b which deals with sample analyses from the RV PELAGIA cruise (64PE388) to the Rainbow vent site.

SITE DESCRIPTION

The original plan of installing the material samples for DeepCorr-on-site project in the “Lucky Strike” vent field was abandoned because of logistical reasons, explained in NIOZ cruise report (64PE388). The actual site explored was the Rainbow vent field (36 14’N, 33 54’W, 2250 m depth) (Fig. 2.1). The site is situated in the discontinuity between two segments of the mid-Atlantic ridge and it is affected constantly by a hydrothermal plume.

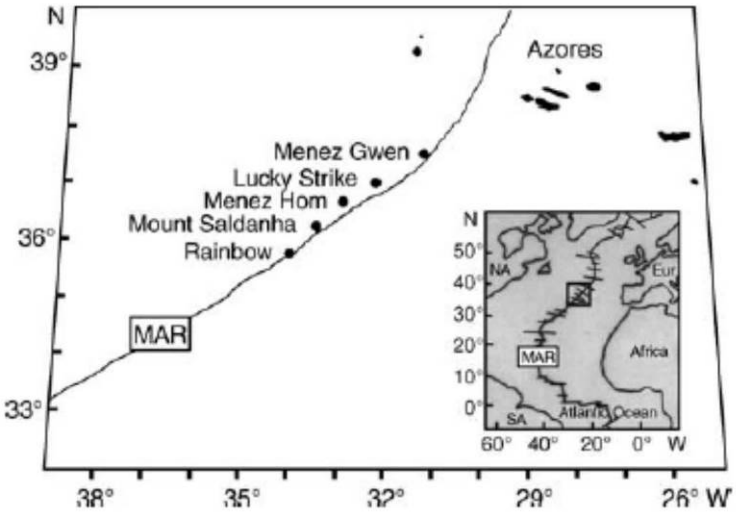

Figure 2.1. Representation of the Mid Atlantic Ridge and the location of common sites, including the Rainbow vent site. Source: (Gadanho and Sampaio 2005).

This vent field consists on more than 30 groups of active, small sulphide chimneys over an area of around 15 km2. It is based on ultramafic rocks (igneous rocks with very low silica content but high content of iron and magnesium). The acid vent fluids common in this site are rich in sulphur, calcium, iron and copper. Especially sulphur at (S> 17%) is dominant in these plumes. The site produces the strongest plume of its kind known on the Mid-Atlantic Ridge (MAR) (Khripounoff et al. 2001). Although macro fauna is reported to be low, some diffusive vents surround the black smokers with small mussel beds and shrimp swarms. Temperatures have been measured to fluctuate between 3.6°C and 10.1°C.

MICROBIOLOGICALLY INFLUENCED CORROSION

The process by which the presence and activities of microorganisms lead to increased and unexpected corrosion is known as Microbiologically Influenced Corrosion (MIC). MIC is therefore not a different corrosion mechanism *per se* but rather a particular set of environmental conditions influencing corrosion rates and types. Microorganisms are ubiquitous in the environment and show an enormous capacity for adaptation. Because the main impact on microbial corrosion is not due to the microbial species but rather their activity, MIC can be a risk in any environment in which human industrial activity is possible. Although traditionally, it has been assumed that the main groups of microorganisms involved in biocorrosion are those belonging to the sulphate-reducing group, it is now evident that SRB influenced corrosion is just one of the possible mechanisms. A short overview of MIC follows which later will be put in the context of the specific environment to which this review refers.

Microorganisms are ubiquitous in nature and in man-made structures provided nutrients, water and biologically useful energy are available. A fundamental characteristic of MIC is the ability of microorganisms to attach to a substratum (e.g., metallic structure) and form biofilms. Biofilms are composed of attached microorganisms and their extracellular polymeric products (slime).

Provided microorganisms are present, biofilm formation starts as soon as the water enters in contact with target surfaces. Most of the times biofilm formation is preceded by the accumulation of organic and inorganic compounds at the interface. It is still controversial if these adsorbed substances are a prerequisite for biofilm formation but indeed they contribute to its development. In this respect and because biofilms continue to be places of accumulation, a vibrant community of microorganisms can thrive even though if nutrients at the water phase are low.

Corrosion can be stimulated by the mere presence of biofilms. Biofilm formation results in the formation of concentration cells. In this direct interaction, the types of microorganisms are irrelevant provided the biofilm is patchy and localized. Consumption of oxygen in these “patchy” biofilms can be so high that oxygen cannot reach the metallic surface under the biofilms. Oxygen exclusion from certain localized areas of the metal structure forms concentration cells which result in pitting corrosion as illustrated in Fig. 2.2.

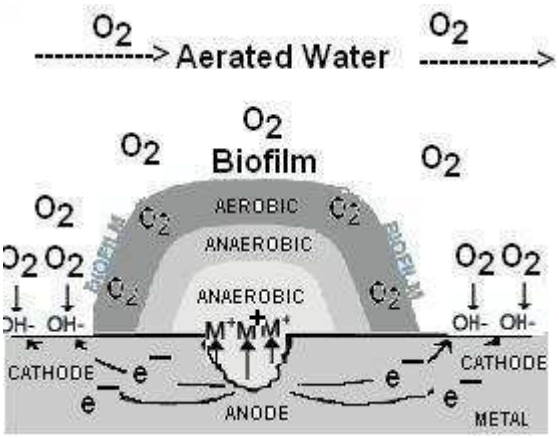

Figure 2.2. Simplified diagram depicting a biofilm-formed oxygen concentration cell. Under the biofilm, low oxygen concentration as compared to its surroundings, results in the formation of an electrochemical cell in which the region under the biofilm acts as the anode (corrodes) and regions with no biofilm act as cathode. Source: (Borenstein 1994).

Certainly MIC is not limited to concentration cell effect due to the bare biomass accumulation. Diverse microbial activities within the biofilm also play a major role on determining MIC. The oxygen concentration gradient created in biofilms will result in diverse communities driven by the available electron donors and acceptors. As oxygen gets consumed in upper parts of the biofilms, anaerobic communities can thrive underneath with processes highly relevant for corrosion (Fig 2.3). One of the most important is the production of hydrogen sulphide (H_2S) which is a highly corrosive acid, catalysing the penetration of hydrogen into steels in a process called H_2S-induced crackingure. Furthermore, the corrosion rate of iron in the presence of H_2S is accelerated by the formation of iron sulphide minerals. With electrical current established, carbon steel behaves as an anode and electron transfer occurs through the iron sulphide. The organisms responsible for this process are known as sulphate-reducing bacteria (SRB).

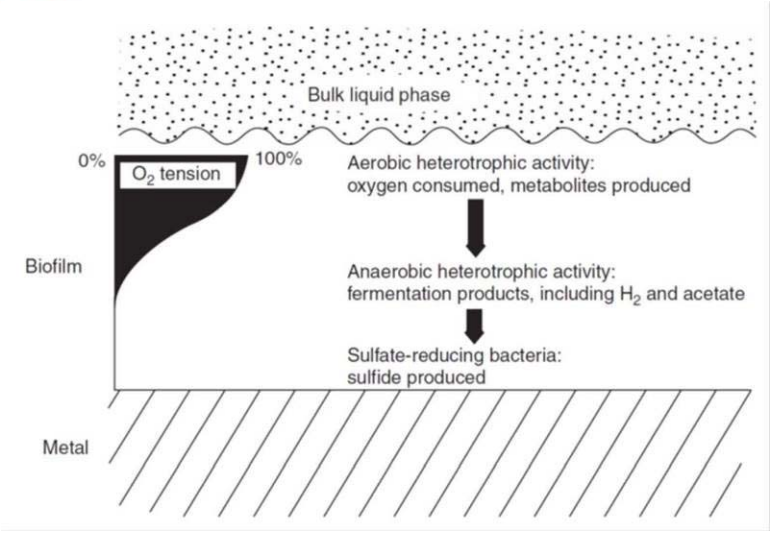

Figure 2.3. Schematic representation of corrosion relevant activities determined by the presence of biofilms and the concentration of oxygen in the system. Source: Little et al. 2007.

Another important process in a MIC attack is the production of acid. Acid can result from the oxidation of sulphur, thiosulphates and H2S among others to sulphuric acid. This process is driven by sulphur-oxidizing bacteria (SOB). Another source of acid is the heterotrophic fermentation of organic substrates which results in the production of organic acids by acid-producing bacteria (APB). The impact of acidic metabolites is intensified when trapped at the biofilm-metal interface. Local acid production by microorganisms can accelerate corrosion of metals. When active, anaerobic acid producing microorganisms can acidify the medium in which they are growing in a matter of 1 or 2 days. The MIC risk posed by acid producing microorganisms is by creating local acid environments within biofilms which might increase corrosion rate of many metals including carbon steel. These localized low pH environments might not be detectable with standard water testing procedures.
The complementary activities of iron oxidizers and iron reducers (IOB, IRB) are determinant on the stability of iron and therefore are key on corrosion processes in which some form of iron is involved. In acidic conditions, acidic iron oxidizers (AIO) can promote the oxidation of ferrous iron to ferric iron which results on the deposition of iron oxides and hydroxides and/or the formation of iron chloride salts which can be highly corrosive. In the other hand iron reducers can reduce ferric iron to ferrous (mobile) iron. By doing this iron reducers can disrupt passivation layers which are known to protect several metals from corrosion. The main difference of these two processes is that microbial induced iron oxidation occurs in aerobic conditions, while iron reduction is an anaerobic respiration process.

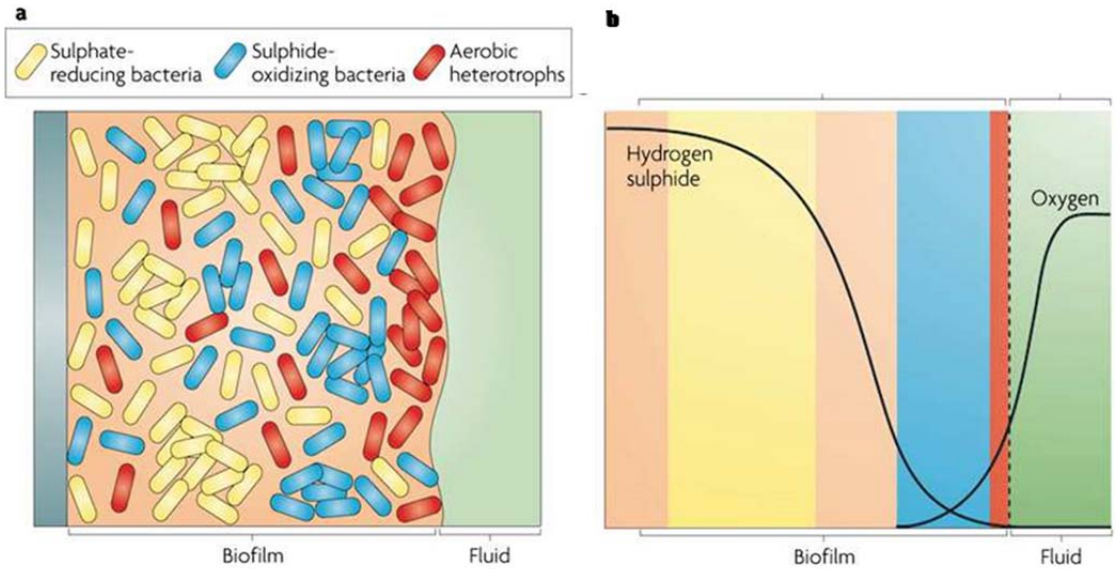

Figure 2.4. Sharp microenvironments created inside biofilms due to microbial action. Source: Stewart and Franklin 2008.

It is important to stress that MIC does not imply a new type of corrosion reaction, corrosion is strongly associated with the biofilm and its extracellular polymeric substances, EPS and that most engineered alloys are susceptible.
Another misconception is that microbial activity is limited to certain pH or temperature ranges. Although many microorganisms have pH optima around neutrality, several MIC relevant microorganisms can be active at pHs ranging from 1 up to 9 and also at temperatures from 4 up to 45°C or even higher. A good example of this versatility in terms of pH is found with the sulphur-oxidizing bacterium *Thiobacillus thiooxidans* which has been found to be able to grow at the mentioned range although with optimum pH at around 3.5.
Traditionally, SRB are believed to be major players in biocorrosion. There have been several theories about the exact mechanisms but basically SRB are believed to accelerate corrosion by: (a) generating H2S; (b) creating oxygen concentration cells; (c) forming insoluble sulphides when metal ions combine with sulphur and (d) by cathodic depolarization. In most environments SRB are participating in the cycling of sulphur in which SOB participate by oxidizing reduced sulphur compounds generated by SRB metabolism (see example for hydrothermal system in Dick et al. 2013).
Microbiologically Influenced Corrosion (MIC) in the deep sea depends exclusively on the viability and activity of microbial species which are known to influence corrosion processes. The activity and structure of these communities will in turn depend on the physicochemical characteristics of the surrounding environment. From a biological perspective, in order to be active, microorganisms need a relatively constant source of energy and nutrients, as well as a way to eliminate waste products excreted during their metabolism. All these conditions are met in most open deep sea environments. Reports on bacterial presence in the deep sea date back to more than 50 years (ZoBell and Morita 1959). There are numerous reviews accounting for the great diversity found in these environments, changing in this way the previous misconception that the deep sea environment was largely unpopulated (Arakawa et al. 2006; Santelli 2007; Mason et al. 2010). In fact deep sea microbiology is already an established field with dozens of papers and books describing common methodologies for dealing with these microorganisms (e.g. Paul 2001; Michiels et al. 2008).
In terms of corrosion relevant microorganisms, and microbial activities linked to corrosion processes in the deep sea, information is scarcer. Reports are, however, constantly emerging on microbial groups known for their role in corrosion processes, able to thrive on high pressure conditions as found in these environments. High pressure is the defining factor when speaking about deep sea microbiology because other physicochemical parameters can change depending on the location. For example there can be extremely hot places poor in oxygen while other relatively cold places with pockets rich in oxygen. Microorganisms able to live under the high pressures found in deep sea are known as piezophilic and comprise a wide variety of microbial groups ranging from fungi to archaea.
MIC-related piezophilic (or moderately piezophilic) organisms have been isolated including acid producing bacteria (Nogi et al. 1998, 2007); iron related bacteria (Liu et al. 1997; Edwards et al. 2004; Edwards et al. 2003; Bailey et al. 2005) and sulphate reducing bacteria (Bale et al. 1997; Barnes et al. 1998). Quite importantly, the ability of microorganisms to form biofilms on native and foreign structures has been also reported (Venkatesan et al. 2003).

OVERVIEW OF MIC-RELATED MICROORGANISMS ABLE TO GROW AT CONDITIONS RESEMBLING TARGET ENVIRONMENT

Slime and biofilm forming bacteria - As mentioned earlier, the formation of biofilms is a pre-requisite for the onset of bio-corrosion. Reports have emerged in which the formation of biofilms is reported at depths and temperatures relevant for the target situation. Groudieva et al. (2003) reported the isolation of a novel psychrotolerant, biofilm-forming bacterium which was named as *Psychromonas arctica* sp. The organism was grown at 4°C using starch as carbon source. Growth at temperatures above 27°C was not observed. pH for optimum growth was found to be between 8.5 and 8.8 and the organism grew in the presence of 1-7% NaCl with an optimum at 2% NaCl (close to seawater concentration). The production of Extracellular Polymeric Substances (EPS) and biofilm formation has been often reported as a microbial strategy to survive adverse environmental conditions. A known example is the production of exopolysaccharide by the deep sea psychrotolerant bacterium *Pseudoalteromonas* sp. SM9913 which increased as the culture temperature decreased in the range 30-10C (Qin et al. 2007). These authors report and hypothesize several ecological advantages for the organism by producing these EPS, including enhancing the stability of cold-adapted enzymes.
Acid producing bacteria - Microorganisms with the capacity to produce acid from a wide variety of organic compounds have been found in similar environments as the one relevant for present problem (Nogi et al.

2007). From these, strains of *Shewanella*, which are facultatively anaerobic bacteria wide distributed in deep sea sediments have been found able to produce acid from some sugars in laboratory incubations (Miyazaki et al. 2006). This means these organisms might produce acid provided the conditions are given (e.g. carbon source available). Also barophilic members of the genus *Photobacterium* which are common bacteria in marine environments have been found able to produce acid from fermentable sugars (Nogi et al. 1998). Some of these organisms are able to grow at depths up to 5000 m and with optimum temperatures of around 10°C.

Iron and manganese related microorganisms - Iron oxidizing and reducing bacteria have been an active subject of research in deep sea environments (Edwards et al. 2003). Interesting about these organisms is that many are autotrophs (able to obtain their carbon directly from CO_2) and do not require organic compounds for growth. On Earth environments many of these organisms are acidophiles (growing at low pH) but there are neutrophilic iron oxidizers (growing at neutral pH) as well. They are believed to have an important role in corrosion, especially in acidic conditions where they can outcompete other species.

Sulphate-reducing bacteria - SRBs are widely reported for their important role in corrosion, especially by the process known as cathodic depolarization which can be induced by their hydrogenase system or by iron sulphide precipitation after production of hydrogen sulphide (Coetser and Cloete 2005). Sulphate reduction has been studied quite extensively in seabed sediments at depths and temperatures relevant for the present problem. It is important to notice that normally sulphate reduction will occur inside the sediment where oxygen is depleted. Obviously in the presence of a metallic surface biofilms can develop and anaerobic microenvironments in which SRB are active can exist. If SRBs are in direct contact with the metal, and if there is metal dissolution, either caused by the bacteria or by a galvanic process, SRBs are also able to use electrons directly from metal oxidation (Venzlaff et al. 2013).

In terms of the specific environment, it has been shown that SRBs can be well adapted to relatively cold conditions and depths but sulphate reduction maxima is rarely found at in-situ growth conditions (Isaksen and Jorgensen 1996, Elsgaard et al. 1994) but instead at temperatures well above 15°C. This of course does not mean sulphate reduction will not occur but that the rate at which occurs will be significantly lower in colder environments (such as the problem environment).

KEY BIOGEOCHEMICAL FEATURES INFLUENCING CORROSION IN DEEP SEA ENVIRONMENTS

The deep ocean can be generally divided in zones with hydrothermal influence and zones without hydrothermal influence. Although deep open ocean without or with little hydrothermal influence has been considered as life deserts, in reality there is enough microbial activity to consider. Even in nutrient limited environments such as these, Most microorganisms are in a so-called “starved” condition, with very slow metabolic rates and relatively inactive. However, if organic carbon is suddenly available, these “fasting” organisms will become more active and quickly bring organic carbon levels to oligotrophic conditions. This might also be the case in a completely closed system which is re-opened and fresh nutrients are available. Microorganisms can remain viable (but not active) even for years, until the conditions are good for growth. It is important then to remember that even in very limited conditions, microorganisms do not die off completely but remain inactive in a dormant state until conditions “improve”. This is especially true at surfaces. An example of this is the microbial alteration of basaltic glass.

The biologically induced alteration of basaltic glass is characterized by cavities that could display a granular structure (Fig. 2.5B) or a tunnel-like structure (Fig. 2.5C) (Staudigel et al. 2006).

Microorganisms are living in close association with the basalt rock structure, either forming biofilms on top of it or as crypto-or eu-endoliths (actively boring into the rock structure). Basalts (especially the first 200-500 m) can be highly porous with hydraulic conductivities of 10^{-12} to 10^{-15} m^2 (Fisher 1998). From the point of view of potential corrosive processes eu-endoliths have a big relevance since probably similar processes could take place with foreign surfaces being introduced into these environments. Even though the active involvement of endoliths on the degradation of basalts is highly likely, until fairly recently, not many studies were available about the mechanisms involved or the physiology and identity of these microorganisms. The reason for this was technical limitations especially for sampling and microbial diversity analysis. This has been changing over the last decade due to important advances in both molecular biology and sampling technologies.

Finally, physiological characteristics as well as identities of basalt euendoliths are starting to emerge. Edwards et al. 2003, for example, found an unexpected high diversity of organisms directly involved in rock weathering at the ocean-floor. These organisms were mainly involved with the dissolution of sulfide minerals also an important constituent of the ocean crust. This was confirmed by the abundant presence of cells and various Fe-oxides in weathering and colonization experiments done in situ. These results suggest the activity of

lithotrophic, possibly autotrophic iron oxidizers. Mineralogical data and Fluorescence In-Situ Hybridization (FISH) suggest the presence and activity of neutrophilic iron oxidizers.

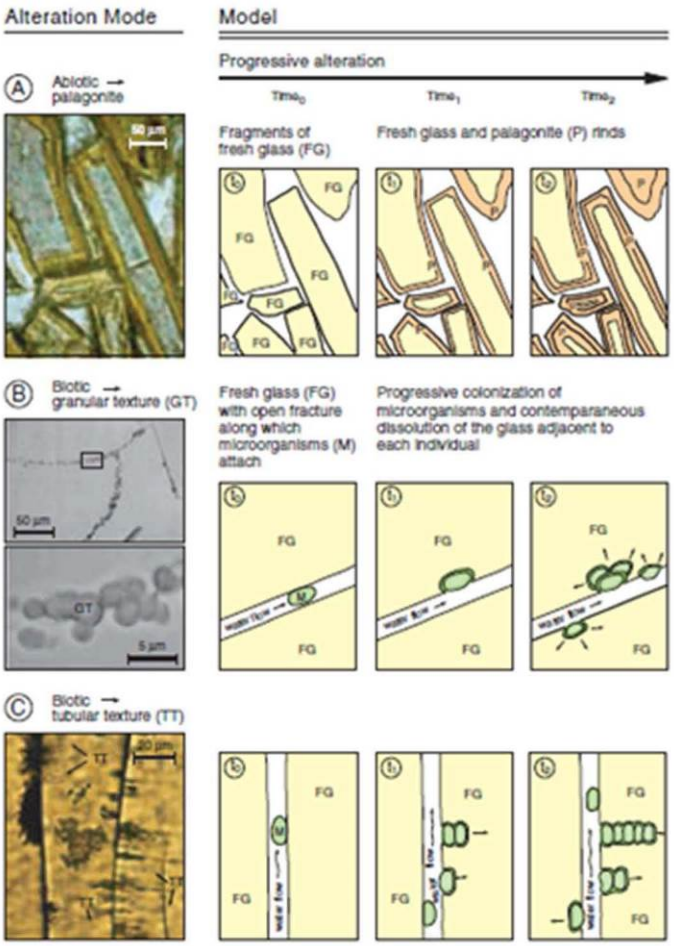

Figure 2.5. Abiotic (A) and biotic (B and C) alteration of the ocean crust surface (basaltic glass). Images in the first left column are actual micrographs while the other three columns are a model of the different processes in time (Staudigel et al. 2006)

The biological and chemical activity of seafloor hydrothermal systems has been widely investigated since their discovery in the 70s. Vents offer a steep physicochemical gradient which stimulates many biological processes. Also it is important to mention that in many locations energy fuelling microbial processes is totally independent from photosynthesis. Also, H2S is considered one of the most important electron donors. The area and type of influence of hydrothermal venting will depend on the depth, the number of vents present, and the age of the system among others. (Mironov et al. 2002) have suggested 5 hierarchies of scale when speaking about the area of venting:
Vent – single, active structure or opening with area of influence of a couple of meters.
Site – comprising a cluster of single vents with area of influence of up to around 10 m.
Field – A cluster of sites with area of influence of up to several hundred meters.
Group of fields – with area of influence of around 1 km.
Ridge segment (sector) with tens of km of influence area.

In zones of hydrothermal convection, close to spreading centers (where new crust is being formed), seawater penetrates deeply into the crust (up to 1 km) (see ISA 2002 and Orcutt et al. (2011). This gives rise to important reactions that determine a great deal of the oceans chemistry in these zones. The radius of a typical convection cell normally goes from 3-5 km (ISA 2002).
The influence of vent fluids on adjacent areas to convection cells, close to or at sea-floor will depend on the amount of reduced compounds being expelled, the rate at which these are mixing with the sea water, the rate at which precipitation reactions are taking place, the fluid velocity regime and the porosity of adjacent

sediments. An idea of the components of a hydrothermal system which determine their area of influence is depicted in Figure 2.6.

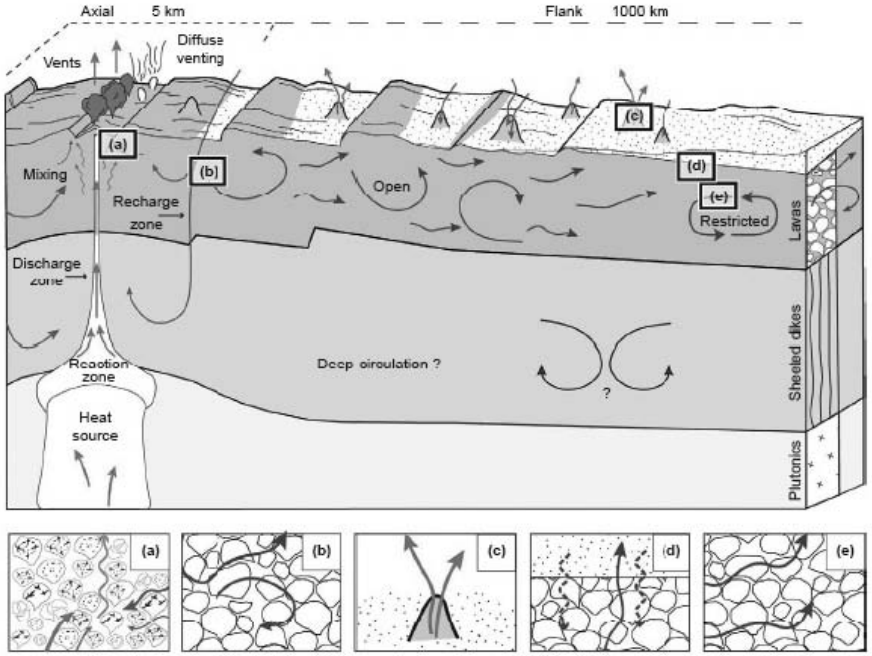

Figure 2.6. Cross-section showing the spatial distribution of fluid flow hydrothermal activity. Even though it has been suggested that the reach of hydrothermal plumes is limited at deep locations, the porosity and hydraulic conductivity of marine sediments can increase several orders of magnitude the reach of venting.

Actual studies have demonstrated that although many chemical compounds precipitate from the vents early on, a significant “plume” of hydrothermal fluids persist over large spatial areas which can be several kilometres away from the source (German and Von Damm 2003). An example of the influence of hydrothermal activity on the surroundings is the fact that concentrations of dissolved metals are higher in water masses above hydrothermal vents. The high concentrations of these metals can persist for several tens of kilometres away from the vent source (Cowen et al. 1986). Another factor to take into account is the permeability of sediments and/or faults and cracks found in the adjacent sub-sea floor. As depicted in Fig. 2.6, advection and massive fluid transport in these saturated porous environments can create authentic “oceans” under the ocean water column. This will have obvious consequences on the reach of venting and all the biogeochemical processes close to and at the sea floor. Sampling and survey campaigns have been already performed in certain regions in order to assess the reach of hydrothermal activity and its influence. One example is the study done on the north-eastern Lau Basin (southwest pacific) which had as a goal identifying the source of previously measured hydrothermal activity in the region (Kim et al. 2009). Signs of hydrothermal vent plume presence include anomalous light transmission, increased methane and dissolved trace metals concentrations, as well as, increased microbial biomass.

In oxygenated marine waters corrosion depends directly on oxygen concentration. The presence of oxygen minimum zones (OMZ) located a few hundreds of meter below the surface, are well documented globally (Ulloa et al. 2012). These zones have important effects on both corrosion and microbial processes (Dick et al. 2013).

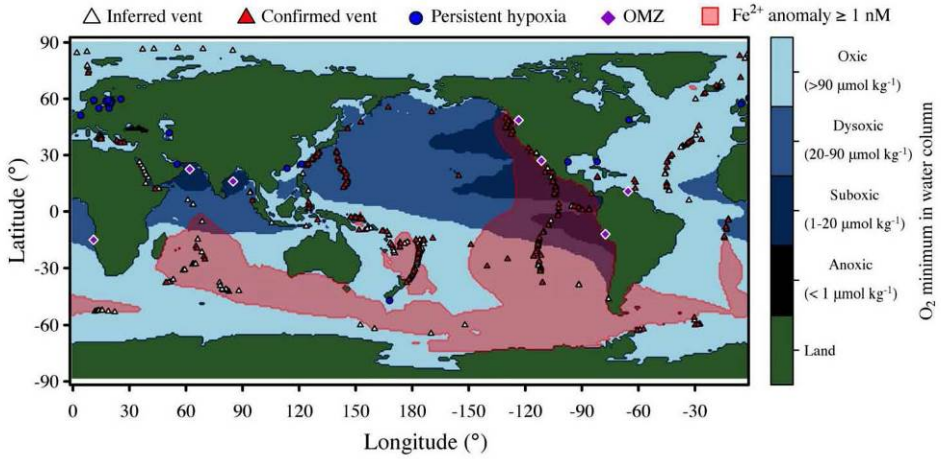

Figure 2.7. Global distribution of deep sea hydrothermal systems and low oxygen environments. Yellow circle represents target location. Modified from Dick et al. (2013).

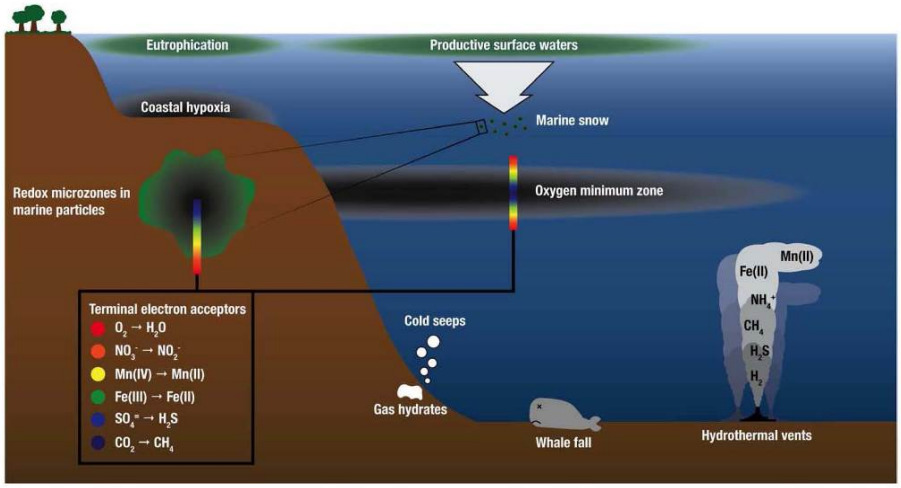

Figure 2.8. Water column profile with different marine habitats which are source of electron donors for microbiological activity. Note the alternative electron acceptors for microbial respiration in the OMZ. Source Dick et al. (2013).

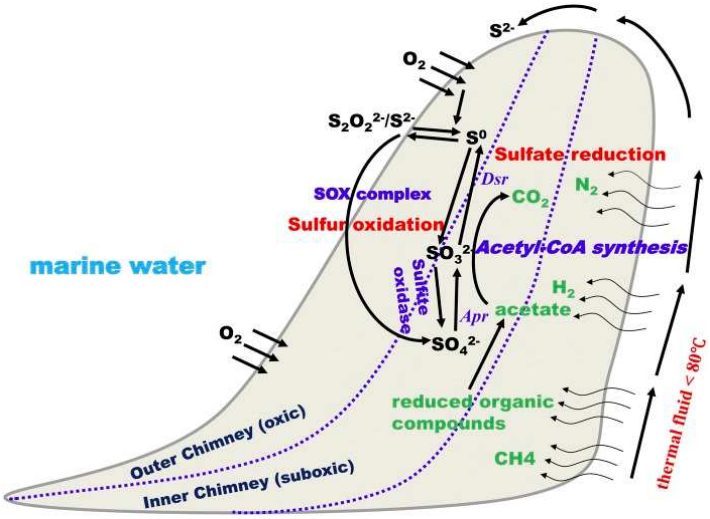

Figure 2.9. Schematic diagram showing sulphur transformations in a hydrothermal chimney.

The Rainbow site, which is located in the aphotic zone is not influenced by any known OMZ. Under these conditions potential transformations of sulphur close to vent chimneys could be occurring as depicted in Fig. 2.9. Dissolved O2 concentrations in deep Atlantic waters could be at least as high as surface concentrations. A comparative plot of Pacific and Atlantic waters can be seen in Fig. 2.10.

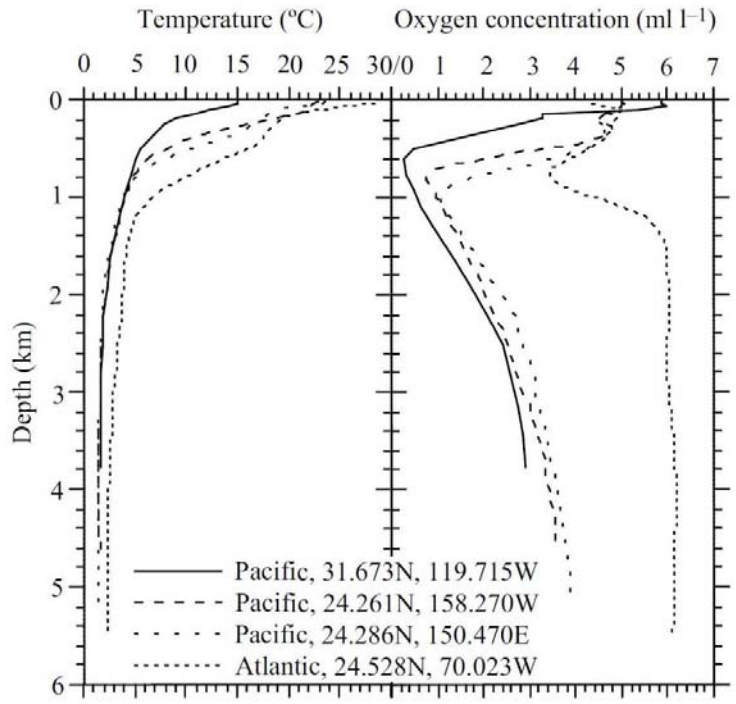

Figure 2.10. Temperature and dissolved oxygen conditions with depth at oceanic stations in the Pacific and Atlantic Oceans. Source: (Childress and Seibel 1998).

CORROSION RISK AT RAINBOW VENT SITE WITH FOCUS ON MIC

Not all vent sites are the same and with respect to the ones studied along the MAR it is possible to say that sites show characteristics that make them unique. In a study along the MAR including several vent sites, important differences in fluid composition are evident. Especially interesting for the Rainbow vent site is the high concentrations of Fe(II) and H2 (Figs 2.11, 2.12).

Site[b]	Year	Depth (m)	*T*, °C	pH	S^{-II}	CH_4	Fe^{II}	H_2
Menez Gwen (1)	1994–1997	840–850	265–284	4.2–4.8	<1.5	1.35–2.63	<0.02	0.02–0.05
Lucky Strike (1, 2)	1993–1994–1997	1560–1730	170–324	3.4–5	0.6–3.3	0.5–1	0.03–0.92	0.02–0.73
Rainbow (3)	1997–1998–1999–2001	2280	342–362	2.5–3.1	1–2.5	1.7–2.5	24	10–16
Broken Spur (4–7)	1993	3100–3300	356–364	–	8.5–11	0.06–0.13	1.68–2.16	0.43–1.03
TAG (4, 7–9)	1986–1993–1994–1995	3670–3700	270–366	2.5–3.8	2.5–6.7	0.05–0.62	1.6–5.2	0.15–0.37
Snake Pit (10–11)	1986–1988–1990–1996	3460	313–356	3.4–3.9	2.7–6.1	0.02–0.06	1.83–2.56	0.19–0.48
Logatchev (1, 4, 12)	1996–2005	3000	347–352	3.3–3.9	0.5–3.6	2.1–3.5	2.4–2.5	12–19
Lost City (13)	2000	700	40–76	9–9.9	0.06	0.13–0.28	NP	0.25–0.43

[a]Concentrations are in mmol kg^{-1}; NP is not published.
[b]Sources given in parentheses are 1, *Charlou et al.* [2000]; 2, *Von Damm et al.* [1998]; 3, *Charlou et al.* [2002]; 4, *Douville et al.* [2002]; 5, *Jean-Baptiste et al.* [1991]; 6, *Rudnicki and Elderfield* [1992]; 7, *Edmonds et al.* [1996]; 8, *Gamo et al.* [1996]; 9, *Charlou et al.* [1996]; 10, *James et al.* [1995]; 11, *Lein et al.* [2000]; 12, *Schmidt et al.* [2007]; and 13, *Kelley et al.* [2001].

Figure 2.11. Parameters important for the prediction of corrosion risk at the Rainbow vent site. Source: (Le Bris and Duperron 2010).

It is important to acknowledge that H_2 is a common electron donor for microbial respiration such as sulphate reduction, which could be key in corrosion processes. Chemolithotrophic organisms participating in these processes do not need the presence of organic compounds in order to be active. This means that low organic content does not mean low microbial activity.

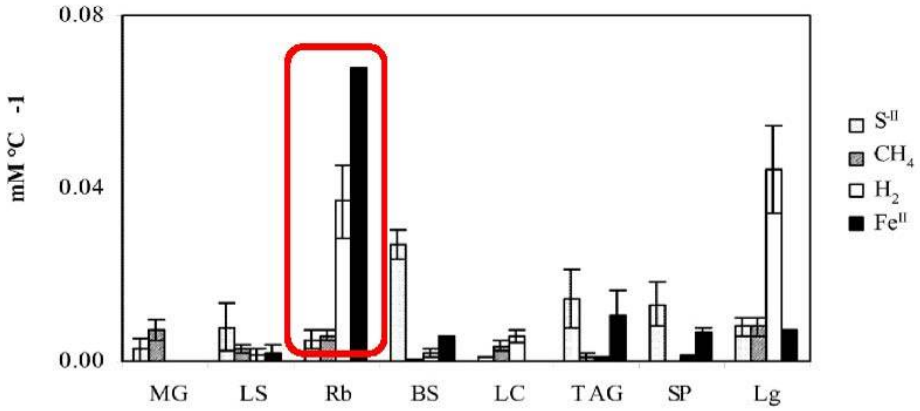

Figure 2.12. Electron donor contents in MAR vent fluids normalized to temperature (in mmol kg^{-1} $°C^{-1}$). MG:Menez Gwen; LS: Lucky Strike; Rb: Rainbow (red square); BS: Broken Spur; LC: Lost City; SP: Snake Pit; Lg: Logatchev. Note high levels of Fe(II) and H2 as potential electron donors (energy sources) at Rainbow site. Source: (Le Bris and Duperron 2010).

As observed in Fig. 2.13, most sulphide found in the Rainbow site is present as S^{2} and $Fe(HS)^{+}$. Other species such as H2S are found in relatively low concentrations as compared to other sites. These analyses have been done in the fluid phase, which does not tell anything about the presence of sulphur species at surfaces, where they are the most important for corrosion processes. Not many studies are available about the Rainbow vent site microbiology, however, microbial induced processes are known for other similar systems and knowing presence of particulates and key elements for biology a possible scenario of microbial transformations can be constructed based on available data and the results of microbial analyses. One of the few studies of plume microbiology was done by O'Brien et al. (1998) who collected microbial biomass from the plumes using 293 mm, 0.2 µm filters. Genomic DNA was later extracted from the collected biomass and analysed by molecular biology methods. Although the study was limited to general microbial groups, it was clear that the plumes were dominated by members of the domain Archaea as compared to the surrounding seawater.

A more complete investigation involving fluids, chimney fragments and sediments comparing several sites including the rainbow site was done more recently by Roussel et al. (2011). In these studies, both phylogenetic genes (16S rRNA) were assessed as well as functional genes for methanogenesis, sulphate reduction, and other metabolic activities.
In terms of corrosion, organisms attached at surfaces are the most relevant. In hydrothermal systems, the symbiotic interactions between microorganisms and macro fauna has been studied for their impact on the cycling of several elements. Although macro faunal species (e.g. shrimps mussels) do not change greatly from site to site, the attached microbial community can be highly diverse. The metabolic diversity of epibiotic microbial communities growing on the surfaces of hydrothermal shrimps has been studied. Even though sulphur processes have been mainly studied because of their dominance in hydrothermal systems, the possibility of a diverse attached microbial community participating on the transformation of iron, sulphur and methane has been demonstrated (Zbinden et al. 2008). All these processes might also occur on foreign structures (e.g. infrastructure) operating close to the site.

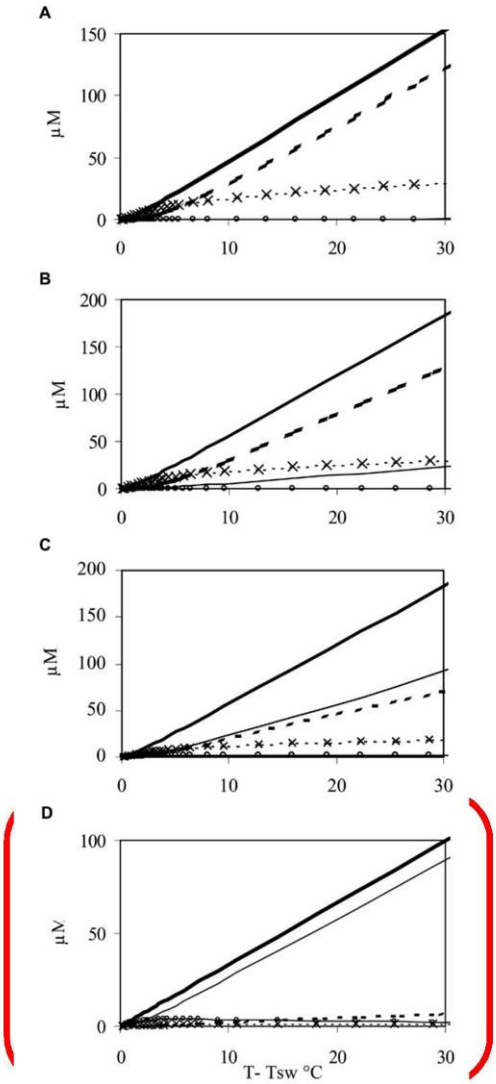

Figure 2.13. Abundance of sulphide species as function of temperature for different vent fluids at different sites. In the red circle values for Rainbow site. Bold line: S^{-2}, thin line: $Fe(HS)^{+}$; dotted line: H2S; line with crosses: HS^{-}; line with circles: FeSaq. Source: (Le Bris and Duperron 2010).

In the specific case of the Rainbow site a good example on the impact of epibiotic microbial communities on the stability of iron is given by the unique abundance of iron oxyhydroxides in the branchial chamber of the shrimp *Rimicaris exoculata*. This accumulation (Fig. 2.14) is believed to be due to microbial activity.

Figure 2.14. Iron oxyhydroxide deposits associated with *Rimicaris* shrimp (inhabitant of Rainbow vent site). (A) Specimen in a late stage of the molting cycle. Scale bar: 2 cm. (B) Dissected parts of a shrimp throax. (C) Inner face of carapace showing mineral accumulation. The arrow indicates circulation of water in the branchial chamber.

An important consequence of this phenomenon, is that at the macroscale, this biological interaction might be enhancing local iron precipitation. A potential scheme on the impact of shrimp swam presence and absence at the Rainbow site can be seen in Fig. 2.15.

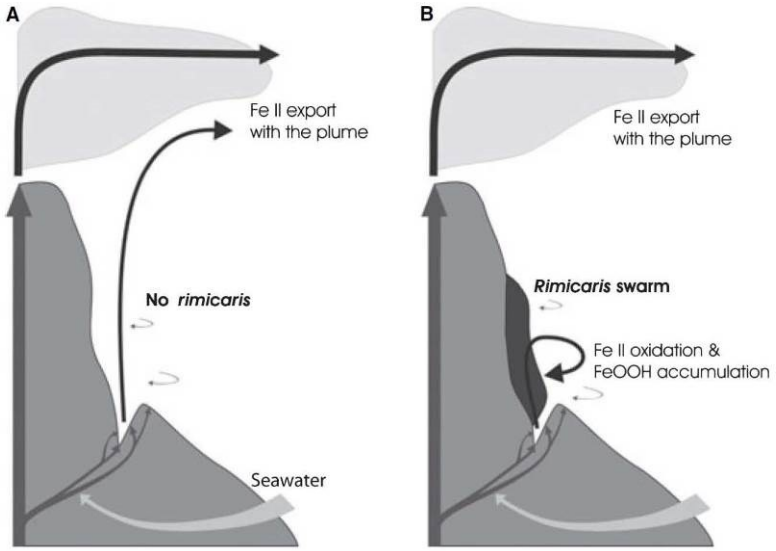

Figure 2.15. Local iron transport pathways from primary and secondary fluid sources on Rainbow hydrothermal chimneys, in the absence (A) or presence (B) of a *Rimicaris* swarm.

It is widely accepted that iron stability have a huge impact on corrosion processes. The knowledge that there are microbial processes at surfaces able to promote the local accumulation of iron is an important aspect of potential corrosion processes in such an environment. Whether or not microbiota able to influence iron precipitation processes can also attach and grow on metallic structures in a similar way as they do on the *Rimicaris* shrimp remains an open question worth to be investigated.

CONCLUDING REMARKS

- The Rainbow site is highly influenced by vent activity. The high concentration of sulphur in the plumes means that with exposed new infrastructure, microbial corrosion processes might be relatively high.
- Relatively low pH might also increase corrosion rates, especially if acidophilic microorganisms are present which could promote corrosion even in absence of oxygen.
- High copper levels at the site could indicate copper adapted microorganisms, which also mean a negative impact on MIC risk.
- Known corrosive activities stimulated by microorganisms are present at the Rainbow site (in fact acidophilic iron oxidizers were found in samples analysed from the site)
- Iron/sulphur related biofilms are very likely to be abundant at the site. It is commonly agreed that these types of biofilms can be highly corrosive.
- If materials known to be susceptible to microbial attack are to be used in this type of environments then the risk of accelerated corrosion should be considered.
- Because MIC rate will be directly linked to the growth and activity rate of these organisms, more detailed studies on site biogeochemistry should be documented. Data on actual microbial growth rates and activities are needed in order to have better chances of at least predicting worst case scenarios and possibly MIC rates under these conditions.

REFERENCES

Arakawa S et al. (2006) *Bioscience, Biotechnology, and Biochemistry* 70: 749–52.
Bailey B et al. (2005) http://adsabs.harvard.edu/abs/2005AGUFM.V51C1505B.
Bale S J et al. (1997) *International Journal of Systematic Bacteriology* 47: 515–21.
Barnes S et al. (1998) *Geomicrobiology J.* 15: 67–83.
Borenstein, SW (1994) Woodhead Publishing.
Childress JJ, BA Seibel (1998) *Journal of Experimental Biology* 201: 1223.

Coetser SE, TE Cloete (2005) *Critical Reviews in Microbiology* 31: 213–32.
Cowen, JP et al. (1986) *Nature* 322 (6075): 169–71..
Dick GJ et al. (2013) *Extreme Microbiology* 4: 124
Edwards, KJ et al. (2004) *Geomicrobiology J.* 21: 393–404.
Edwards, KJ et al. (2003) *Appl. Environ. Microbiol.* 69: 2906–13.
Elsgaard L et al. (1994) *Geochimica et Cosmochimica Acta* 58: 3335–43.
Fisher AT (1998). *Reviews of Geophysics* 36: 143–82.
Gadanho M, JP Sampaio (2005) *Microbial Ecology* 50 (3): 408–17.
German CR, KL Von Damm (2003) In *Treatise on Geochemistry*. Vol. 6. Oxford: Elsevier.
Groudieva T et al. (2003) *International Journal of Systematic and Evolutionary Microbiology* 53 (2): 539–45.
ISA (2002) D:\tosync\papers_old\ISA2002.pdf.
Isaksen MF, BB Jorgensen (1996) *Applied and Environmental Microbiology* 62: 408–14.
Khripounoff, A et al. (2001) *Journal of Marine Research* 59: 633–56.
Kim, J et al. (2009) *Geochemical Journal* 43: 1–13.
Le Bris N, S Duperron (2010) In *Geophysical Monograph Series*, edited by PA. Rona et al. (eds) 188:409–29. Washington, D. C.: American Geophysical Union.
Liu, SV et al. (1997) *Science* 277 (5329): 1106–9.
Mason, OU et al. (2010) *PLoS ONE* 5 (11): e15399.
Michiels C et al. (2008) In *Biology of hydrothermal systems*, 410–55. Moscow: KMK Press.
Miyazaki M et al. (2006) *International Journal of Systematic and Evolutionary Microbiology* 56: 1607–13.
Nogi Y et al. (2007) *International Journal of Systematic and Evolutionary Microbiology* 57: 1360–64.
Nogi Y et al. (1998) *Extremophiles: Life Under Extreme Conditions* 2: 1–7.
Nogi Y et al. (1998) *The Journal of General and Applied Microbiology* 44: 289–95.
O'Brien, D et al. (1998) *Earth and Planetary Science Letters* 157 (3–4): 223–231.
Orcutt BN et al. (2011) *Microbiol. Mol. Biol. Rev.* 75 (2): 361–422.
Paul JH (2001) *Marine Microbiology*. Gulf Professional Publishing.
Qin G et al. (2007) *Microbiology* 153 (5): 1566–72.
Roussel EG et al. (2011) *FEMS Microbiology Ecology* 77: 647–65.
Santelli CM (2007) Massachusetts Institute of Technology and the Woods Hole Oceanographic institution.
Staudigel H et al. (2006) *GSA TODAY* 16 (10): 4–10.
Stewart PS, MJ Franklin (2008) *Nature Reviews Microbiology* 6 (3): 199–210.
Ulloa O et al. (2012) *Proceedings of the National Academy of Sciences* 109 (40): 15996–3.
Venkatesan R et al. (2003) *Indian Journal Of Engineering And Materials Sciences*.
Venzlaff H et al. (2013) *Corrosion Science* 66: 88–96.
Zbinden M et al. (2008) *Journal of Experimental Marine Biology and Ecology* 359: 131–140.
ZoBell CE, RY Morita (1959) *Galathea Rep* 1: 139–154.

3. LITERATURE STUDY ON MARINE CORROSION

3.1 Introduction

Seawater is not a simple solution of inorganic salts in water. It is a complex mixture containing many different salts, dissolved gases, trace elements, suspended solids, decomposed organic matter, and living organisms. Its composition can vary between wide limits; for example, the dissolved salt content of the Baltic Sea is about 7 g/kg, whereas the Persian Gulf has about 43 g/kg [1]. The temperature of seawaters range variably from -2 ºC at the poles to 35 ºC right on the equator and it is subject to seasonal variations, winds and currents [4]. As such, seawater can be an aggressive and unpredictable medium. For most metals and alloys, it is capable of causing degradation or corrosion. Corrosion can be defined in a number of ways but "the chemical or electrochemical reaction of a metal or an alloy with its environment" provides a reasonable explanation of the term corrosion [4]. This can take the form of general thinning or more localised penetration in a variety of guises. The corrosion behaviour of metals in seawater is largely influenced by the oxygen content, seawater velocity, temperature, pollution and marine organisms [1].

The importance of seawater as a corrosive environment has increased during the last few decades because of offshore exploration of oil and gas [3]. Since metals are used for engineering structures because of their unique mechanical properties (strength and hardness combined with ductility), the corrosion product (powdery, non-adherent, friable compound) will result in deterioration of metallic structures [4].The majority of alloys are susceptible to corrosion in seawater in one way or another. Their successful application relies on knowledge of the types of corrosion each alloy may be susceptible to and how to avoid potential problems by material selection as well as good design, fabrication and operational practices [1]. Corrosion of alloys is an electrochemical phenomenon. Alloys are mixtures of two or more different metals and many have the capability of improving the properties of individual constituents but corrosion can affect this quality effectively [3].

3.2 PRINCIPLE OF CORROSION

3.2.1 Introduction

Corrosion in aqueous solutions is by far the most common of all corrosion processes. The aqueous medium is provided by water, seawater and various process streams in industry. Corrosion of metals in aqueous environments is almost electrochemical in nature. It occurs when two or more electrochemical reactions take place on a metal surface and as a result, some of the elements of the metal or alloy change from a metallic state into non-metallic state. The electrochemical reactions occur uniformly or non-uniformly on the surface of the metal which is called electrode. The ionically conducting liquid is called an electrolyte [8].

Electrochemical reactions are usually discussed in terms of the change in valence that occurs between the reacting elements, that is oxidation and reduction. Oxidation and reduction are commonly defined as follows: Oxidation is the removal of electrons from atoms or groups of atoms, resulting in an increase in valence and reduction is the addition of electrons to an atom or group of atoms. Electro-chemical reactions are often further defined as cathodic reactions and anodic reactions [2].

By definition, cathodic reactions are those types of reactions that result in reduction and anodic reactions are those types of reactions that result in oxidation:

- $M(aq)^{2+} + 2e^{-}$ → $M(s)$
- $M(s)$ → $M(aq)^{2+} + 2e^{-}$

The schematic for electrochemical reactions for Fe is shown in figure 3-1,

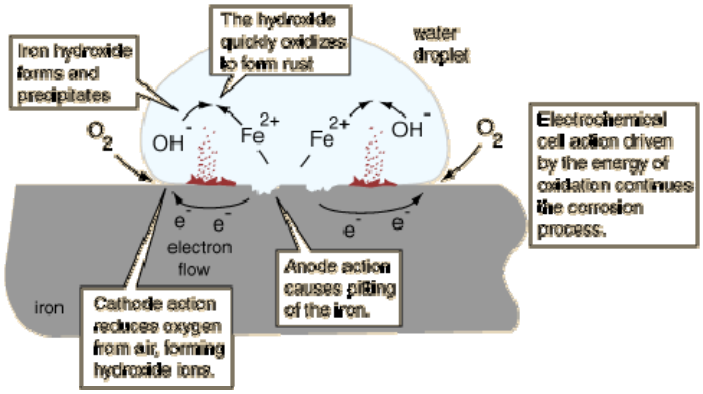

Figure 3-1 Schematic diagram of corrosion cells on iron[3].

3.2.2 Forms of corrosion

Introduction

Aqueous corrosion of metals and alloys takes place in a variety of environments containing water. While different terms serve to describe certain typical characteristics of corrosion pertaining to an environment, in this section the focus is on “marine corrosion“ and consideration is given to the more common forms of such corrosion [4].

Localised Corrosion

Metals corrode because of their thermodynamic instability in a particular environment and the mechanisms involve the existence of anodic and cathodic sites on the metal surface. In general corrosion, the sites change from being predominantly anodic to cathodic and vice-versa. In some situations however this happens to a lesser extent or not at all. Therefore the corrosion becomes localised at a number of anodic areas, the general surface being predominantly cathodic. This type of corrosion is usually complex and unpredictable in the sense that it is not usually possible to predetermine exactly where the attack will occur or even its extent. The most important forms of localised corrosion are discussed here [4].

Pitting Corrosion

Pitting is a form of localised attack in which small areas of the surface are corroded with penetration of the alloy at these areas. Usually the depth of penetration into the alloy is greater than the nominal diameter of the surface corrosion. Once it has been initiated, its continuation is determined by reactions within the pit, which at the points of attack is anodic, with the outer surface being cathodic. Sometimes pits penetrate to a certain depth and

then the downward attack stops or may continue horizontally within the metal. The effect of oxygen depletion and acid formation in the pit have to be taken into account. An example of pitting corrosion is shown in figure 3-2 [2,4].

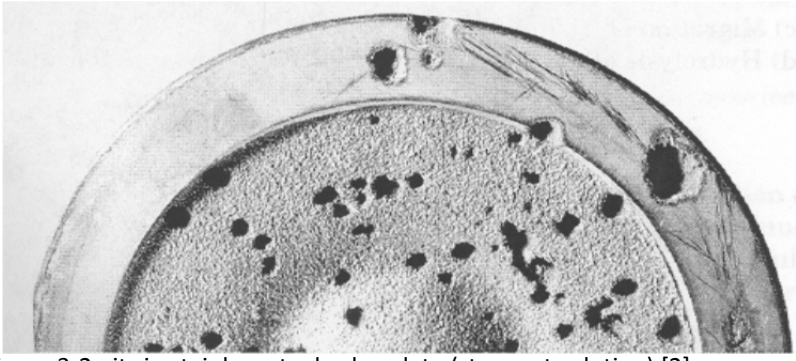

Figure 3-2 pits in stainless steel valve plate (stagnant solution) [2].

Crevice Corrosion

This type of corrosion arises when a crevice is formed between two surfaces with the inside of the crevice being anodic to the external surface. The large cathodic current acting on the small anodic area in the crevice results in an intensive local attack. Typical engineering situations where crevice corrosion may occur are at bolted joints, washers and flanges. The nature of the crevice is important because its influence is very much affected by the overall size and strength of the joint concerned. An example and an illustration of the principle of crevice corrosion are shown in figure 3-3 [2,4].

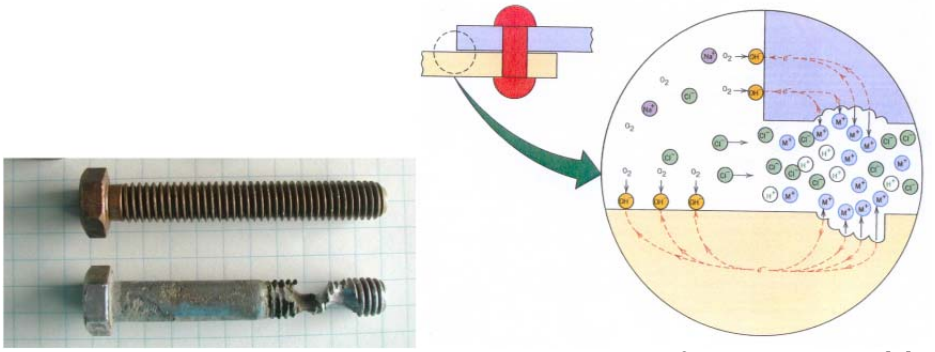

Figure 3-3 A schematic picture of crevice corrosion [2].

Selective Leaching

This form of attack is sometimes called de-alloying, which explains its nature. Alloys are composed of different metals and, which certain of them, under specific conditions selective leaching of one metal can occur. The most common examples are the selective removal of zinc from brasses (dezincification), the selective removal of iron from cast iron, known as graphitization and the de-alloying of aluminium bronze in sea water. Other alloys are also susceptible to this form of attack, particularly in acids, but those noted above are most likely to be encountered in marine situations[4].

Intergranular Corrosion

In some alloys under certain environmental conditions grain boundaries are much more active areas than the matrix. In such cases preferential corrosion may occur at the grain boundaries, leading to intergranular or intercrystalline corrosion. A common example of this form of attack occurs in austenitic stainless steels. When these alloys are heated within a certain range of temperature, they become what is termed 'sensitised' or susceptible to intergranular corrosion. This susceptibility results from the depletion of chromium near the grain boundaries. As stainless steels depend upon chromium for their corrosion resistance, a marked reduction in the amount of this element leads to a much reduced level of resistance. Microscopic feature of intergranular corrosion is shown in figure 3-4 [2,8].

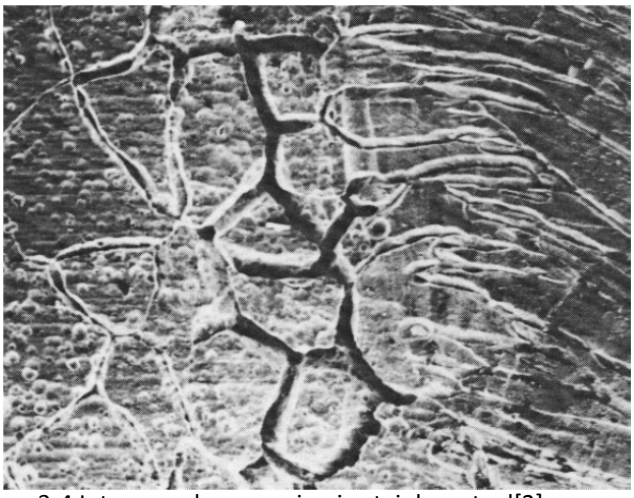

Figure 3-4 Intergranular corrosion in stainless steel[2].

Erosion-corrosion

Movement of sea water and, incidentally, other fluids, can cause mechanical action, i.e. erosion, as well as the corrosion arising from its electrochemical nature. Erosion-corrosion can lead to the removal of protective films from the surface of alloys and even removal of the metal itself if abrasive particles are entrained in the water. Generally the rate of attack increases with velocity of sea water [4].

Figure 3-5 Erosion-corrosion sample[2].

Stress Corrosion Cracking

The general corrosion of structural metals leads to the loss of cross-section so eventually they may fail under a load that they could originally sustain. SCC (stress corrosion cracking) is the initiation and slow growth of cracks under the simultaneous influence of tensile stresses and aggressive environment. Protective coating are applied to steels to control the loss of metal and hence prevent mechanical failures. There are, however, situations where the simultaneous effects of a tensile stress and corrosion are greater than the sum of these factors acting separately. Their effect is described as stress corrosion cracking and can lead to rapid failure of an alloy, unlike a structural failure arising from ordinary corrosion over long period [4].

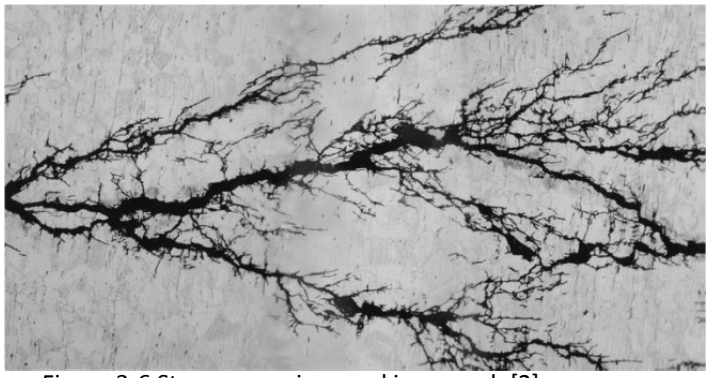

Figure 3-6 Stress corrosion cracking sample[2].

Corrosion Fatigue

Fatigue is the tendency for a metal or alloy to fracture under conditions of repeated cyclic stresses at loads below the ultimate tensile strength of the material. Corrosion fatigue occurs in metals as a result of the combined action of a cyclic stress and a corrosive environment. The importance of conjoint action should be emphasised because the separate effects are not usually as severe as the joint effects. Corrosion fatigue is dependent on the interactions among loading , environmental and metallurgical factors. For a given material, the fatigue strength generally decreases in the presence of an aggressive environment [2,4].

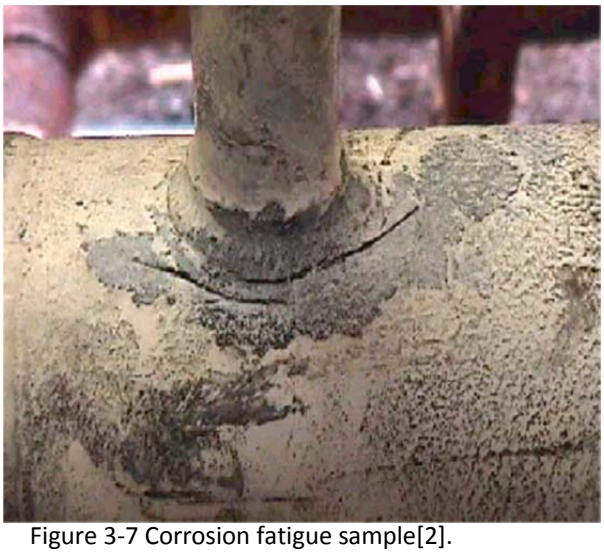

Figure 3-7 Corrosion fatigue sample[2].

Fretting Corrosion

Fretting corrosion is the damage that occurs at the interface of two closely fitting surfaces when they are subjected to slight relative movement or slip. Fretting corrosion is a combined wear and corrosion process in which material is removed from contacting surfaces when motion between the surfaces is restricted to very small amplitude oscillation. Oxidation is the most common element in the fretting process. In oxidizing systems, fine metal particles removed by adhesive wear are oxidized and trapped between the fretting surfaces [4].

3.3 MARINE ENVIRONMENT

3.3.1 Introduction

Seawater covers two-third of the earth's surface and its environment has been always important with respect to constructional materials. The importance of the marine environment has increased considerably in the last few decades because of the exploration for natural resources in the sea [4]. On the other hand, regarding design and engineering, sea water has always been important because of its high salt content and its aggressive and corrosive environment has been a critical issue for engineers. Figure 3-1 shows the corrosion rate of iron in aqueous sodium chloride (NaCl) solutions of various concentrations. The maximum corrosion rate occurs near 3.5% NaCl (the approximate salt concentration of sea water) [2].

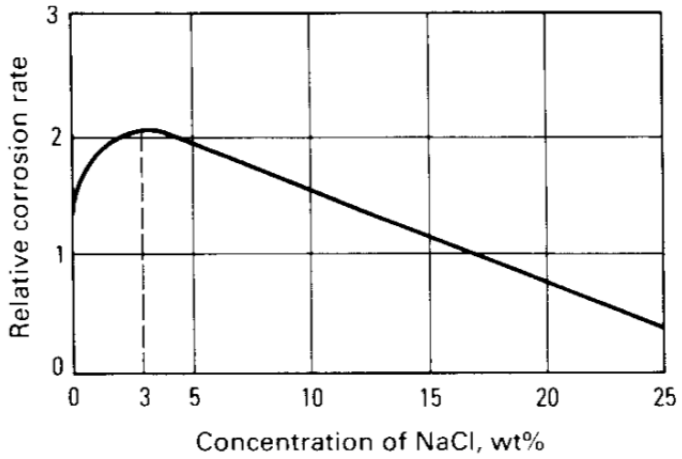

Figure 3.3-8 Effect of NaCl concentration on the corrosion rate of iron in aerated room-temperature solutions [2].

Other variables in seawater and in the marine environment affect corrosion rates in different ways. The most important variables are discussed in the next sections.

3.3.2 Salinity

The most commonly measured property of seawater is salinity (S in parts per thousand [‰]), which has historically been defined as the total weight in grams of inorganic salts in 1 kg of seawater when all bromides and iodides are replaced by an equivalent quantity of chlorides and all carbonates are replaced by an equivalent quantity of oxides. Salinity is usually determined by measuring either the chlorinity or the electrical conductivity of the seawater. The total salt content of open ocean seawater varies from 32 to 36‰. Salinity variations with depth at given locations in the Atlantic and Pacific Oceans are shown in figure 3-9 [2].

The main effects of salinity on corrosion result first from its influence on the conductivity of the water and second from the influence of chloride ions on the breakdown of passive films. The high conductivity of seawater means that the resistance of electrolyte plays a minor role in determining the rate of corrosion reactions and that surface area relations play a major role. The second effect of salinity on corrosion in seawater is related to the role of chloride ions in the breakdown of passivity on active-passive metals such as stainless steels and aluminium alloys. The higher the salinity of the water, the more readily chloride ions succeed in penetrating the passive film and initiating pitting and crevice corrosion at localized sites on the metal surface [2].

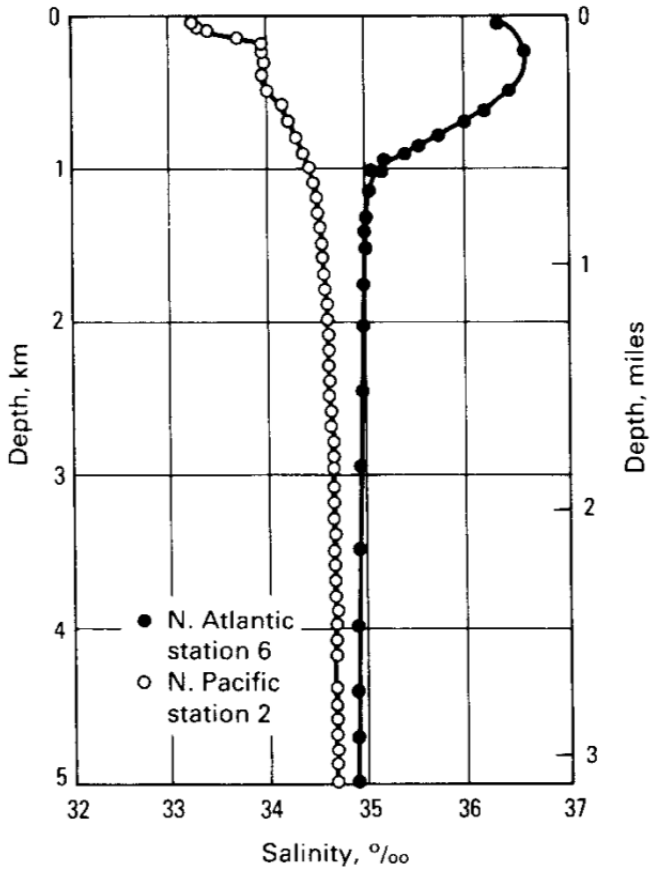

Figure 3.3-9 Comparison of salinity-depth profiles for open ocean [2].

3.3.3 Temperature

When all other factors are held constant, an increase in temperature increases the corrosiveness of seawater. If dissolved oxygen concentration is held constant, the corrosion rate of low-carbon steel in seawater will approximately double for each 30 º C increase in temperature. Open ocean temperature variations are shown in figure 3-10. From these data alone, one would expect corrosion rates in tropical surface waters to be about twice those in the polar regions or in deep water. Corrosion rates are usually higher in warm surface waters that in cold deep waters, as illustrated in figure 3-11 and 3-12 [2,8].

The saturation level of dissolved oxygen increases as the temperature decreases, and the effects of dissolved oxygen on the corrosion rate are often stronger that those of temperature. Short-term local temperature fluctuations and the effects of bio-fouling and scaling films must also be considered.

Summarizing, sea temperature decreases with depth in irregular ways depending on the season and location. Deep ocean water has a temperature of about 3 ºC . As water depth increases temperature decreases, this decrease in temperature affects the ability of calcareous deposits to form. Calcareous deposits are the result of the cathodic protection polarization process. These deposits are critical in the cathodic protection process as they act like crude coating systems to reduce the current required from the anodes, thus it is possible to provide cathodic protection for a very long lifetime with relatively small anodes.

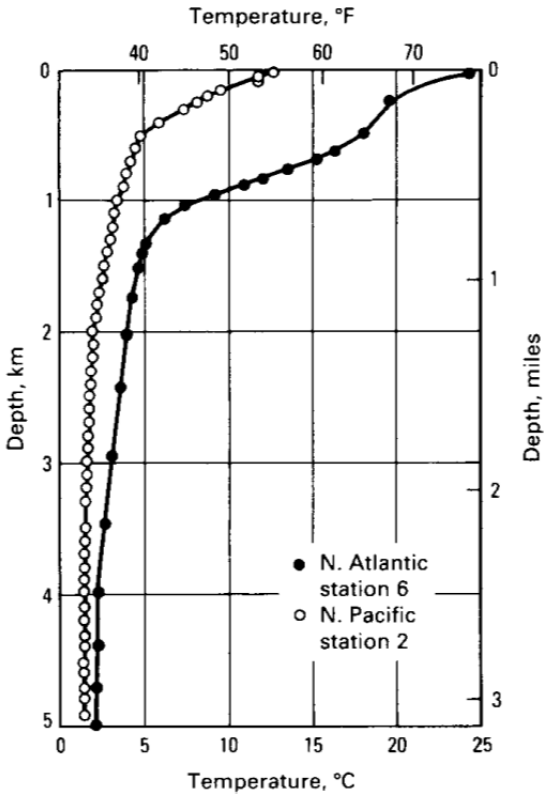

Figure 3.3-10 Comparison of temperature-depth profiles for open ocean [2].

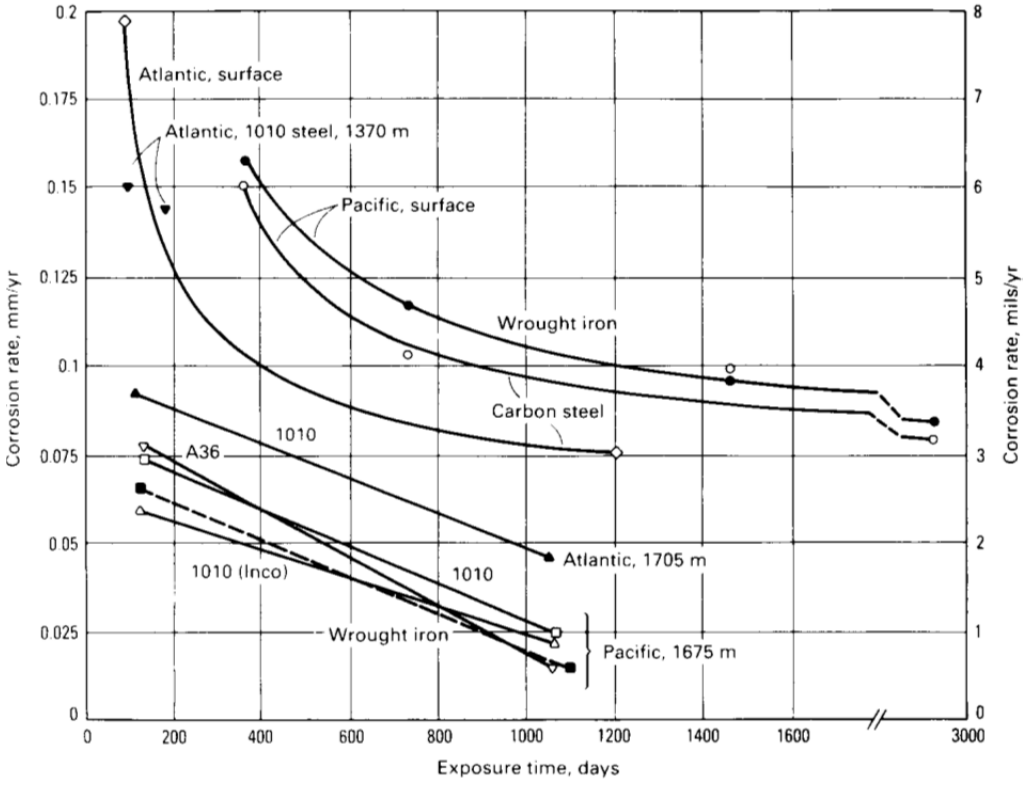

Figure 3.3-11 Comparison rates of carbon steels and wrought iron in the Atlantic & Pacific Oceans at various depths [2].

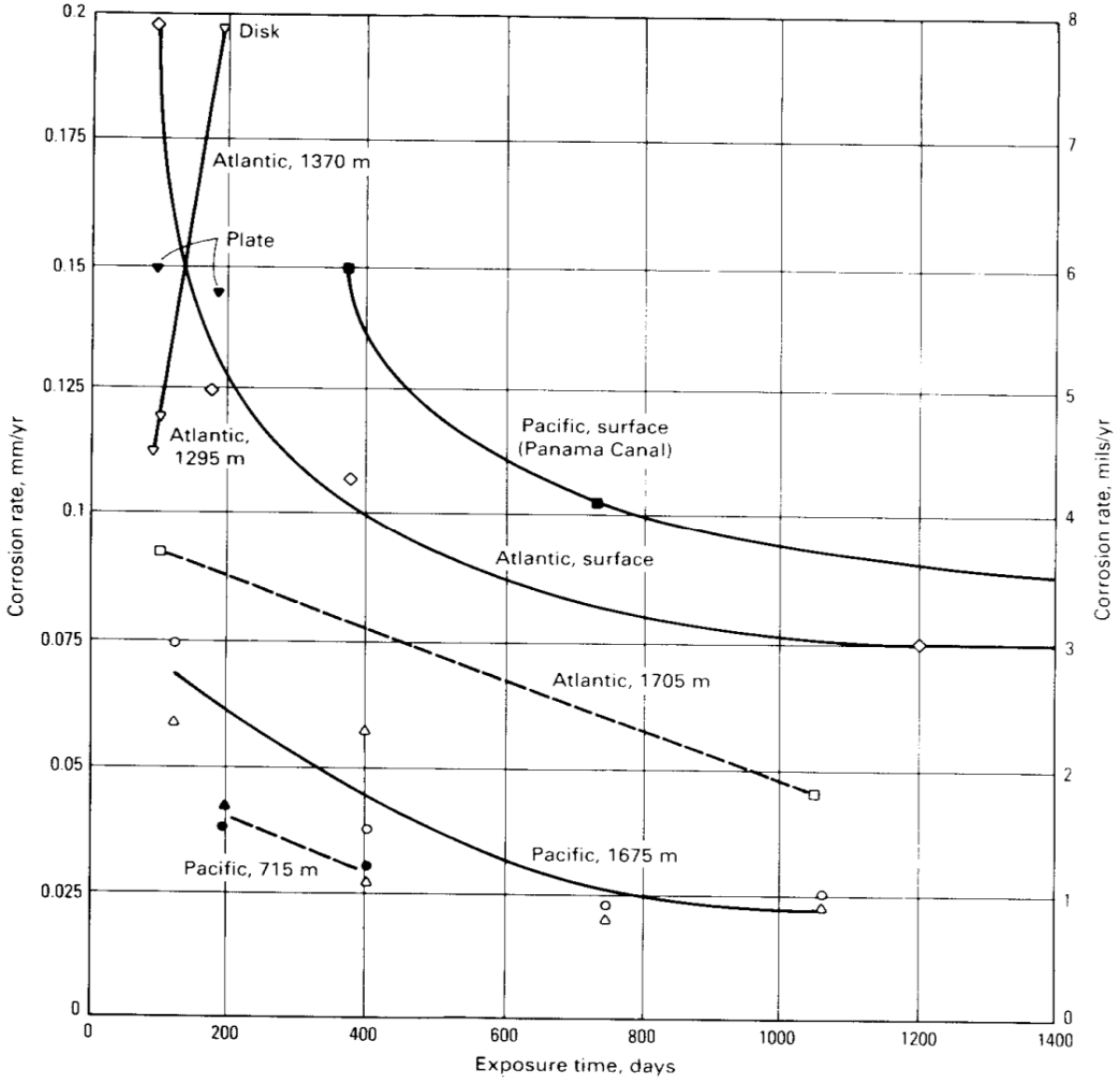

Figure 3.3-12 Comparison rates of low-carbon steels in the Atlantic & Pacific Oceans at various depths [2].

3.3.4 Dissolved Oxygen (DO)

Generally, the surface waters of the ocean are in equilibrium with the oxygen in the atmosphere at a specific temperature. Surface waters are either saturated or supersaturated with oxygen at atmospheric conditions. In contrast, deep waters are often under-saturated because of the consumption of oxygen during biochemical oxidation of organic matter. This decrease in oxygen concentration with depth is shown clearly in figure 3-13. The oxygen profiles for the open Atlantic and Pacific stations both go through a minimum at intermediate depths and increase again at great depths. Summarizing, at shallow depths the oxygen supply is close to saturation, the concentration decrease till to a layer of minimum oxygen content, generally at depths to between 500m and 1000m, at greater depths in oceans oxygen levels rise again because of cold, dense, oxygenated water sinking in the polar regions [2,7]. In spite of the increase in the oxygen bulk concentration at low temperatures, the mass-transfer of oxygen does not increase significantly because of the lower diffusion coefficient under these conditions.

The corrosion rate of active metals in aerated electrolytes such as seawater at constant temperature is a direct linear function of the dissolved oxygen concentration, as shown in figure 3-14. When oxygen and temperature vary together as they do in the marine environment, the oxygen effect tends to predominate. This trend is illustrated by data for the corrosion rate of steel at various depths in the Pacific Ocean in figure 3-8 [2].

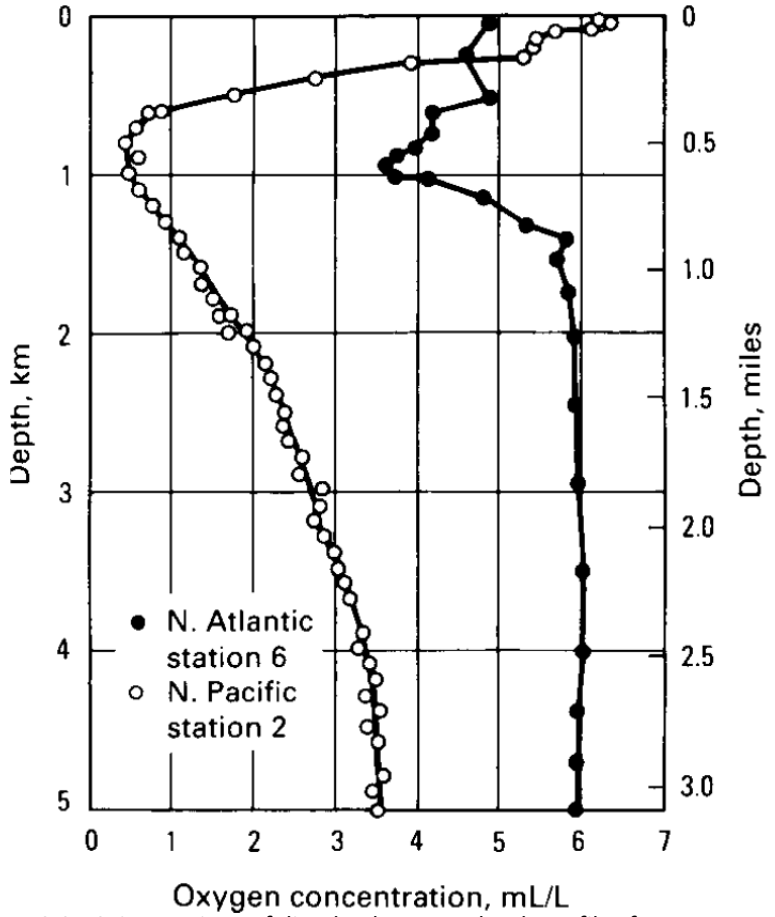

Figure 3.3-13 Comparison of dissolved oxygen-depth profiles for open ocean [2].

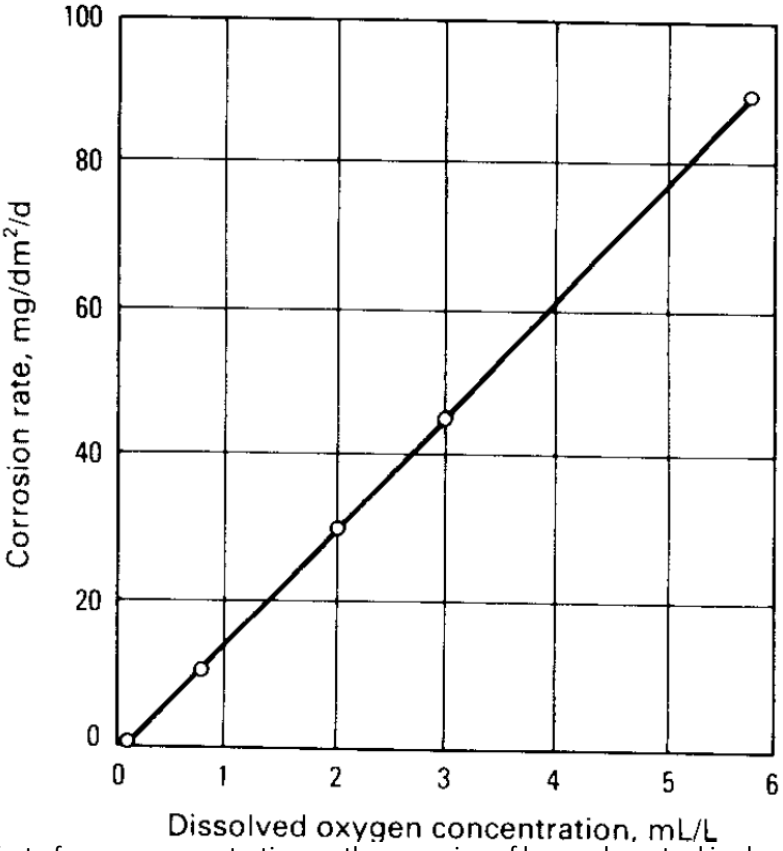

Figure 3.3-14 Effect of oxygen concentration on the corrosion of low-carbon steel in slowly moving water containing 165 ppm CaCl2 [2].

The corrosion rate decreases with dissolved oxygen down to the oxygen minimum, then increases again with oxygen at greater depths, despite a continuing decrease in temperature.

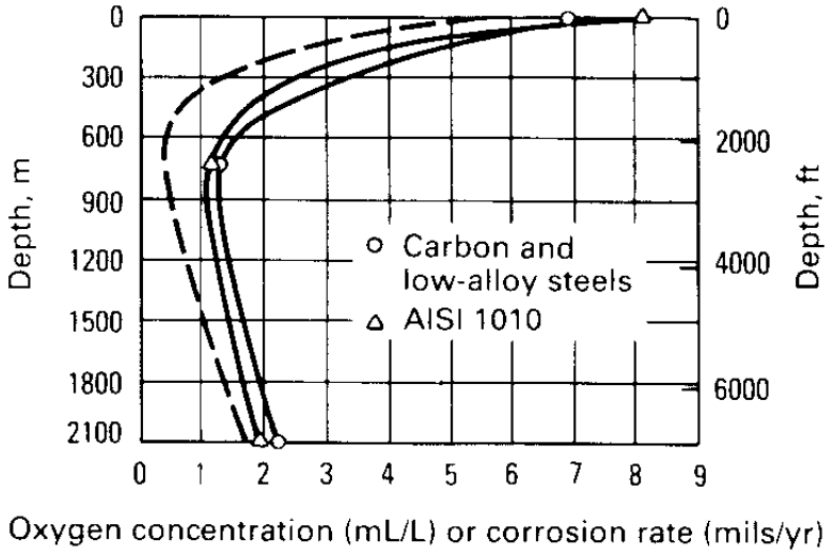

Figure 3.3-15 Corrosion of steels versus depth after 1 year of exposure compared to the shape of the dissolved oxygen profile(dashed line) [2].

The corrosion rates of nickel and nickel-copper alloys are somewhat less affected by oxygen concentration, as shown in figure 3-16.

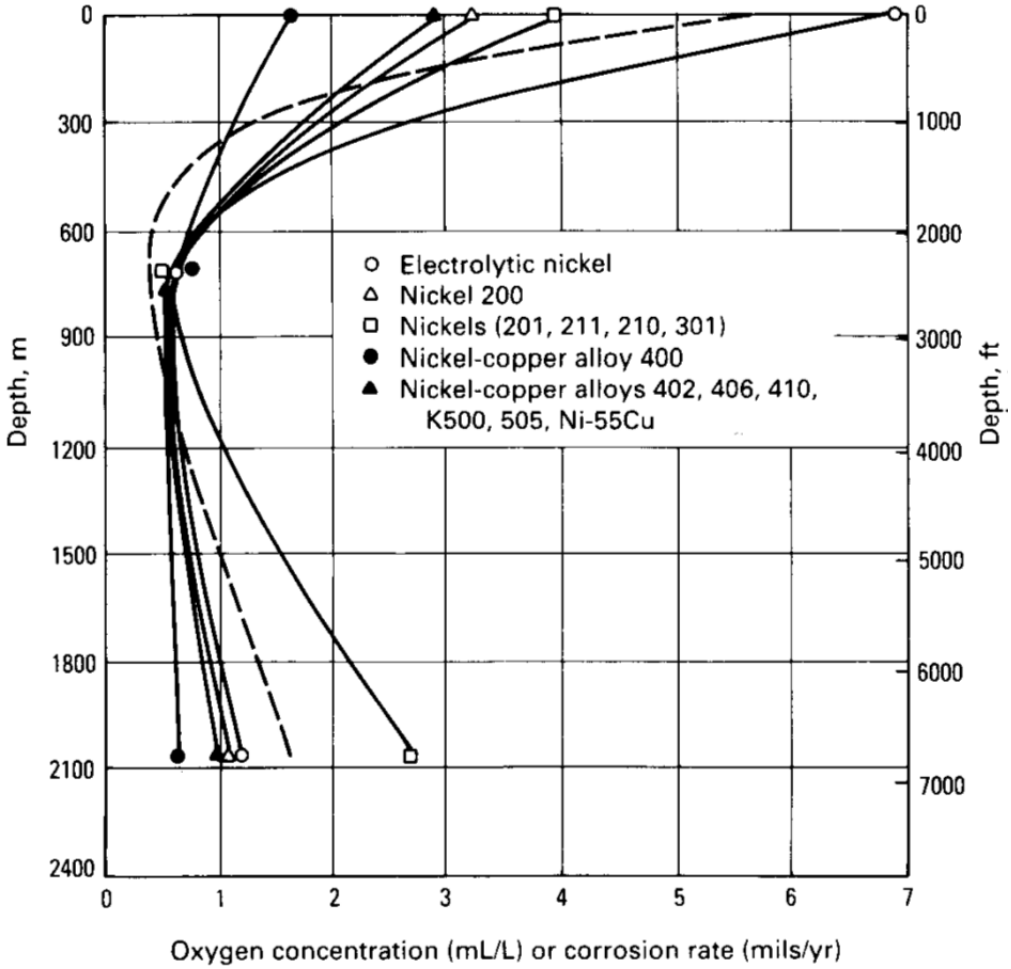

Figure 3.3-16 Corrosion of nickels and nickel-copper alloys versus depth after 1 year of exposure compared to the Shape of the dissolved oxygen profile(dashed line) [2].

The effect of oxygen on the corrosion rates of active-passive metals, such as the aluminium and stainless steel alloys, can be quite variable, as shown in figure 3-17. In such alloy systems, high oxygen concentrations tend to promote healing of the passive film and this retard initiation of pitting corrosion. On the other hand, high oxygen favours a vigorous cathodic reaction and tends to increase the rate of pit and crevice propagation after initiation [2,7].

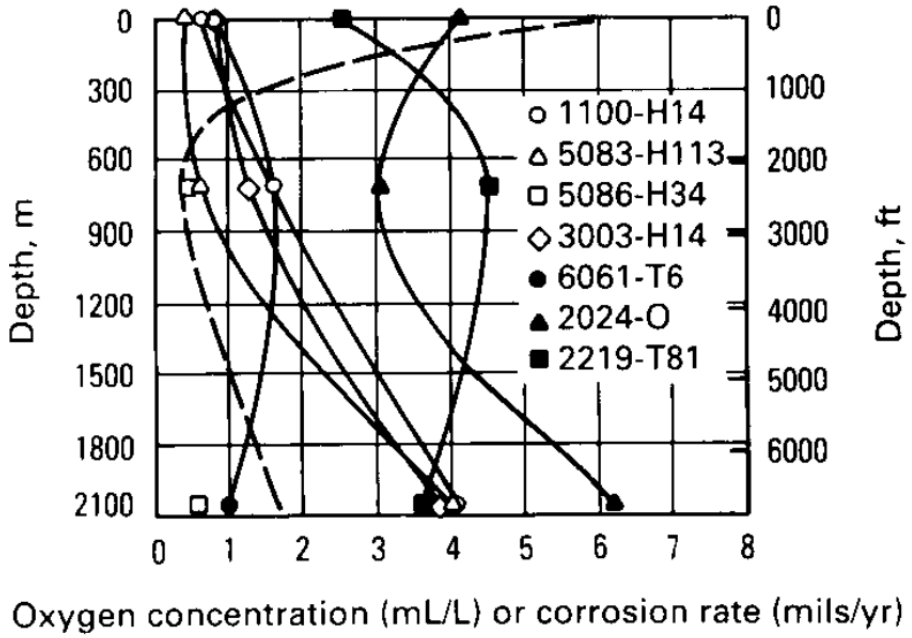

Figure 3.3-17 Corrosion of aluminium alloys versus depth after 1 year of exposure compared to the shape of the dissolved oxygen profile (dashed line) [2].

3.3.5 pH

The pH value of open ocean water ranges from about 7.5 to 8.3. Changes within this range have no direct effect on the corrosion of most structural metals and alloys. Exceptions to this general statement are aluminium alloys. A decrease in the pH value from the surface water value of 8.2 to a deep water value of 7.5 to 7.7 causes a marked acceleration in the initiation of both pitting and crevice corrosion, which accounts for the reported increase in corrosion of aluminium alloys in the deep sea. The concentrations of carbon dioxide and oxygen are closely coupled and related to the pH value of seawater through the process of photosynthesis and biochemical oxidation. Profiles of pH values with depth for 2 open ocean locations are shown in figure 3-18. A comparison of the corresponding pH values and oxygen profiles in figure 3-13 and 3-18 reveals their closely coupled nature through the carbon dioxide system as discussed above [2,7]. It can be concluded that the change of the pH value with depth does not directly affect the corrosion of metals and alloys. Figure 3-19 shows the effect of depth on 4 variables: oxygen, temperature, pH value and salinity in seawater and in the marine environment.

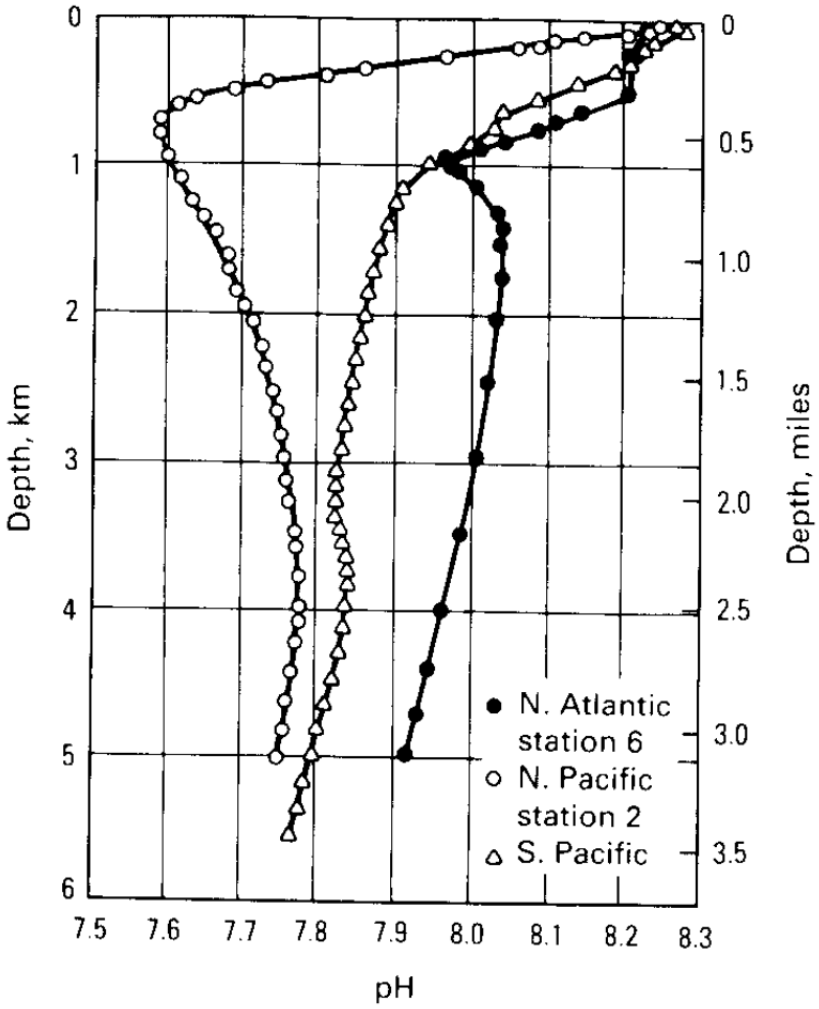

Figure 3.3-18 Comparison of PH-depth profiles for open ocean sites [2].

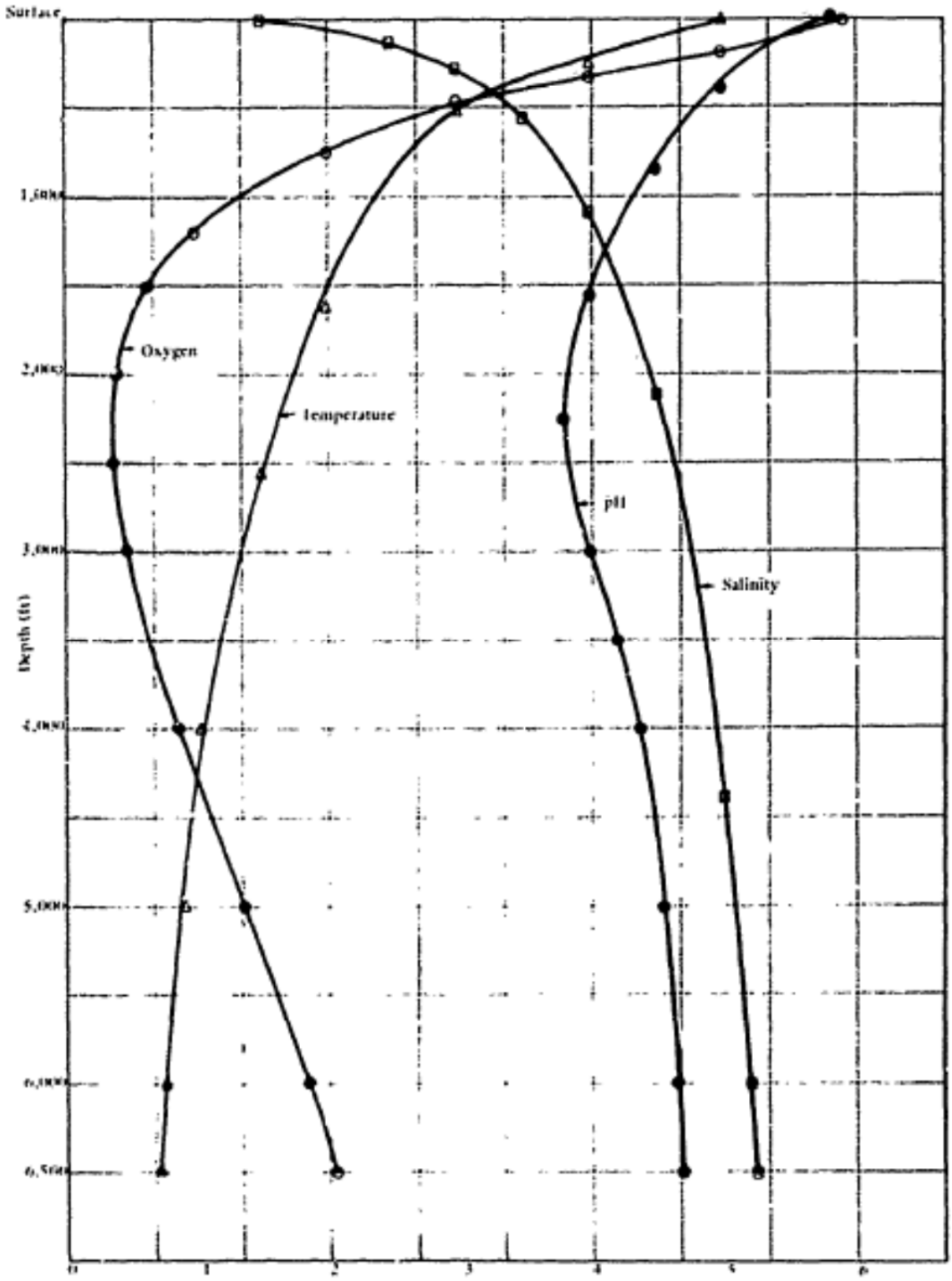

Figure 3.3-19 The variation of temperature, PH, salinity, oxygen content of seawater with depth [10].

3.3.6 Dissolved carbon dioxide

The concentration of carbon dioxide is less affected by air-sea interchange that the concentration of dissolved oxygen, because the carbon dioxide system in seawater is buffered by the presence of bicarbonate and carbonate ions. Seawater carbon dioxide affects the rate of corrosion by determining whether or not a protective layer (e.g. calcium carbonate) will precipitate on all metal and alloy surfaces. Seawater in the deep ocean environmental zone is generally under-saturated in carbonates, which reduces the likelihood of forming protective calcareous layers [2,7].

3.3.7 Duration of exposure

In general, the effect of duration of exposure in sea water depends on the depth of exposure and the kind of material which is exposed in that depth, Consequently there is not a general rule for explaining the effect of the duration of exposure on materials. The corrosion rate of some materials like steels, cast iron and copper alloys decreases with increasing of duration of exposure both at the surface and at 6000 foot (~1829 m) depth, figure 3-20 [10]. There are also some materials like aluminium and its alloys which show erratic or not definite correlation with duration of exposure.

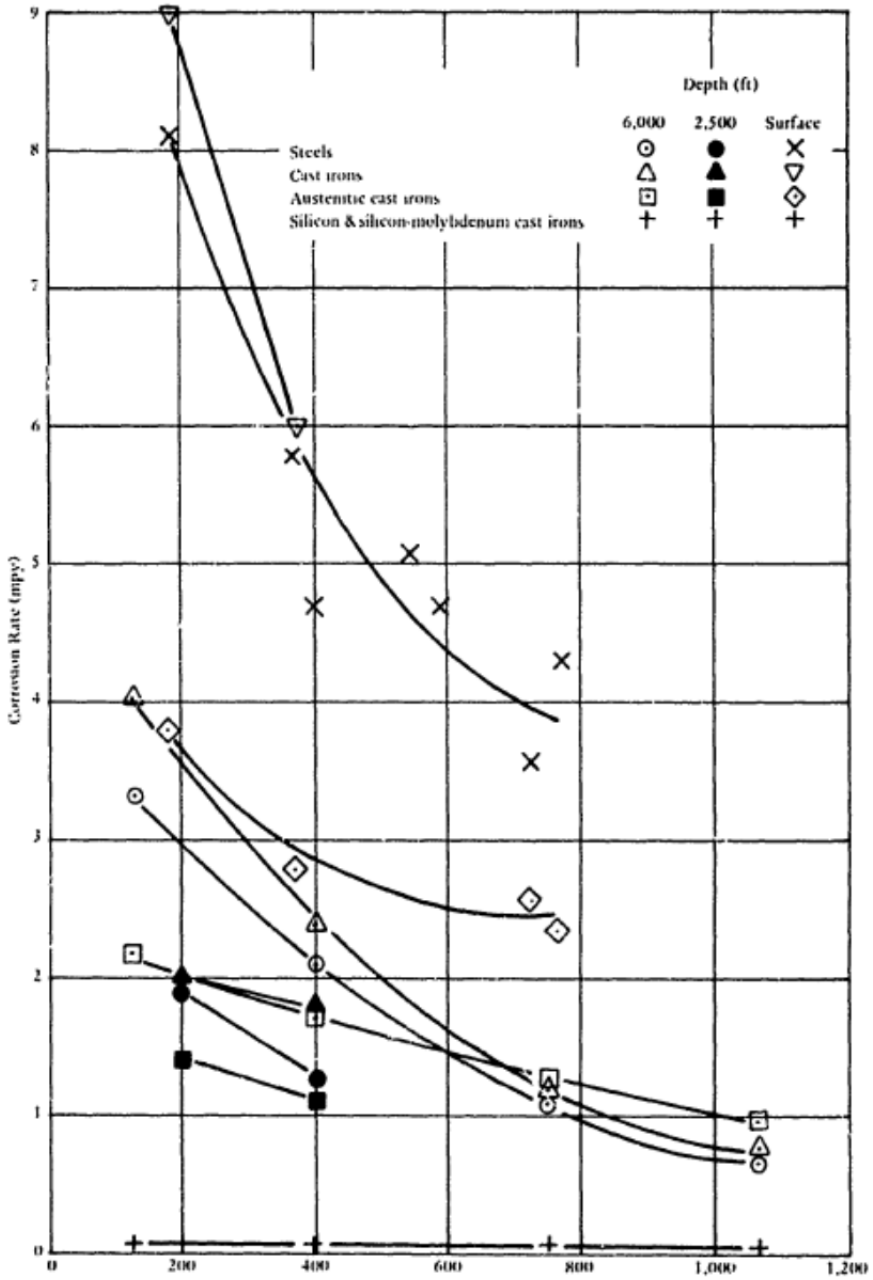

Figure 3.3-20 Effect of duration of exposure on corrosion of steels and cast iron [10].

3.3.8 Environment and corrosion control

The general marine environment includes a great diversity of sub environments, such as full-strength open ocean water, coastal seawater, brackish and estuarine waters, bottom sediments and marine atmosphere. Exposure of structural materials to these environments can be continuous or intermittent, depending on the application. Generally, structures can be exposed simultaneously to five zones of corrosion. Beginning with the marine atmosphere, the structure then passes down through the splash, tidal, continuously submerged and subsoil zones. The relative corrosion rates often experienced on steel structures passing through all of these zones are illustrated in figure 3-21 [2,4].

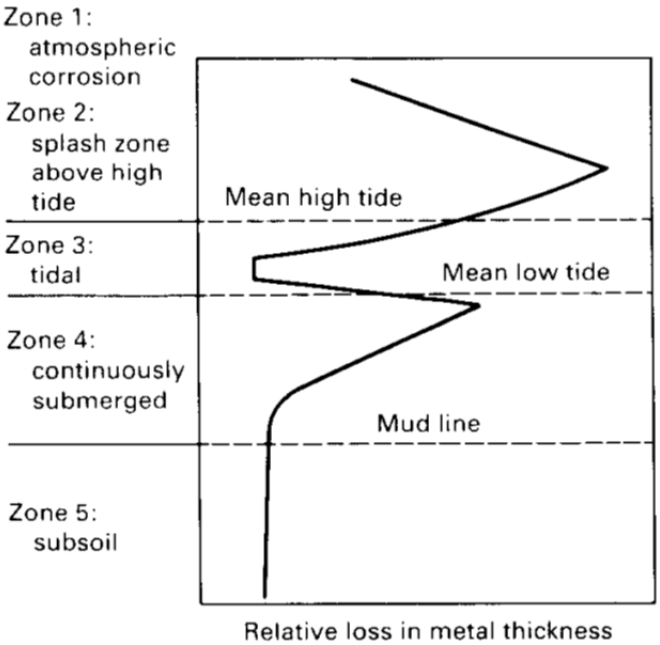

Figure 3.3-21 Effect of NaCl concentration on the corrosion rate of iron [2].

Protection of a steel structure can be achieved by various means; each corrosion zone being separately considered. Three generally accepted methods are cathodic protection, Painting and coating, and sheathing. Table 3-1 and figure 3-22 give results from various sources for the maximum corrosion rate in the splash zone and immersed zone for a range of locations. These show the maximum corrosion rates for the splash zone in the range 150-500 µm/y compared to the immersed zone at 60-140 µm/y [4,9] .

LOCATION		MAXIMUM CORROSION RATE µm/y	
		SPLASH ZONE	IMMERSED ZONE
1970	UK ESTUARY	195	80
1977	TOKYO BAY	500	10 (CP)
1983	UK PORTS	180	140
1983	NETHERLANDS	180	60
1983	CYPRUS	210	110
1983	UAE	220	120
1989	LA GUARDIA AIRPORT[4]	150	25 (CP)
	AVERAGE	230	100
	RANGE	150-500	60-120

Table 3.3-1 Corrosion rates, CP = with cathodic protection [9].

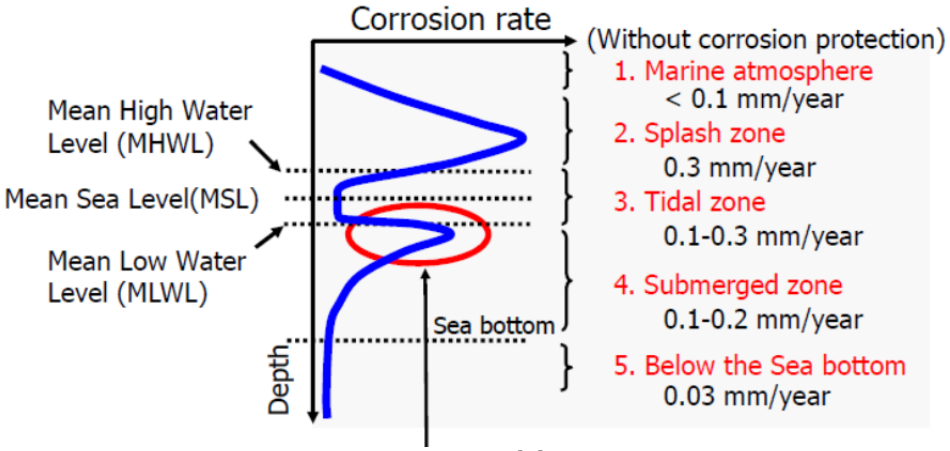

Figure 3.3-221 Corrosion environment and corrosion rate [9]. Concentrated corrosion occurrence just below MLWL.

Steel and concrete offshore structures exist in an environment of oxygen saturated seawater which is particularly detrimental to structural steels. Corrosion will occur if the proper precautions are not taken. An offshore platform is schematically shown in figure 3-16 with an indication of the main problem areas and the methods for controlling corrosion. Clearly, the splash zone is the most aggressive and difficult to maintain because cathodic protection cannot be used and painting has to be carried out. Cathodic protection in this area is ineffective because of the lack of continuous contact with the seawater (electrolyte) and thus no constant current flows [4].

With the huge and expensive installations in deep seawater, and with production equipment and pipelines carrying very aggressive mixtures of hydrocarbons and salt water, strict demands are naturally made on the corrosion technology for this industry. During the last few decades, oil companies have started using more corrosion-resistant materials in production and seawater systems [1]. There are several reasons for this :

- Large inhibitor expenses can be eliminated or reduced substantially.
- Demand for inspection, maintenance, repair and replacement is reduced.
- Weight may be reduced by reducing thickness or by using lighter materials.

The platform structure can from a corrosion point of view be subdivided into three broad zones:

- Submerged zone
- Splash zone
- Atmospheric zone

In this report the main focus is based on submerged zone and the essential factors that influence the choice of control methods are discussed [4].

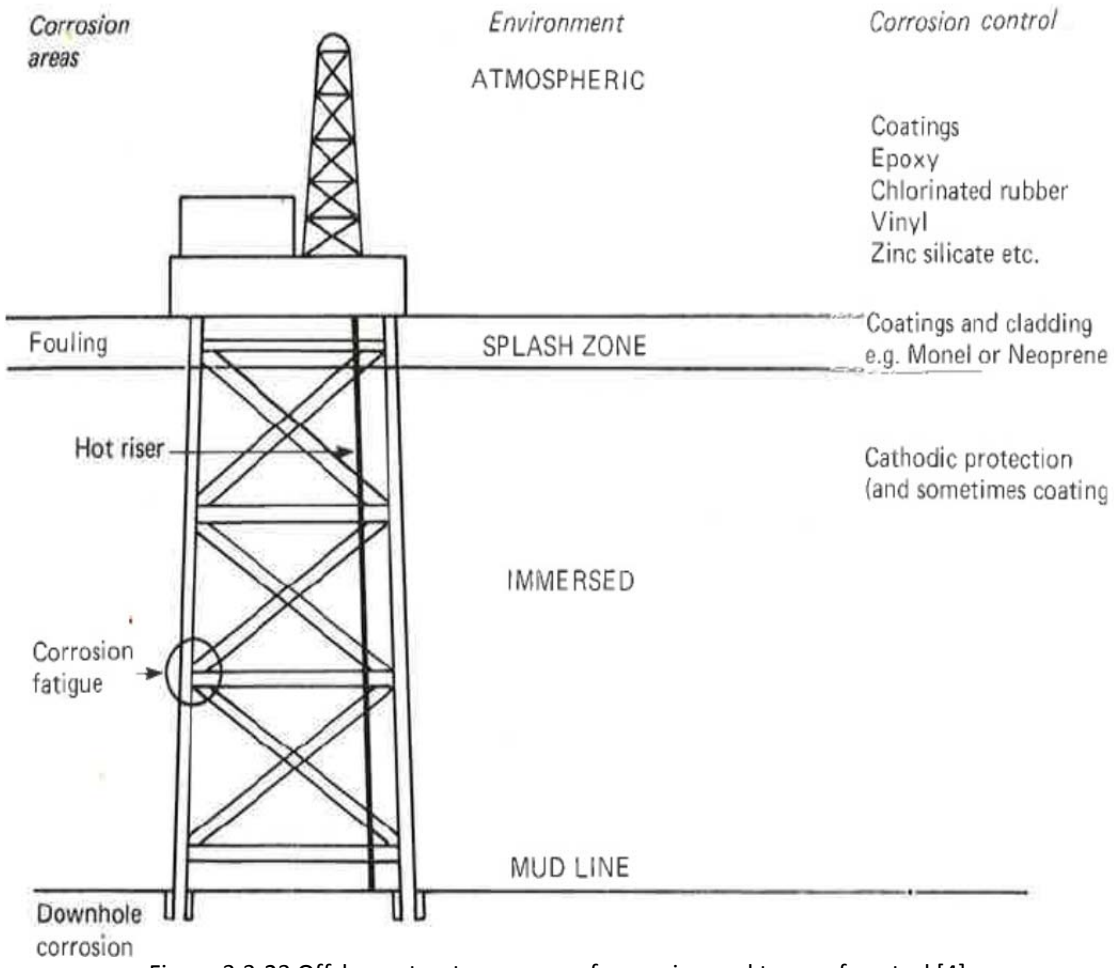

Figure 3.3-23 Offshore structure: areas of corrosion and types of control [4].

Submerged zone

The deep-sea environment is very different from the sea at the surface. It is characterized by total absence of sunlight, high hydrostatic pressure and a low water temperature of about 3 ºC. An exception are hydrothermal vent fields at which the temperature in the vicinity of the vents may be as high as 400 ºC. Despite these severe conditions, more and more effort is being devoted to both scientific exploration and resource exploitation of the deep sea environment [7].

Apart from hydrostatic pressure and temperature, corrosion of a structure in a marine environment is reigned by dissolved oxygen (DO), salinity and pH in addition to other factors such as seawater current, suspended silt, marine biota, decaying organic material, dissolved sulphides and carbonates [2,7].

All steel immersed in seawater is susceptible to corrosion even when it is coated. Defects, damage and deterioration over time may affect the coating's integrity Cathodic protection is the method invariably used in this zone. Generally, protective coatings are not used in conjunction with cathodic protection but in some cases coatings for submerged areas are specified. Fewer anodes would be required for cathodic protection and they would require to be replaced less frequently during the design life of a platform and the anode design life would be expected to be considerably longer. This must of course be balanced by the cost of protecting such a large area of steel work. The coating system would generally be of a two-pack coal-tar epoxy type. Figure 3-24 illustrates the most problematic corrosion types for an offshore platform. As can be seen cathodic protection is often used for submerged areas.

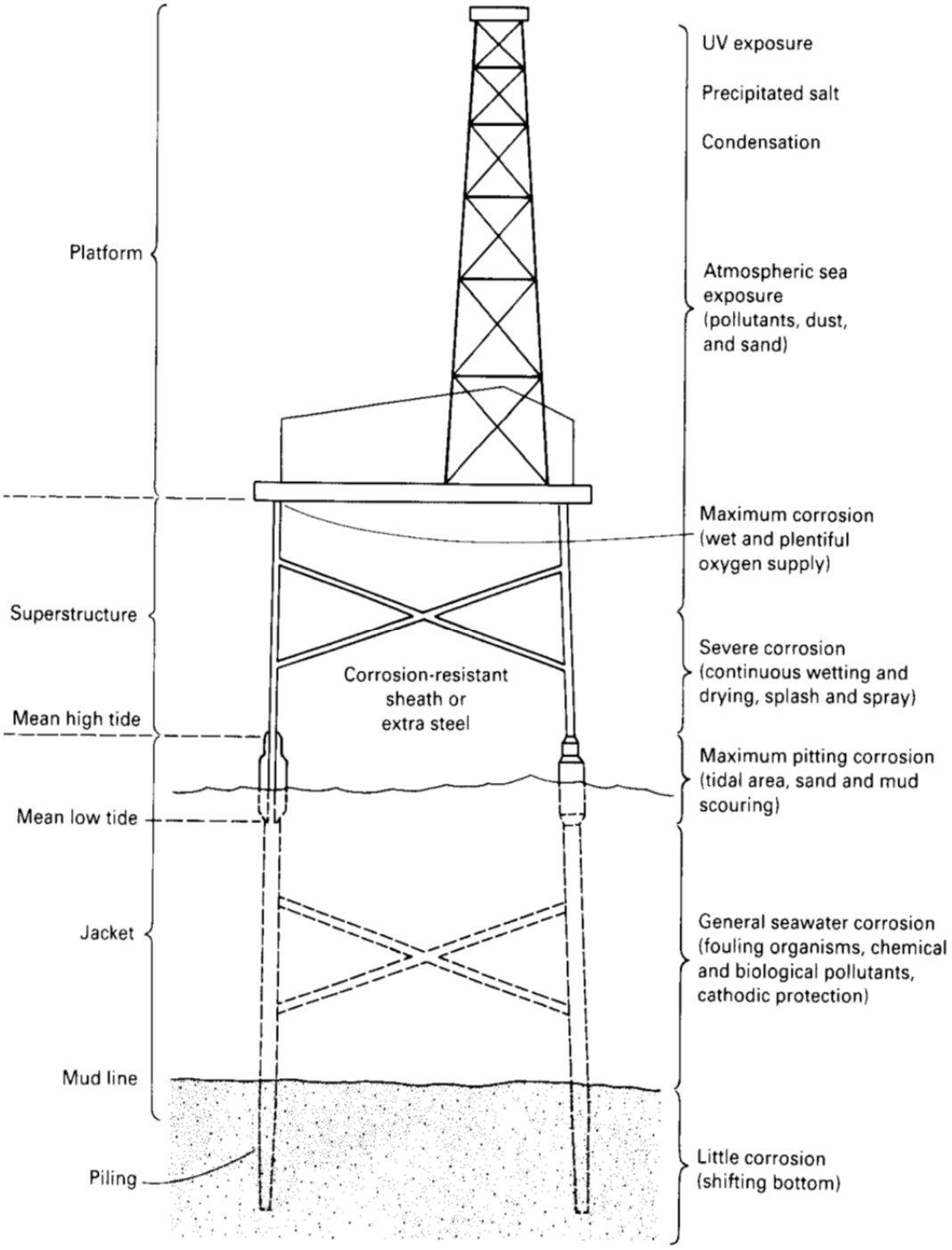

Figure 3.3-24 Zones of severity of environment for a typical drilling structure [2].

Cathodic protection

Introduction

In view of the electrochemical nature of corrosion, it would seem logical for an electrochemical method to be devised to control or prevent it; cathodic protection is such a method. It is based on the reactions that occur in a simple electrolytic cell and provides a situation where an alloy (usually steel) constitutes cathode or non-corroding electrode of the cell. Cathodic protection is restricted to environments of suitable conductivity. It is particularly suitable for steels immersed in sea water. It has been shown that the chemical reactions occurring in the corrosion process can be subdivided into two electrochemical reactions, one of which involves oxidation, the release of electrons, and the other reduction, the consumption of electrons. The following are typical anodic (oxidation) and cathodic (reduction) reactions for the corrosion of iron (or steel) [4].

- Anodic reaction: $2Fe(s) \rightarrow 2Fe^{2+}(aq) + 4e^-$
- Cathodic reaction: $O_2 + H_2O + 4e^- \rightarrow 4\ OH^-$

As can be seen, all the electrons released in the anodic reaction are consumed in the cathodic reaction. If electrons are supplied to the iron from some external source then the anodic reactions will be suppressed and the potential of the iron will be lowered. If the potential of the iron is lowered sufficiently, then eventually no current will flow between the anodes and cathodes on the iron surface and corrosion will cease. During cathodic protection, this situation is brought about and full protection will be achieved. The essential requirement for the cathodic protection is to achieve a situation on the surface of the metal to be protected where no local corrosion currents occur. In electrochemical terms this involves the supply of electrons to steel, which can be achieved in two ways:

- By applying a current through an external source. This is called the "impressed current method".
- By forming a galvanic cell using a block of suitable metal, e.g. zinc, electrically connected to the steel. Provided the attached metal has a more negative potential than the steel, electrons will pass spontaneously from metal to steel. This is called the "sacrificial anode method" because the attached metal is sacrificed to protect the steel [4].

Cathodic protection in fixed offshore structure

Cathodic protection is widely used to protect steelwork immersed in sea water such as offshore structures. Cathodic protection is generally used in conjunction with suitable coating. The protection system only needs to protect areas where the coating has failed to protect the steel, e.g. at pinholes, pores and damaged areas. The underwater steelwork of the majority of offshore platforms in not protected by coatings. This is an economic decision arising from a number of factors such as the overall costs involved in the protection of such massive amounts of steelwork and the time required for coating. This has to be balanced against the greater cathodic protection requirement on uncoated steelwork and the much greater weight involved in using more anodes [4].

All fixed offshore structures associated with the exploration and production of hydrocarbons are provided with cathodic protection. Without effective cathodic protection these structures would suffer general corrosion loss resulting in structural weakening and possibly perforation of members however the most dangerous consequences of insufficient protection is preferential corrosion at or near welds between structural tubular joints with resultant increased concentration of stress and reduction in fatigue life. An increased likelihood of corrosion fatigue problems also arises in this situation [4].

Most platforms are welded steel tubular 'space frames' piled to the sea bed but several steel reinforced concrete gravity-based platforms have also been constructed. Fixed offshore platforms supported by welded tubular jackets are in turn supported by foundation piles driven into the seabed. Normally the piles have no designed corrosion allowance and will require cathodic protection. The jacket carries ancillary steelwork such as mud mats, grout lines, monitoring conduits, temporary or permanent buoyancy chambers, temporary or permanent pile guides, boat bumpers and construction and installation steelworks, e.g. walkways, pad-eyes, valves and spindles etc. All of these should be considered as short- or long-term current demands on the cathodic protection system [4]. Cathodic current density demand to achieve cathodic protection in deep water is known to be greater than for warmer, near-surface waters [7].

3.3.9 Application

Steel

In quiescent seawater, the general corrosion rate of carbon steel and cast iron is 0.1 mm per year. However, cast iron and carbon steel can also undergo increased rates of corrosion under localised attack. General corrosion also increases as the seawater flow rate increases. Austenitic cast iron contains nickel, so it has a lower corrosion rate, typically 0.02 mm per year in quiescent seawater. When steels and irons corrode in seawater, the corrosion rate gradually decreases because the corrosion products restrict diffusion of fresh water to the metal surface. If the dissolved oxygen is maintained at ≤ 20 ppb, the corrosion of carbon steel is low [1].

Steels can undergo pitting to several times the depth of general corrosion under quiescent and flowing conditions. Hence, pitting corrosion is more likely to lead to leaks in carbon steel pipes. Carbon steel and cast irons do not usually develop SCC in seawater. Although austenitic cast irons have a lower general corrosion rate in seawater than grey cast iron, they are susceptible to chloride SCC, particularly in warm seawater [1]. Carbon and low-alloy steels are the most widely used materials in the marine environment, for both structural components and pressure-retaining applications. Table 3-2 lists some of the major applications.

Type	Alloy	Application
Structural	Carbon steel and cast iron	Platforms, jackets, ship hulls, vessels, piling and sheeting, towers, bridges, lock gates, gratings, ladders, cranes, lifts, and loaders
Pressure-containing	Carbon steel, low-alloy steels, cast iron, and austenitic cast iron	Piping, vessels, pumps, and valves

Table 3.3-2 Typical carbon steel and cast iron applications in marine environment [1].

Stainless steels provide a wide range of strengths and corrosion resistance in seawater environments. Some have limitations or require cathodic protection (CP); others have been developed to a sophisticated level and have extremely high corrosion resistance in seawater. The degree of alloying, temperature, seawater flow, oxygen levels and chlorination can all influence the performance of stainless steel. As chromium is added to carbon steel, the corrosion rate in a marine environment decreases until the chromium content has reached 12-14% [1].

Stainless steels have negligible general thinning in seawater because of a protective, predominantly chromium oxide film that forms immediately on their surface upon exposure to air. Oxygen levels present in seawater normally allow the film to repair itself if damaged. Under certain conditions in environments containing oxygenated chloride, the protective surface film on stainless steels can break down locally, leading to pitting, crevice corrosion, or chloride stress corrosion cracking (SCC) [1].

Pitting of stainless steels is usually seen in welds used beyond their service limits, or in the weld/heat-affected zone of poorly fabricated joints. Typical areas for crevice corrosion are found beneath O-rings, flange faces under gaskets and threaded connections. Stainless steels become more resistant to crevice corrosion if they are exposed to a less corrosive environment for some time before contact with a more aggressive environment [1].

More recently investigations have been performed on the effect of hydrostatic pressure in NaCl solutions on the corrosion behaviour of Fe–20Cr alloy, Ni–Cr–Mo–V high strength steel and nickel. Investigations were performed on the details of the pit corrosion mechanism and it was found that the corrosion susceptibility increases in the presence of a higher hydrostatic pressure [7].

In a further study regarding Ni–Cr–Mo–V high strength steel it was found that with the increase of hydrostatic pressure, the pit growth rate parallel to the steel surface increases and that the coalescence rate of neighbouring pits was promoted. Therefore it took shorter time to complete the evolution from wide-shallow shape pits to uniform corrosion as a result of the interaction between electrochemical corrosion and elastic stress [7]. Table 3-3 provides examples of how stainless steels are used in marine environments.

Conditions	Alloy type	Applications
Marine atmospheres	UNS S31600 (316)/ UNS S31603 (316L); Superduplex	Instrumentation tubing, electrical connectors, instrument housings, rebar in concrete, handrails, cable trays, platform module cladding, fasteners, and boat hardware
Seawater with galvanic protection	UNS S31600 (316)/ UNS S31603 (316L); UNS S32205 (2205)	Tube sheets, hull-mounted equipment, pump impellers, valves, stems and trim, fasteners for Al and steel, and pump shafts
	Lean duplex Duplex	Thermal desalination plants Subsea flow lines handling wet CO_2 and instrumentation tubing
	Precipitation-hardened grades	Special fasteners
Seawater without galvanic protection	UNS N08904 (904L)	Pipes, trays, and spray heads in thermal desalination plants
	6% Mo	Power plant condensers, condenser tubing, firewater, ballast and seawater pipes, pumps, valves, and reverse osmosis (RO) desalination
	Superduplex	High-pressure oilfield injection pumps, seawater and firewater pumps, shafting, propellers, retractable bow plane systems, seawater piping and valves, fasteners, heat exchangers (tubes and plates), umbilicals, and RO desalination piping
	Superferritics	Power station condenser tubing
Deaerated brines	UNS S31600 (316)/ UNS S31603 (316L); Duplex	Desalination flash chamber lining and water injection tubing

Table 3.3-3 Typical stainless steel applications in marine environment [1].

Aluminium

Aluminium alloys are favoured for uses for which their high strength-to-weight ratio, as well as a high corrosion resistance, are particular advantages. The corrosion rate of aluminium increased when increasing the hydrostatic pressure, in prevalence as an effect of increasing in localized corrosion; deeper pits were formed on 6061 T6 aluminium alloy as well, but generalized corrosion of this alloy decreased due to the formation of a Mg–Al oxide layer, which was more protective than aluminium hydroxides.

To round up the main results about general corrosion: the effects of depth were either negligible or in the order of reducing the consumption rates with the exception of aluminium alloys which were detrimentally affected. The typical pitting and crevice corrosion of aluminium in seawater were more severe at depth than at the surface.

In figure 3-25 two examples of aluminium alloy specimens as retrieved from the sea after 12 months of exposure are shown: 6082 T6 alloy showing typical pitting corrosion of aluminium alloys (left); 6082 T6 hard anodized alloy (right). In the latter case corrosion products affect only the margins where the surface treatment is weaker. While at atmospheric pressure the bayerite (Al(OH3)) is the main component of the corrosion layer of the 6000 series aluminium alloys, the pseudo bohemite (AlO(OH)) is the prevalent one at high hydrostatic pressure and the presence of magnesium compounds becomes very noticeable.

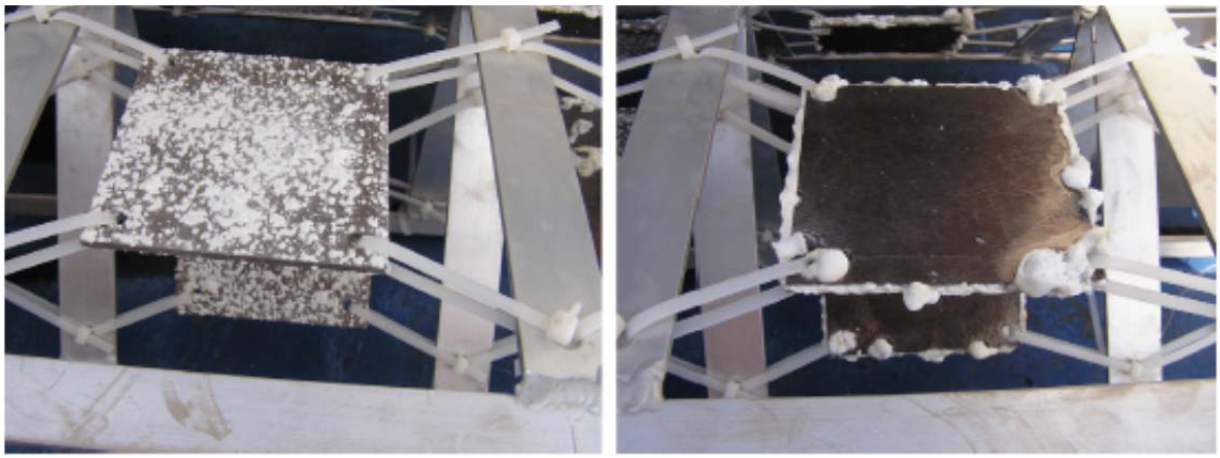

Figure 3.3-25 Examples of aluminium alloy specimens as retrieved from the sea after 12 months of exposure at a depth of about 3350 m within the KM3NeT framework. Left: Al 6082 T6 alloy showing typical pitting corrosion of aluminium alloys. Right: Al 6082 T6 hard anodized alloy, corrosion products affects only the margins where the surface treatment is weaker.

Contrary to mild steel, a protective oxide passive film is formed on sea water immersed aluminium alloys. In general, oxidizing conditions favour the preservation of this passive film, while reducing conditions destroy it. Chloride ions are particularly aggressive in destroying this passive film. Deep-sea lower DO and higher salinity with respect to shallow water favour typical pitting and crevice corrosion of aluminium alloys. Increasing hydrostatic pressure was found to be a further detrimental factor for aluminium pitting in sea water. However generally speaking, from in situ experiments increasing hydrostatic pressure was not found to be an influencing factor for corrosion of metals and alloys in a deep-sea environment.

3.4 ACID SULPHATE SOIL (ASS)

3.4.1 Fundamentals of corrosion of metals in soil

In general the most corrosive soils contain large concentrations of soluble salts, especially in the form of sulphates, chlorides, and bicarbonates which may be characterized as very acidic (low pH) or highly alkaline (high pH). The corrosion mechanism of ferrous and other metals in soils is essentially electrochemical of nature. For corrosion to occur there must be a potential difference between two points that are electrically connected in the presence of an electrolyte. Under these conditions a current will flow from the anodic area through the electrolyte or soil to the cathodic area and then through the metal to complete the circuit. The anodic area becomes corroded by the loss of metal ions to the electrolyte.

Clayey and silty soils are characterized by fine textures, high water-holding capacity and, consequently, by poor aeration and poor drainage. They are also prone to be potentially more corrosive than soils of coarse nature such as sand and gravel in which there is greater circulation of air. Buried metals corrode significantly by the process of differential aeration and sometimes by bacterial action. Corrosion by differential aeration may result from substantial local differences in type and compaction of the soil or variations in the oxygen or moisture content resulting thereof. Such a phenomenon is generally associated with fine-grained soils. Bacterial corrosion is associated with the presence of anaerobic sulphate-reducing bacteria that reduce any soluble sulphates present in the soil to sulphides.

Although most chemical elements and their compounds are present in soil, only a few exert an important influence on corrosion. In areas of high rainfall, the passage of time has resulted in the leaching of soluble salts and other compounds rendering these soils generally acidic. In arid locations soluble salts are brought to the upper soil layers through capillary and evaporative processes, causing the soils to be generally alkaline.

3.4.2 Acid Sulphate Soil

Acid sulphate soil is the common name given to sediments and soils containing iron sulphides that, after exposure to oxygen (drying) and rewetting generate sulphuric acid. The majority of acid sulphate sediments have formed by natural processes in recent geological time (the last 10,000 years). The conditions of their formation usually limit the occurrence of these soils to low lying parts of coastal floodplains, rivers and creeks. Acid sulphate soils are generally blue-grey to greenish-grey clay or blue-grey sandy clay deposits, often mottled, occurring in low lying coastal lands or floodplains of tidal creeks. Generally the acid sulphate soil deposits are covered by a layer of alluvial soil, which varies in thickness depending on factors such as the frequency and intensity of floods and human disturbance.

Acid sulphate soils contain pyrite (iron sulphide). When this type of soil is disturbed and the pyrite is exposed to air and water it generates sulphuric acid. The acidic leachate reacts with clay to release minerals/elements and/or contaminants such as aluminium and a red iron hydroxide precipitate. The drainage from acid sulphate soil lands can create conditions which are totally toxic to aquatic and terrestrial life. The presence of potential acid sulphate soil is an important consideration when developing a site with any structures that contain steel or concrete. Without some form of management, it is likely that these structures will deteriorate over time as the acid from the soil will cause structural damage.

Pyrite (FeS2) containing soils may become extremely acidic (pH<4) due to the oxidation of pyrite into sulphuric acid (H2SO4). In its simplest form this chemical reaction is as follows:

- $2\ FeS_2 + 9\ O_2 + 4\ H_2O \rightarrow 8\ H+ + 4\ SO_4^{2-} + 2\ Fe(OH)_3$ (solid)

In general there are two types of acid sulphate soils :

1) Potential acid sulphate soils: the iron sulphides are contained in a layer of waterlogged soil. This layer can be clay, loam or sand and is usually dark grey and soft. The water prevents oxygen in the air reacting with the iron sulphides. This layer is commonly known as potential acid sulphate soil (PASS) since it has the potential to oxidise to sulphuric acid.

2) Actual acid sulphate soils: when the iron sulphides are exposed to air and produce sulphuric acid they are known as actual acid sulphate soils. The soil itself can neutralise some of the sulphuric acid. The remaining acid moves through the soil, acidifying soil water, groundwater and eventually surface waters.

Sulphuric acid produced by acid sulphate soils corrodes concrete, iron, steel and certain aluminium alloys. It has caused the weakening of concrete structures and corrosion of concrete slabs, steel fence posts, foundations of buildings and underground concrete water and sewerage pipes.

Figure 3-26 An example of where acid water derived from acid sulphate soils has corroded concrete.

3.4.3 Speculation

Based on the articles covered in this section, the most detrimental effect of acid sulphate soil is in the coastal and inland areas and in deep sea the effect of ASS is less. This is because of the exposure to oxygen in the air as it was described before. We can speculate that for deep sea structures, because of the lack of oxygen and the presence of low temperatures compared to coastal regions, the immunity of structures is higher. However according to figure 3-6 the amount of dissolved oxygen in the deep layers of the North Atlantic ocean is higher than in surface waters which implies a different conclusion.

On the other hand, Actual acid sulphate soils (AASS) can change the pH value of the soil (pH<4) and referring to section 3.1, the average pH value in deep water has a value of 7.5 to 7.7 which is not significant and does not directly affect corrosion rates except for that of aluminium. So based on these estimations, if there are AASS in the deep sea, then the pH value can affect the corrosion rate of materials on the ocean floor; however the rate can be different for different materials. As is depicted in figure 3-27 and 3-28, the corrosion rate of iron in water at room temperature for pH<4 is higher than for other values but for aluminium the pH value for the increment of corrosion rate is pH<2; however for the deep sea environment all these values can be different.

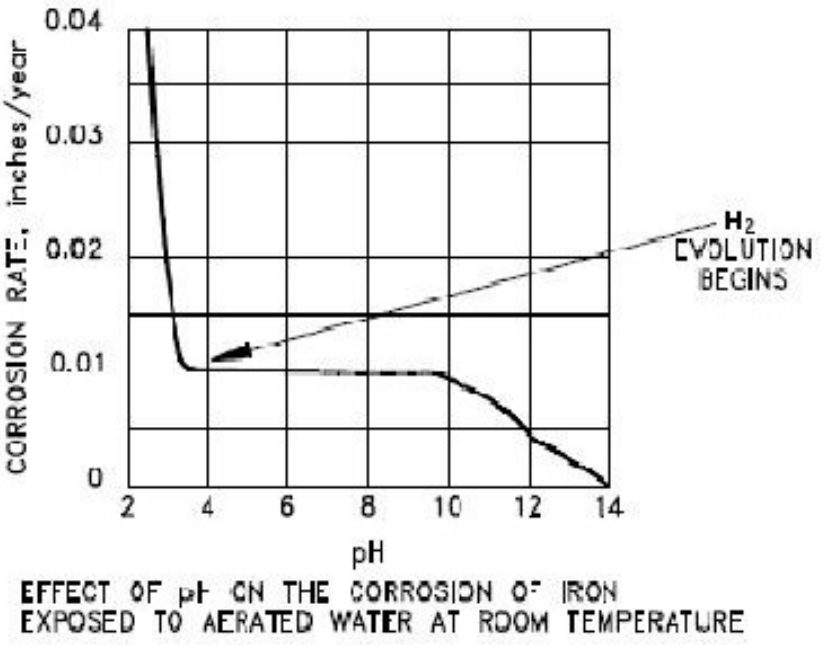

Figure 3-27 Effect of pH on Iron Corrosion rate in water.

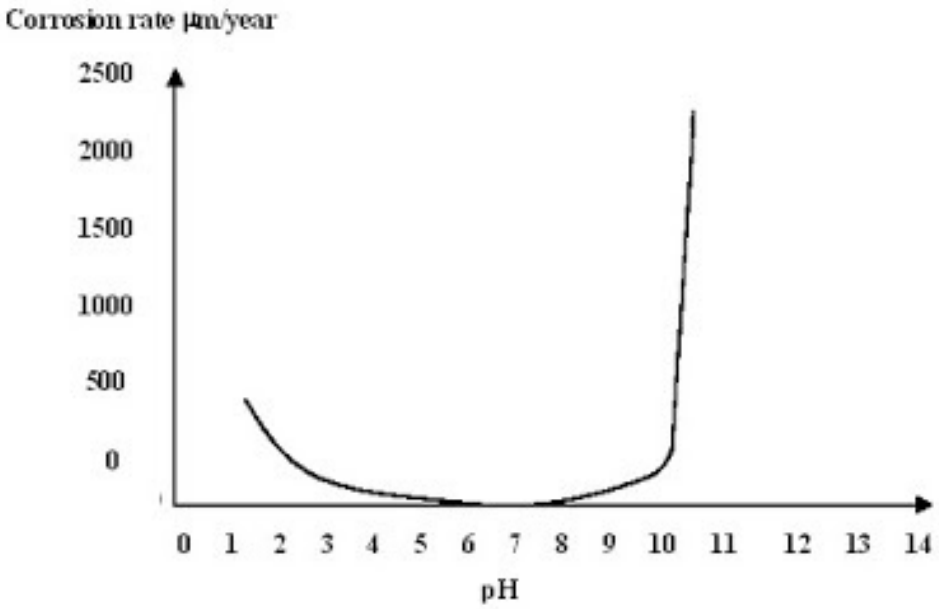

Figure 3-28 Effect of the pH value on aluminium corrosion rate in water.

3.5 Conclusion

Several studies conducted on corrosion of metals and alloys in the deep sea environment are confidential (e.g., performed in the framework of defence-related activities) and so not available in the public domain. Furthermore, the deep sea is characterized by total absence of sunlight, high hydrostatic pressure and low water temperature so because of its complex environment experiments are expensive and technically demanding. Therefore the available literature on this topic is scarce and the comparison of the results is difficult because they are influenced by experimental features and local effects. Nonetheless some main issues can be highlighted. The concentration of dissolved oxygen in seawater, low sea water temperatures and microbial communities seem to exert a major influence on deep sea corrosion of metals and alloys. Lastly, it should be noted that the deep sea is not a uniform environment and local conditions can be very different.

Different experiments in different places have been conducted on corrosion rate of carbon steel, mild steel, stainless steel, copper, brass and aluminium alloys. Hydrostatic pressure did not greatly influence the corrosive behaviour of metals tested but temperature has a great influence on the corrosion rate. Very dependent on the local situation stainless steel in the deep sea can suffer severe corrosion: pitting corrosion, galvanic corrosion,

crevice corrosion and corrosion by stray currents. In coastal waters, stainless steel is severely subject to pitting corrosion. The deep sea results for mild steel compared to shallow water is four times lower (about 0.35 mm per year to 0.08 mm per year). In general the corrosion rate of metals decreases in the deep sea due to lower dissolved oxygen and lower temperatures, except for aluminium. Contrary to mild steel, a protective oxide passive film is formed on sea water immersed aluminium alloys. In general, oxidizing conditions favour the preservation of this passive film while reducing conditions destroy it. Chloride ions are particularly aggressive in destroying such passive films. Deep sea lower DO and higher salinity with respect to shallow water favour typical pitting and crevice corrosion of aluminium alloys. In many situations seawater resistant aluminium performs very well in the deep sea.

The change of pH with depth does not directly affect the corrosion of metals and alloys, but sea water carbon dioxide affects the rate of corrosion by determining whether or not a protective layer (e.g. of calcium carbonate) will precipitate on all metal and alloy surfaces. Seawater in the deep ocean environmental zone is generally under-saturated with respect to carbonates, which reduces the likelihood of forming protective calcareous layers. Cathodic protection and epoxy coating systems have proved to be effective in deep sea environments..

3.6. Recommendation

In the short span of time devoted to this general research the primary and general information about marine corrosion have been discussed by means of different books and articles. However for better depth of understanding, the absolute and further research based on experimental tests can be fulfilled. Throughout this research, it was tried to put highlights on deep sea corrosion, however because of the very complicated nature of the deep sea there are not so many resources and references in this area. One of the obscure and unknown characteristics of the deep sea is the effect of acid sulphate soil on the corrosion rate of structures. As described in this report the hydrostatic pressure does not have a significant effect on corrosion rate so by providing other variables similar to those in the deep sea, the deep marine environment can be simulated in the lab and experimental tests regarding the effect of acid sulphate soil on corrosion rate can be executed. ASS can change the pH value of the soil (pH<4) and ocean water has a pH value in the range of 7.5 to 8.2 . In such research it can be discovered how different pH values in an environment affect the corrosion rate of different metals.

3.7. References

[1] Carol Powell, Roger Francis, The corrosion performance of metals for the marine environment, 2012.

[2] ASM handbook Vol 13 Corrosion, 1992.

[3] E.Bardal, Corrosion and protection, 2003.

[4] Kenneth A Chandler, Marine and offshore corrosion, 1985.

[5] Gaute Svenningsen, Corrosion of Aluminium Alloys, Department of Materials Technology, 7491 Trondheim, Norway.

[6] P. R. Roberge, Handbook of corrosion engineering, New York: Mc Graw Hill Handbook, 1999.

[7] Pierluigi Traverso, Elisa Canepa, A review of studies on corrosion of metals and alloys in deep-sea environment, Ocean Engineering 87(2014) 10-15.

[8] U.K. Chatterjee ,S.K. Bose, Environmental degradation of metals, 2001.

[9] Martin Smith & Colin Bowley, In situ protection of splash zone, 2002.

[10] CIVIL ENGINEERING LABORATORY (NAVY), CORROSION OF METALS AND ALLOYS IN THE DEEP OCEAN, 1976.

4. Forecast of the chemical/physical and biological environment of the Rainbow vent area – a literature study

(NIOZ - M.S.S. Lavaleye & G.C.A. Duineveld).

A short overview of the physical, chemical and biological environment extracted from literature is given below. It includes a brief description of the geological features of the area. The physical parameters will include current speed and direction, temperature and particle flux. The description of chemical parameters will focus on fluids and composition of the particles emitted by the hydrothermal vents and SMS deposits. In terms of biology a description of the benthic environment of the area is given.

GENERAL AND GEOLOGICAL FEATURES

The Rainbow vent field was discovered in 1997 with the manned submersible Nautile during the FLORES cruise with RV L'Atlante, and is situated at $36^0$14'N at a depth of 2275m on the west flank of a relatively small mountain ridge in the discontinuity between two segments of the MAR and it produces a strong and persistent hydrothermal plume. It is one of the most active hydrothermal vent fields discovered in the North Atlantic with more than 30 groups (Fig. 4.1) of small but extremely active black smokers spread over 15000m^2 most without visible fauna (Desbruyeres et al. 2000 & 2001). Some diffusive vents are also present, located 25–100 m from the black smokers with small mussel beds and shrimp swarms (Desbruyères et al. 2001). The most active smokers are located at the western and eastern ends of the hydrothermal field. The west zone has the roughest relief, while the sites at the east are located on a sedimentary plateau. The highest developed sites are situated in the centre, but are either active or extinct chimneys. Because of the great number of inactive chimneys, and the change in activity of individual vents within an 1-year period, this vent field has an unstable character in time and place, which is unusual for a slow spreading ridge (Desbruyeres et al. 2000). The Rainbow hydrothermal field has the strongest plume of its kind known on the Mid-Atlantic Ridge (German et al. 1996; Fouquet et al. 1997). The entire vent field is located in an ultramafic environment, and only some old basalt exists about 1 km east of the active vents (Fouquet et al. 1998) . The rocks consist mostly of coarse and fine grained, porphyritic and non-porphyritic serpentinites (Fouquet et al. 1998). During the MoMARDREAM cruises (2007, 2008)
extensive rock sampling throughout the massif that constrains the geological setting of hydrothermal activity in the Rainbow area has been done. The lithology is heterogeneous with abundant serpentinites surrounding gabbros, troctolites, chromitites, plagiogranites, and basalts (Andreani et al. 2014). There is little evidence of recent volcanic activity at Rainbow (Desbruyeres et al. 2000). Dating of shells on the basis of ^{14}C of vesicomyid shells of a *Phreagena* species, found at 2.5 km east of the active vent field, suggest that hydrothermal activity in this area dates back to at least 25.5 kyr (Lartaud et al. 2010).

PHYSICAL ENVIRONMENT

Currents - Khripounoff et al. (2001) deployed several moorings at and near the Rainbow vent field (see Fig. 4.2). The results showed that the residual near bottom current is directed northwards with a residual current speed between 1.1 and 4.5 cm/s. According to the former paper the tidal currents at Rainbow are semi-diurnal, and had a low mean speed of 6 cm/s with a maximum of 19 cm/s (Table 4.1).

Temperature - although the blacksmokers of the Rainbow vent field produce the strongest plume at the MAR and the water that is emitted is very hot (360^0C), the high temperature of the plume is very quickly dampened by the ambient cold deep-sea water (3.7^0C). This is obvious from the results of a mooring placed at 2m away from one of the vents (Khripounoff et al. 2001). It measured the temperature at 3.5 mab, and these temperatures never reach more than $10\ ^0$C (Fig. 4.3). The mooring at 500m away from the vent did not record a temperature anomaly that could be linked to the hot vent.

Particle flux- the total mean particle flux measured with the sediment traps of long-term moorings varied little between moorings (11-25 mg/m^2.d), and showed the normal seasonal changes (Khripounoff et al. 2001). Meaning that the flux in winter is very low, and peaked in June due to the spring bloom in the surface waters. In his mooring (M500) at 500 m N of the vent field the plume of the black smokers could still be observed at 150 to 300m a.b. (Table 2). This was determined by the significantly higher sulphur, iron and copper concentrations of the particles in comparison to the M.Pelagic mooring samples (Fig. 4.2). Also according to Khripounoff et al. (2001) the particle flux near the vent area (6.9 g/m^2.d) is 500 times higher than at a nearby pelagic site not under the influence of the vent. However the variation in the vent particle flux was quite large within a period of 16 days. It varied from 0.28 to 19.2 g/m^2.d. In comparison to the other well-known vent areas on the Mid Atlantic Ridge the particle flux caused by the Rainbow vents is significantly higher (Table 4.3). The shallower vents Lucky Strike (1600m depth) and Menez-Gwen (850m depth) do not have black smokers but emit translucent fluids with low particle content, respectively 0.26 g/m2.d and 0.64 g/m2/d, which is on average 10 times lower than at Rainbow (Khripounoff et al. 2000; Desbruyeres et al. 2001).

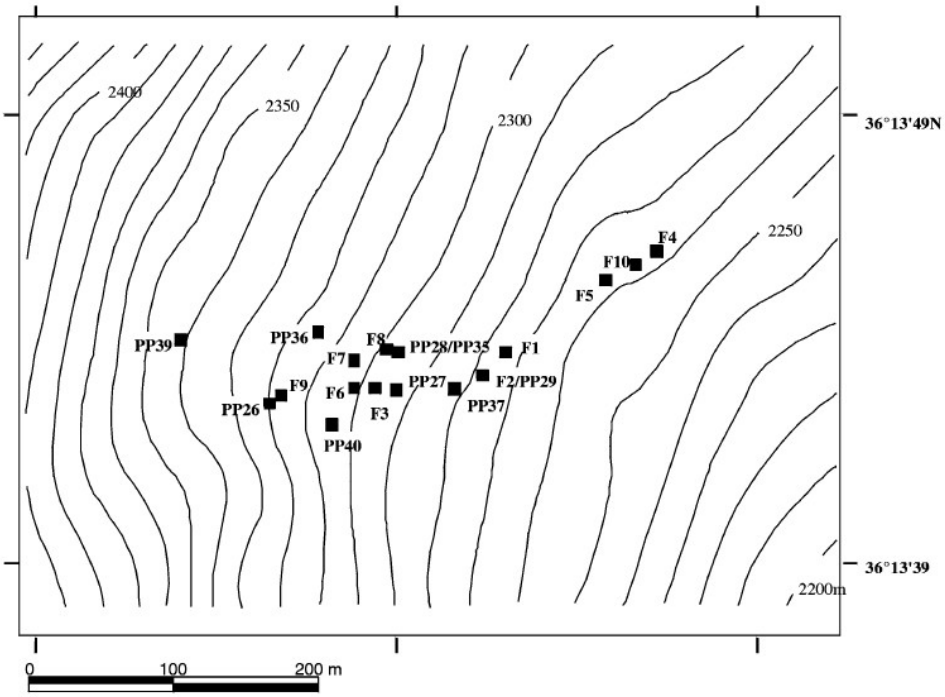

Figure 4.1. Map of the Rainbow vent field with the distribution of the active vents (from Desbruyeres et al. 2001)

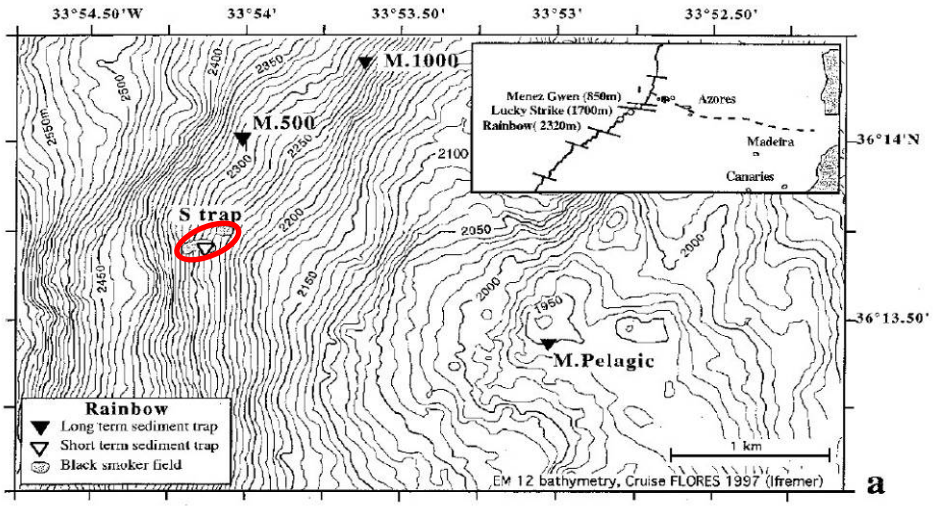

Figure 4.2. Map of the surroundings of the Rainbow vent field with the position of the 4 moorings of Khripounoff. The vent field itself is situated within the red circle. Source: Khripounoff et al. 2001.

Table 4.1. Current data obtained with current-meters fixed on the short (Mooring S) and the long-term moorings (M Pelagic, M500 and M1000). Source: Khripounoff et al. 2001

Moorings	Duration (days)	Altitude (a.b.)	Residual current direction	Mean speed	Max. speed	Residual current speed
Mooring S	16	1.5 m	N330°	9 cm s^{-1}	19 cm s^{-1}	2.9 cm s^{-1}
M Pelagic	304	210 m	N310°	5 cm s^{-1}	14 cm s^{-1}	1.1 cm s^{-1}
M500	304	310 m	N005°	6 cm s^{-1}	17 cm s^{-1}	3.1 cm s^{-1}
M500	304	160 m	N020°	6 cm s^{-1}	18 cm s^{-1}	4.5 cm s^{-1}
M1000	304	310 m	N355°	6 cm s^{-1}	17 cm s^{-1}	1.5 cm s^{-1}
M1000	304	160 m	N355°	6 cm s^{-1}	18 cm s^{-1}	3.4 cm s^{-1}

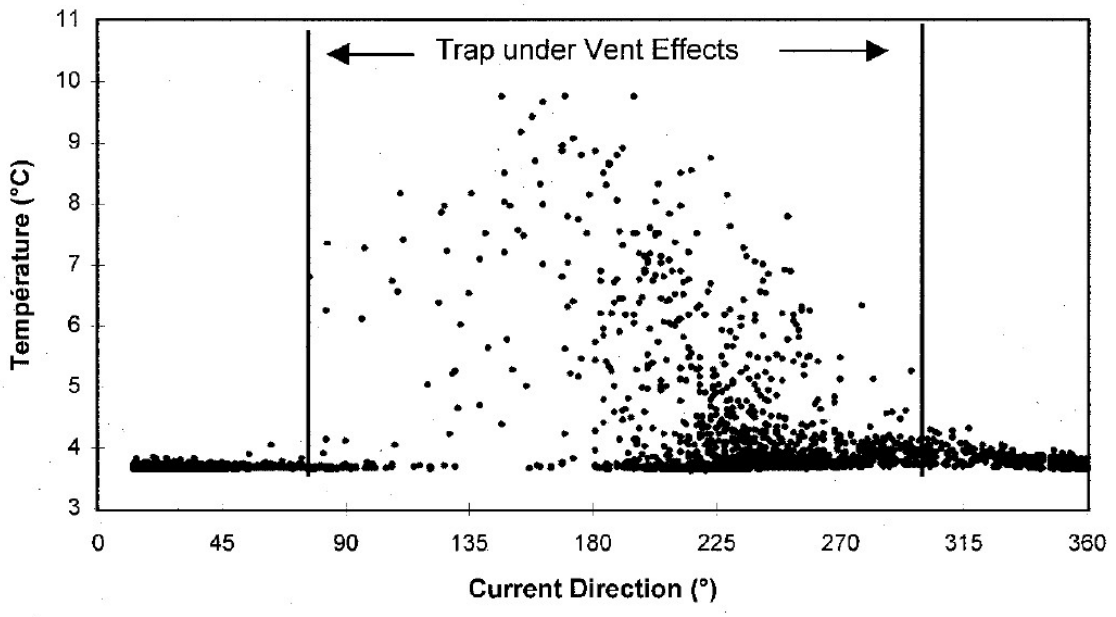

Figure 4.3. Changes in temperature in relation to current direction over 14 days at 3.5 m above the bottom and 2 m off an active vent of the Rainbow vent field. Source: Khripounoff et al. 2001

Table 4.2. Mean particle flux sampled in large traps (Long-term-moorings). Source: Khripounoff et al. 2001

	M Pelagic	M 500		M 1000	
	200 m a.b.	150 m a.b.	300 m a.b.	150 m a.b.	300 m a.b.
Mass flux (mg m^{-2} d^{-1})	11.2	11.3	10.6	17.5	25.0
Organic C. (mg m^{-2} d^{-1})	0.62	0.47	0.66	0.82	1.28
Inorg. C. (mg m^{-2} d^{-1})	1.32	0.63	1.02	1.43	2.10
Sulphur (mg m^{-2} d^{-1})	0.04	0.94	0.10	0.05	0.06

CHEMICAL COMPOSITION OF THE FLUIDS AND PARTICLES EMITTED BY THE VENTS

The composition of the fluids emitted by the vents are influenced by phase separation processes at these depths, the temperature and by the nature of the basement rock, and therefore here consist of metal enriched brines with a gas-enriched vapour phase (Desbruyeres et al. 2000). The fluids have a pH between 2.8 and 3.1. The chlorinity is more than 750mmol/kg, with silica at about 7mmol/kg. The H_2S content is relatively low, but H_2 and CH_4 are very high especially in contrast to Lucky Strike (Table 4.3). The high figures for H_2 and CH_4 are affected by the serpentinization in the ultramafic rock of the slow spreading MAR (Fouquet et al. 1998, Desbruyeres et al, 2000). The fluid is strongly enriched with Mn, Fe, Co, Ni, Cu, Zn, Ag, Cd, Cs, Pb, Y, and rare earth elements (REE). REE and transition metal abundance (particularly Fe and Mn) is dramatically higher than in other MAR fluids. The abundance of trace element and REE enrichment is due to the greater solubility of these elements that is strongly favored by Cl-complexation at low-pH and high-temperature conditions (Douville et al. 2002).

Sulphides are still relatively high in the plume at 2km distance from the vent with levels up to 2.1 nmol L^{-1}, but levels below and above the plume were undetectable (Radford-Knœry et al. 2001). With help of calculations of the

sulphide removal rates, derived from experiments with Rainbow vent samples, it was estimated that the sulphide emitted by the Rainbow vent field will reach undetectable levels at 10 km distance downstream from the vent site, but presumable at a lower distance because plume dilution was not accounted for in these estimations. The removal of sulphide is due to abiotic (oxidation by dissolved oxygen) and biotic (sulphide-oxidizing bacteria) reactions (Radford-Knœry et al. 2001).

Table 4.3. Comparison of temperature and chemical composition of the vent fluids between 7 different hydrothermal vents on the MAR. MG = Menez-Gwen, LS = Lucky Strike, Rb = Rainbow, BS = Broken Spur, T.A.G. = Trans Atlantic Geotraverse, SP = Snake Pit, Lg = Logatchev. Source: Desbruyeres et al. 2000.

Site	MG	LS	Rb	BS	T.A.G.	SP	Lg
T	265–284	152–333	360–365	356–364	270–363	335–356	>353
pH	4.2–4.8	3.5–4.9	2.8–3.1		2.5–3.4	3.7–3.9	<3.3
Si	8.2–11.2	9.1–17.5	6.9–8.0		18–22	18–20	7–8.2
Cl^-	360–400	410–540	>750	469	633–675	550-563	515–522
CO_2	17–20	8.9–28	<16		2.9–4.1	10.63	
H_2S	1.5–2	1.4–3.3	1–2.5	9.3	2.5–6.7	2.7–6.1	<1
CH_4	1.35–2.63	0.5–0.97	2.2–2.5	0.065	0.14–0.62	0.046–0.062	2.1
Fe	0.002–0.018	0.13–0.86	24	1.68–2.16	1.64–5.45	1.8–2.56	2.50
Mn	0.068	0.45	2.25	0.26	1	0.49	0.33

The particles emitted by the black smokers were characterized by a high concentration of sulphur (17.2% in the form of $CaSO_4$), iron (7%) and copper (3.5-5.5%) and a very low concentration of organic carbon (0.13%), inorganic carbon and silica (Table 4 and 5). The isotopic composition were 1.9‰ for $\delta^{15}N$ and -21‰ for $\delta^{13}C$. During the 16 days of the short mooring experiment there was hardly any variation in the chemical composition of the particles (Khripounoff et al. 2001).
Particles collected by the traps in the moorings further away showed normal back ground levels indicative for the oligotrophic part of the Atlantic Ocean. Only the trap at 150m a.b. in the mooring that was situated 500m north of the vent, the particles had a much higher sulphur, iron and copper signal. This clearly shows that the plume can still be detected at 500m distance. The trap in the same mooring but at 300m a.b. had slightly higher concentrations of sulphur and iron, from which it can be concluded that the plume can be traced in the vertical at least from 150 to 300m a.b. (Table 4.4). The sulphur concentrations in the particles are comparable to Menez-Gwen (18.2%) and higher than Lucky Strike (11%) (Desbruyeres et al. 2001).

TOTAL AMOUNT OF EXITING FLUID, CHEMICALS AND SMS DEPOSITS

German et al. (2010) estimated the total amount of hot water produced and exiting the total vent field of Rainbow. Based on the flux of Mn or CH_4 the amount was calculated at 400 and 450 L/s respectively. They also calculated the amount of different elements emitted by this vent system (Table 6). Iron (Fe) has by far the highest flux, followed by methane (CH_4), phosphor (P), manganese (Mn), copper (Cu), zinc (Zn) and Vanadium (V).
The abundance of the SMS deposits of the Rainbow vent area is estimated to be between 300,000-1,000,000 tonnes and is rated among the 14 largest out of 165 investigated SMS sites of the world oceans by Hannington et al. (2011). The chimneys and SMS deposits are enriched in Cu, Zn, Co and Ni in comparison to the Lucky Strike and Menez-Gwen (Fouquet et., 1997). The copper content of the SMS deposits can be up to 28 wt%, while the chimneys can have a Zn content of up to 5 wt% (Marques et al. 2006)

Table 4.4. Mean chemical composition (%) pf particles in the sediment traps of Kripounoff et al. (2001). The figures in a blue square indicate a strong depletion in comparison to the normal deep-sea back ground, while those within a red square show a strong increase. Source: Khripounoff et al. 2001.

(%)	S trap (Vent composition)	M500 150 m a.b. (Plume composition)	M500 300 m a.b.	M1000 150 m a.b.	M1000 300 m a.b.	M Pelagic 200 m a.b.
Organic C.	0.13	4.9	7.3	5.5	5.9	7.2
Inorganic C.	≈0	5.3	8.0	8.4	8.4	9.0
Phosphorus	0.45	0.8	0.3	0.21	0.5	0.2
Sulphur	17.2	13	0.90	0.31	0.35	0.31
Calcium	22.6	13.5	22.7	21.2	22.6	22.6
Iron	7.2	22.5	2	0.83	0.84	0.58
Copper	5.0	9.1	0.59	0.45	0.41	0.33
Silica	0.35	3.8	7.1	6.44	7.2	7.21

Table 4.5. Particle fluxes measured by sedimenttraps at 2m distance from 4 different hydrothermal vents on the MAR. Source: Desbruyeres et al. 2000.

Site	Location from the vent	Total flux mg m^{-2} d^{-1}	Organic C flux mg m^{-2} d^{-1}	Inorganic C flux mg m^{-2} d^{-1}	Total Nitrogen flux mg m^{-2} d^{-1}	Total S flux mg m^{-2} d^{-1}
TAG	2 m northward	9024.7	48.8	not detected	4.46	2733.7
	pelagic reference	11.3	0.49	0.95	0.05	0.2
Rainbow	2 m Southwest	6890	9.3	not detected	0.9	1171
	Pelagic reference	11.2	0.62	1.32	0.07	0.04
Lucky Strike	2 m southward	264.5	12.06	9.4	2.0	29.0
	Pelagic reference	7.7	0.55	0.75	0.09	0.07
Menez Gwen	2 m southward	704	11.26	not detected	0.85	126.7
	Pelagic reference	28.5	2.51	2.18	0.41	0.11

BENTHIC ENVIRONMENT

The special macrofauna community around hydrothermal vents is dependent on chemoautotrophic bacteria. These bacteria need the H_2S, CO_2 and CH_4 emitted by the vents as a source of carbon and energy, and the multicellular animals harvest these bacteria or live in symbiosis with them. In Rainbow no obvious concentrations of larger animals were detected around the main black smokers, which is in contrast to many of the other Atlantic hydrothermal vents. This may be explained by the fact that the fluids of hydrothermal vents also contain toxic substances like sulphides and heavy metals. In Rainbow the sulphide concentrations are rather low, but those of heavy metals are relatively high. The youngest and most active vents in the eastern and western part of the vent field are therefore nearly azoic. The surrounding hard substrates were non the less covered with a fairly dense cover of hydroids. In the eastern part the polychaete *Spiochaetopterus* sp. formed dense and patchy populations in sediments near the vents. In the west of the field relatively dense aggregations of shrimps were seen. The shrimps consists for the greater part of *Rimicaris exoculata*, especially in depressions between chimneys, but also two other species were found in lower abundance (*Mirocaris fortunata* on chimneys with low diffusion rates and *Chorocaris chacei*). No mussels were observed around the active vents, but at some diffusive vents, located 25–100 m from the black smokers, small mussel beds were present (Desbruyères et al. 2001). The mussel beds consist of *Bathymodiolus azoricus,* but these beds are smaller and with lower densities compared to Lucky strike and Menez-Gwen (Fouquet et al. 1998). The very high production of inorganic particles by the blacksmokers of Rainbow probably negatively affect the filtration of these mussels and also the growth of juveniles (Desbruyeres et al. 2000). Further some crabs (*Segonzacia mesatlantica*) and fish (*Lycenchelys* sp.) were observed along the active chimney walls and mussel beds. At the sediment covered parts ophiuroids, gastropods and pycnogonids occurred. A list of all the fauna of the Rainbow vent field is given by Desbruyeres et al. (2001), and contains 32 species so far. In Table 4.7 a comparison of the main megafaunal species of 7 vent communities along the MAR is shown. From this it can be concluded that shrimps (*R. exoculata*) prefer high mineral particle fluxes, high clorinity and high levels of metals, while mussel beds (*B. azoricus*) prefer low levels of metals and low mineral particle fluxes (Desbruyeres et al. 2000). Further, it was concluded by Desbruyeres et al. (2001) from a comparison of the species composition of the different MAR vent fields, that they have a low specific similarity (20-30%), and therefore can be better seen as distinct biogeographic islands than as a single biogeograpical province.

Table 4.6. Export fluxes from the Rainbow vent site. Source: German et al. 2010.

	Export Flux	Units
Heat	0.5	(GW)
Vent-fluid flux [CH4]	450	(Ls^{-1})
Vent-fluid flux [Mn]	400	(Ls^{-1})
^{3}He	7.6×10^{-9}	($mols^{-1}$)
CH_4	1.0	($mols^{-1}$)
Mn	0.9	($mols^{-1}$)
Fe	9.6	($mols^{-1}$)
Cu	0.11	($mols^{-1}$)
Zn	0.05	($mols^{-1}$)
Cd	5.2×10^{-4}	($mols^{-1}$)
Ag	1.1×10^{-4}	($mols^{-1}$)
Pb	4.5×10^{-4}	($mols^{-1}$)
P	0.94	($mols^{-1}$)
V	0.036	($mols^{-1}$)
Co	2.5×10^{-3}	($mols^{-1}$)
U	4.9×10^{-6}	($mols^{-1}$)
Y	2.6×10^{-4}	($mols^{-1}$)
La	1.2×10^{-4}	($mols^{-1}$)
Ce	4.9×10^{-5}	($mols^{-1}$)
Pr	2.4×10^{-5}	($mols^{-1}$)
Nd	9.6×10^{-5}	($mols^{-1}$)
Sm	1.8×10^{-5}	($mols^{-1}$)
Eu	1.1×10^{-5}	($mols^{-1}$)
Gd	1.9×10^{-5}	($mols^{-1}$)
Tb	3.3×10^{-6}	($mols^{-1}$)
Dy	2.0×10^{-5}	($mols^{-1}$)
Ho	4.3×10^{-6}	($mols^{-1}$)
Er	1.2×10^{-5}	($mols^{-1}$)
Tm	1.5×10^{-6}	($mols^{-1}$)
Yb	9.5×10^{-6}	($mols^{-1}$)
Lu	1.3×10^{-6}	($mols^{-1}$)

In the trap of the short term mooring of Kripounoff et al. (2001) hundreds of larvae belonging to the hydrothermal bivalve *Bathymodiolus azoricus* were collected, but numbers varied dramatically in this short time period of 16 days. Other larvae of benthic organisms belonged to polychaetes (families Spionidae, Hesionidae, Glyceridae, Syllidae, Poecilochaetidae, Polynoidae, Aphroditidae, Archinomidae, Ophelidae, Typhloscolecidae), gastropods (*Shinkailepas* and *Phymorhynchus*, both hydrothermal vent species), another bivalve, nematodes, ostracods, amphipods, tanaids, isopods, cirripeds, halacarids, ophiuroids and asterids. Further lots of holoplankton animals were found, especially copepods and euphausids. The high densities of bivalve larvae probably originate from a mussel bed at 120m SW of the trap. In June 1997 and Aug 1998, however, hardly any larvae were found. In the trap at 150m a.b. and 500m north of the vent still typical hydrothermal vent animals, like *B. azoricus* and the polychaete family Archinomidae were found. The trap at 300m a.b. only had a few larvae of *B. azoricus.* Common holoplankton, such as copepods, were found to be more abundant near the vent then further away. This shows that they are highly tolerant to plume chemicals (in contrast to e.g. Euphausiacea) and maybe were attracted by local nutrient enrichment. The abundance of free-living bacteria fed by the plume is the common explanation for this increase in plankton biomass (McCollom 2000).
Isotope signals of the vent mussels and shrimps suggest that the mussels in contrast to shrimps did not directly consume organic particulate material of the vents (Colaço et al. 2001). The numbers of non-hydrothermal species around hydrothermal vents, the so-called penetrating species, are the highest in the shallower vent fields like Lucky Strike and Menez Gwen, and lower in Rainbow and Snake Pit. This difference is probably due to a much lower fluid toxicity (sulphide and heavy metals) in the first two vent fields (Desbruyeres et al. 2000)

Table 4.7. Description of the main hydrothermal vent communities from 7 hydrothermal vent fields on the MAR. Number in square brackets indicate the abundance of the megafauna species: [1] = rare, [2] = patchy, [3] = common, [4] = dominant, [5] = exclusive. Source: Desbruyeres et al. 2000.

	Dominant species on chimneys walls	Dominant species on chimneys bases	Dominant species on surrounding blocs within active area	Dominant accompanying species	Dominant carnivorous	Dominant peripheral species
Logatchev (Gebruk et al., 1997a; Gebruk et al., 1997b)	*Bathymodiolus* cf. *puteoserpensis* [3] + *Branchipolynoe seepensis* [3] *Rimicaris exoculata* [2]	*Bathymodiolus* cf. *puteoserpensis* [3] + *Branchipolynoe seepensis* [3]		*Ophioctenella acies* [3] *Mirocaris hilgyki* [3]	*Segonzacia* sp.	Actiniaria gen. sp. [2]
Snake Pit (Segonzac, 1992; Segonzac et al., 1993)	*Rimicaris exoculata* [4]	*Chorocaris chacei* [2] *Alvinocaris markensis* [1]	*Bathymodiolus puteoserpensis* [1] + *Branchipolynoe seepensis* [1] *Ophioctenella acies* [1]	*Pseudorimula midatlantica* *Peltospira* sp.	*Segonzacia mesatlantica* [2] *Paclychaus thermophilum* [2]	*Parasicyonis legolfi* [2] *Candelabrum serpentarii* [1] *Charistopterus* sp. [1]
TAG (Gebruk et al., 1997a; Van Dover, 1995)	*Rimicaris exoculata* [4]	*Chorocaris chacei* [2] *Alvinocaris markensis* [1]	*Ophioctenella acies* [1]	*Stygiopontus pectinatus*	*Segonzacia mesatlantica* *Paclychaus thermophilum* [1]	*Charistopterus* sp. *Parasicyonis* ? sp. [3] *Munidopsis* sp.
Broken Spur (Murton et al., 1995; Gebruk et al., 1997a)	*Rimicaris exoculata* [2]	*Mirocaris fortunata* [1]	Spionid polychaetes [2] *Bathymodiolus puteoserpensis* [1] & *Bathymodiolus azoricus* *Branchipolynoe seepensis* [1] *Ophioctenella acies* [2]		*Segonzacia mesatlantica* [2]	*Charistopterus* sp. Actiniaria gen. sp.
Rainbow (Desbruyères et al., subm)	*Rimicaris exoculata* [3] *Mirocaris fortunata* [2]	*Mirocaris fortunata* [2] *Chorocaris chacei* [1]	*Bathymodiolus azoricus* [2] + *Branchipolynoe seepensis* [1]	*Amaga luzi*	*Segonzacia mesatlantica* [2]	*Charistopterus* sp. [1] *Prionospio* sp. [2]
Lucky Strike (Desbruyères et al., subm) (Van Dover et al., 1996)	*Bathymodiolus azoricus* [5] + *Branchipolynoe seepensis* [5] *Chorocaris chacei* [2] *Mirocaris fortunata* [3]	*Bathymodiolus azoricus* [5] + *Branchipolynoe seepensis* [5] *Mirocaris fortunata* [3]	*Bathymodiolus azoricus* (young specimens) [3] + *Branchipolynoe seepensis* [3]	*Amathys luzi* *Lepetodrilus* n. sp.	*Segonzacia mesatlantica* [2]	*Candelabrum phrygium* [2]
Menez Gwen (Desbruyères et al. subm) (Colaço et al., 1998)		*Bathymodiolus azoricus* [3–5] according to the vent sites *Mirocaris fortunata* [2–3] *Chorocaris chacei* [1]	*Bathymodiolus azoricus* [3–5] according to the vent sites *Mirocaris fortunata* [2–3] *Chorocaris chacei* [1]	*Protolyra vahvatnikae*	*Chaceon affinis* [2] *Segonzacia mesatlantica* [1]	*Eudendrium* sp. *Gravieria alticola*

REFERENCES

Andreani M et al. (2014) *Geochemistry, Geophysics, Geosystems* 15: 3543–3571.
Colaço A et al. (2001) *Deep-sea Research I* 49: 395-412.
Desbruyères D et al. (2000) *Hydrobiologia*, 440: 201–216.
Desbruyères D et al. (2001) *Deep-Sea Research I* 48: 1325–1346.
Douville E et al. (2002) *Chemical Geology* 184: 37-48.
Fouquet Y et al. (1997). *Eos Transactions American Geophysycial Union*, 78: 832.
Fouquet Y et al. (1998). *INTERRIDGE News* 7: 24-28.
German CR et al. (1996). *Geophysical Research Letters* 23: 2979–2982.
German CR et al. (2010) *Deep-Sea Research* I 57: 518-527.
Hannington M et al. (2011) *GSA data repository* 2011342: 1-20.
Khripounoff A et al. (2000) *Journal Marine Systems* 25: 101–118.
Khripounoff A et al. (2001) *Journal of Marine Research* 59: 633–656
Lartaud F et al. (2010) *Geochemistry Geophysics Geosystems* 11: 1-17
Marques AFA et al. (2006) *Mineralium Deposita* 41: 52-67.
McCollom TM (2000) *Deep-Sea Research* I 47: 85-101.
Radford-Knœry J et al. (2001) *Limnology and Oceanography* 46: 461-464.

5. **Preparation deployments**

Sets of test materials, both metals and plastics (see Table 5.1) were supplied by the industrial partners. Most test materials consisted of plates with sizes 100x40x6 mm (l x w x t). For easier fixing these test materials to the lander frames they were assembled together in one aluminum frame and isolated from each other and from the aluminum frame by Delrin holders (NIOZ made). The alu frames were attached to the bottom landers (BOBO, ALBEX) at a height of 4 m (BOBO) and 1-2m (ALBEX) above the bottom (Fig. 5.1).

Table 5.1. Sample list of materials attached to 4 landers and a mooring (see Fig. 7), which were deployed during the expedition for one year in the Rainbow area.

			frame 1	frame 2	frame 3	frame 4	Mooring (frame 5)
#	materials in order	marking	mass 1 (gram)	mass 2 (gram)	mass 3 (gram)	mass 4 (gram)	mass 5 (gram)
1	RVS 316	RVS 316	183.1	185	185.1	184.8	183.7
2	duplex		90.3	90.2	89.9	89	90
3	maxtop	-	322.3	315	320.5	319.5	457.8
4	S355 + las	S355W	192.1	190.3	192.8	190.3	192.3
5	S355 + primer	S355P	184.2	184.5	183.7	184.9	184.4
6	355 + Mg	MG	199.1	199.8	199.8	201	200.3
7	355 + Al	AL	201.2	202.4	203.1	203.2	201.6
8	355 paint and scratch	P&S	184.4	186.1	185.7	184.5	185.1
9	Al 5083	AL 5083	19.5	19.9	20.4	20.1	19.5
10	Al 6082	AL 6082	20.5	20.8	21	20.5	20.9
11	Al 1980	AL 1980	48.7	49.5	51.1	50	50
12	Al c22n	AL C22N	49.2	47.7	45.9	48.2	48.5
1	HPE	HPE	y	y	y	y	
2	HMPE1000	HMPE1000	y	y	y	y	
3	HMP 500	HMP 500	y	y	y	y	
4	PP	PP	y	y	y	y	
5	PA6	PA6	y	y	y	y	
6	PTFE	PTFE	y	y	y	y	
7	PU kaboflex U95	PU KABOFLEX U95	y	y	y	y	
8	PU kaboflex V80	PU V80	y	y	y	y	
9	PU kobaflow U95	PU KOBAFLOW U95	y	y	y	y	
10	rubber 38 shore A	38SA	y	y	y	y	y
11	rubber 55 shore A	55SA	y	y	y	y	y
12	rubber 70 shore A	70SA	y	y	y	y	y
13	PA	PA	y	y	y	y	y
14	PE	PE	y	y	y	y	y
15	TPE	TPE	y	y	y	y	y
16	TPV	TPV	y	y	y	y	y
17	nanowire	N.A.	y	y	y	y	
18	rifler	N.A.	y	y	y	y	
19	grease-wire	N.A.	y	y	y	y	
20	PU AWC 800	PU AWC 800	y	y	y	y	
21	PU AWC 850	PU AWC 850	y	y	y	y	
22	PEEK ACW 860	PEEK AWC 860	y	y	y	y	
23	Neoprene (CR) 60 shore	NEO 60S	y	y	y	y	
24	EPDM 60 shore A	EPDM 60SA	y	y	y	y	
25	NBR 65 shore A	NBR 65SA	y	y	y	y	
26	HNBR 90 shore A	HNBR 90 SHORE A	y	y	y	y	
	additional bracket						
13	"beitelplaat"		18.5	18.6	19.2	N.A.	18.4
27	D-glide FC	D GLIDE FC	y	y	y	y	
28	D-glide P	D GLIDE P	y	y	y	y	
14	steel 316 (A4-80)		29.3	29.6	29.2	29.4	29.4
15	"widia plaat"		147.1	146.7	143.2	144.8	135.1
16	"staal hard"		271.1	316.3	320.9	N.A.	275.5
17	special bend+nops		156.7	156.7	153.8	N.A.	153.3

Figure 5.1. Detail of the alu frames holding the sets of test materials on the benthic landers.

6. **Sampling and deployments** (NIOZ - M.S.S. Lavaleye & G.C.A. Duineveld)

Below is a brief summary of the activities during the cruise (Pelagia 64PE388) with particular emphasis on the activities in context of the DeepCorr-On-Site project

DEEPCORR-ON-SITE CRUISE ACTIVITIES

The research of the surroundings of the active Rainbow vent field (Fig. 6.1) started with a CTD survey (40 casts) of the water column from bottom to surface and spread over an area with a radius of 40 km. Most of these casts didn't show a sign of the plume of the black smokers, but importantly a few casts showed a very clear sign of higher turbidity which must be caused by the plume. These signals come from CTD casts north of the Rainbow active vent field. Khripounoff et al. (2001) already showed that the residual near bottom current is directed northwards and had a speed between 1.5 and 4.5 cm/s. According to the former paper the tidal currents at Rainbow are semi-diurnal, and had a mean speed of 9 cm/s and a maximum of 19 cm/s. Near bottom temperatures measured by us were just below 5 °C, and the small variations in time cannot be attributed to the influence of the vents.

To find suitable areas for taking sediment cores and to deploy our 4 landers several video transects with our tethered HD video frame were carried out near the active vent site (Fig. 6.2A). Video grabs from two of those transects are shown in Fig. 6.3 and 6.4. Transect 49 is directly north of the active vent field, while transect 65 is covering an area presumable influenced by the vent plume. On this last transect we found a soft sediment area of a few 100m length were some boxcore samples were taken and were two of the landers were eventually deployed.

Taking undisturbed samples with our large boxcorer (sample diameter 50cm) proofed to be quite difficult, even though we picked out suitable places with soft sediment on basis of our video surveys. Often the boxcore failed because of large stones or because the area was too steep. Eventually only seven samples (out of 17) were more or less suitable for subsampling. For the Deep Corr On Site project samples for microbiota were taken from 5 boxcores, namely on station 63, 68, 69, 70 and 72. The procedure was as follows. When the boxcorer was back on board, the top lid of the core was lifted and the overstanding water was partly drained. The heavy sample was then wheeled carefully away from the boxcore frame to make easy access to the sample possible. After draining the sample completely a sterilised syringe of which the bottom was cut off was pressed into a undisturbed area of the sediment. The syringe with the sediment was then removed from the core, and the sediment sample taken by the syringe transferred to a sterilised Falcon tube. The tube was closed with a lid and sealed with parafilm, and then stored in a fridge at about 4°C. The position of the boxcore sample are shown in Fig. 6.2. Pictures of the sediment surface of these 5 boxcore samples are shown in Fig. 6.5. A list of these samples with positions and short description is given in Table 5.1.

During the expedition four landers were deployed for a couple of days to test instruments and get some first near bottom data about temperature, currents, turbidity, fluorescence and redox. Furthermore sediment trap, plankton samples and video footage of a baited experiment were collected. At the end of the expedition all four landers were deployed for the period of 1 year. For the DeepCorr-On-Site project all four landers carried a frame with a multitude of test materials which are thus exposed to in-situ near bottom deep-sea circumstances including corrosion processes close to an active vent site and at an SMS deposit area.

The positions of the four lander positions is indicated ion Fig. 6.2. Two landers (ALBEX4 and BOBO-A) were positioned NE of the active vent field in the area estimated to be influenced by the plume of the black smokers of the Rainbow active vent field, while the other two landers (ALBEX1 and BOBO-D) were placed respectively SE and S of the active vent field in an area estimated to be hardly influenced by the plume. As a reference for normal oceanic seawater circumstances a fifth corrosion frame was attached to a mooring at about 900 m below the ocean surface in a position South of the Rainbow vent field (Fig. 6.2).

REFERENCES

Hannington M et al. (2011). *GSA data repository* 2011342: pp. 1-20.
Khripounoff A et al. (2001) *Journal of Marine Research* 59: 633–656.

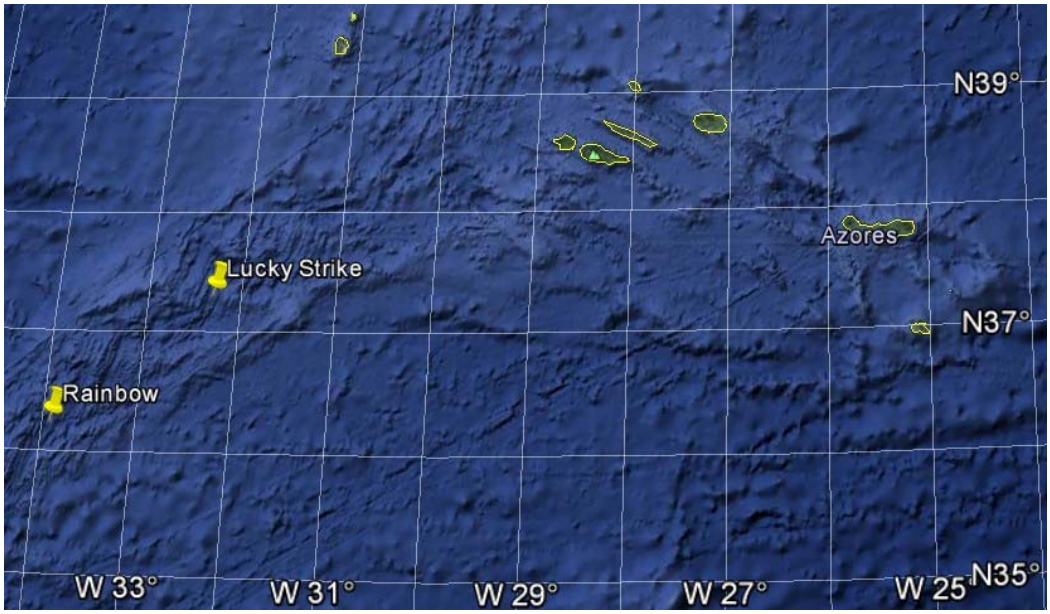

Figure 6.1. Overview of the Mid Atlantic Ridge immediately SW of the Azores. All islands of the Azores and the Lucky Strike and Rainbow sites are shown.

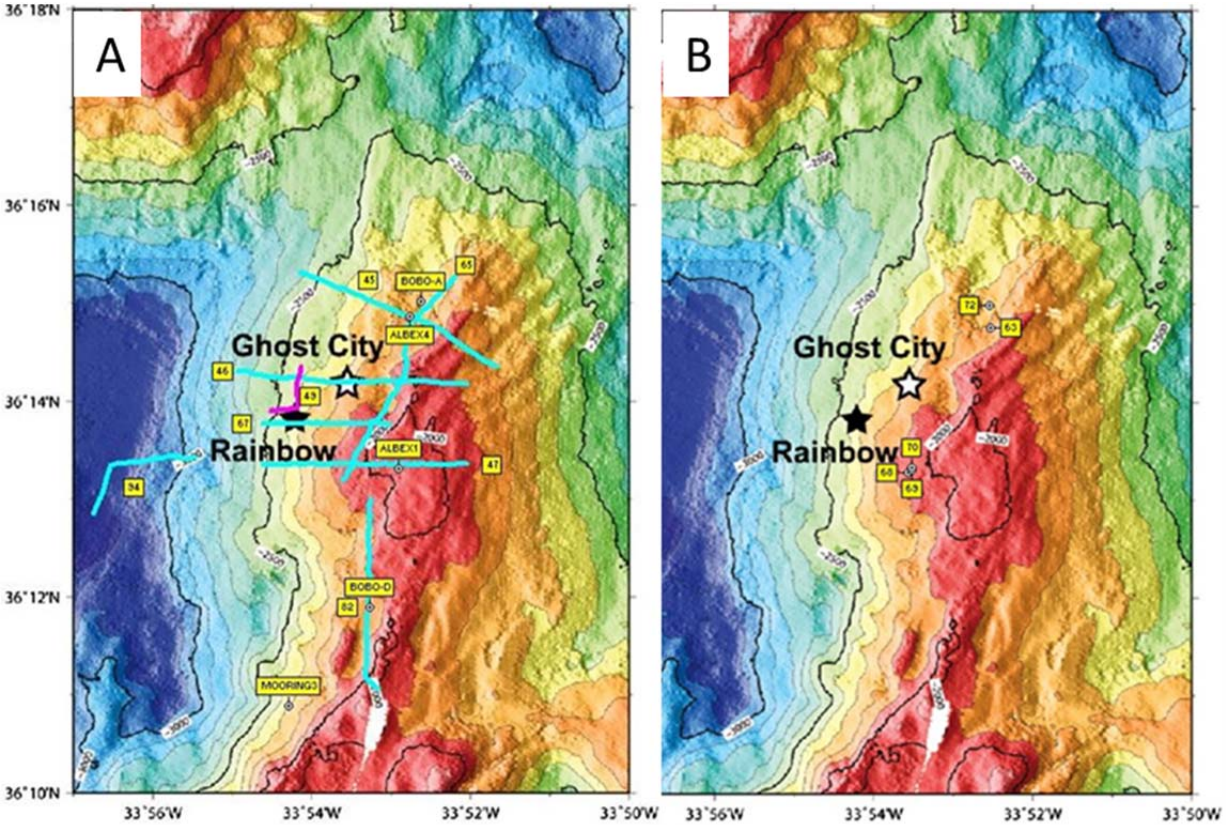

Figure 6.2. A. Map of the bathymetry of the Rainbow vent field with the videotracks (blue) and lander and mooring positions (yellow squares) indicated. Numbers are station numbers of the video survey tracks. ALBEX1 and ALBEX4 are the biological landers (Fig. 6.6B), BOBO-A and BOBO-D are the geological landers with long legs (Fig. 6.6A), while Mooring3 is the 1400m long mooring. B. Positions of the boxcore samples taken for the DeepCorr-On-Site project indicated by yellow squares.

Table 6.2. Position and description of boxcore samples from which subsample for microbiology was taken.

Date	station	result	description	area	deep-cor	Lat	Long	Depth
21-May	**63**	good	soft sediment, very full with only room for a few centimeters of overstanding water	N. of Rainbow	y	N 36° 14.77596'	W 33° 52.53042'	2175
23-May	**68**	heavily disturbed	lot of stones in sediment matrix	S. of Rainbow	y	N 36° 13.29462'	W 33° 53.57058'	2046
23-May	**69**	too full	soft sediment, closing lid touched the surface sediment	S. of Rainbow	y	N 36° 13.31538'	W 33° 53.53176'	2040
23-May	**70**	good	soft sediment	S. of Rainbow	y	N 36° 13.3446'	W 33° 53.52576'	2033
23-May	**72**	good	soft sediment	N. of Rainbow	y	N 36° 14.99304'	W 33° 52.55136'	2240

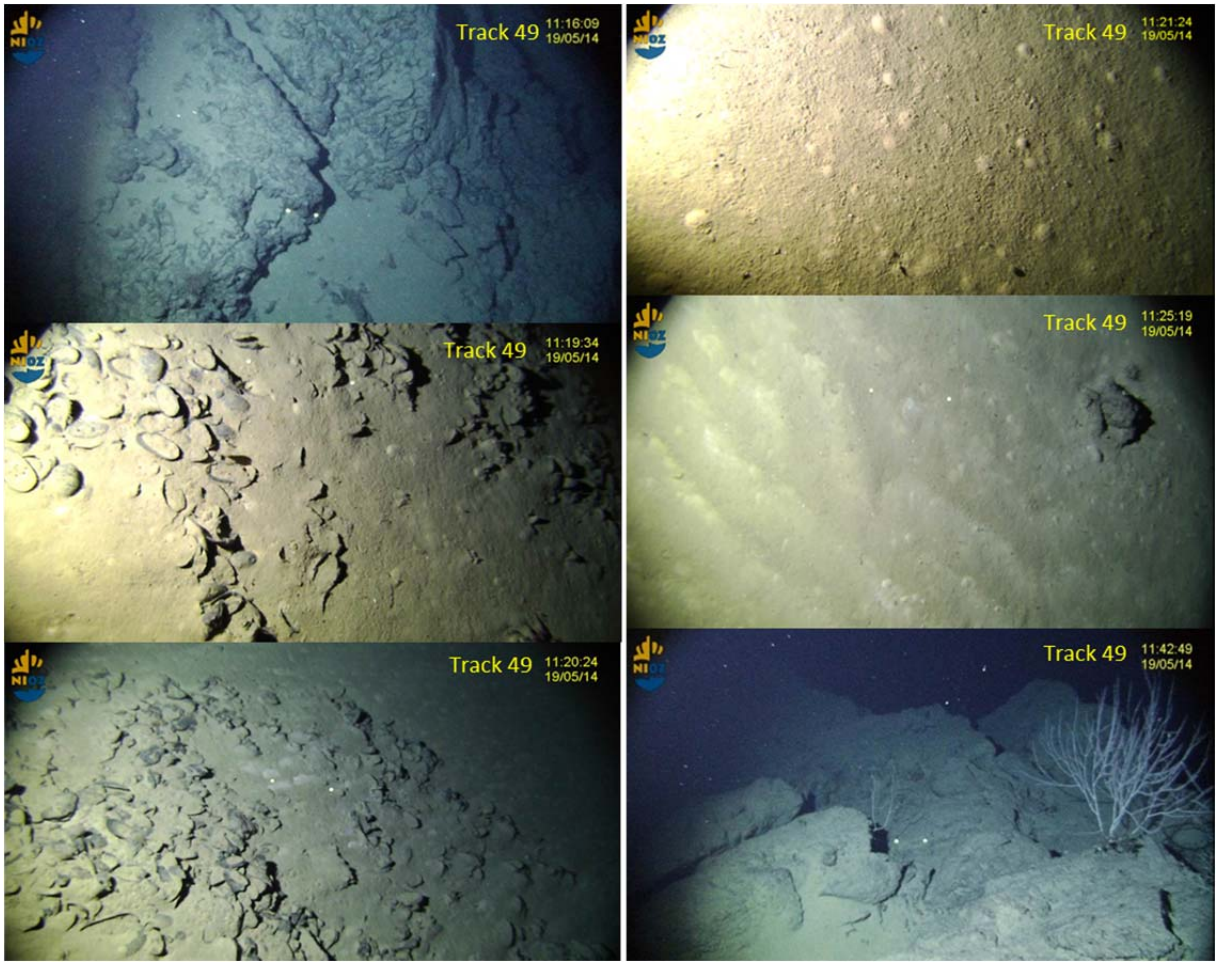

Figure 6.3. Video grabs from video track 49 (near the Rainbow vent field). Distance between laser dots is 30 cm.

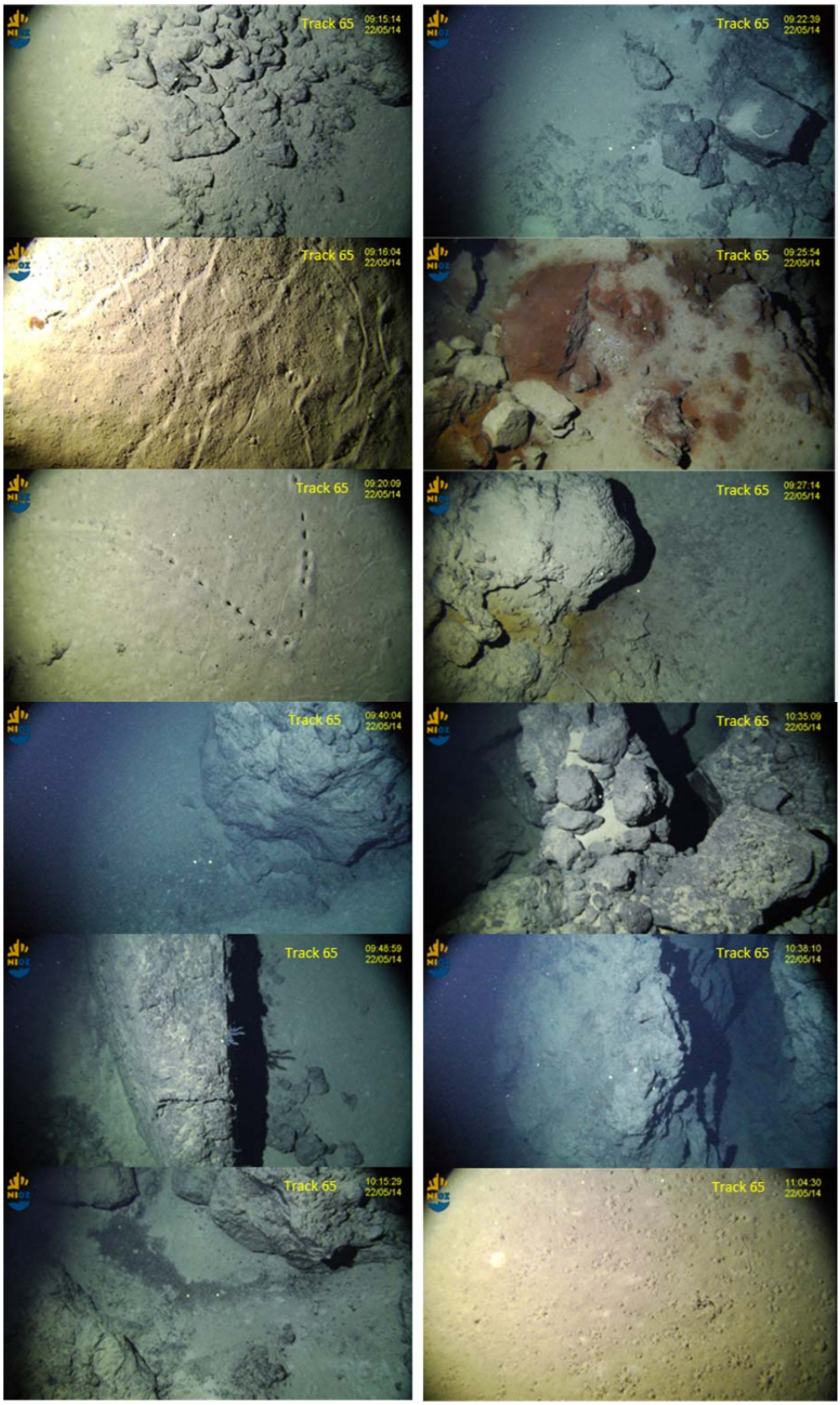

Figure 6.4. Video grabs from video track 65 near the ALBEX4 and BOBO-D positions (see Fig. 2). Distance between laser dots is 30 cm.

Figure 6.5. Surface pictures of the 5 boxcore samples after draining the overstanding water. Diameter of the core is 50 cm. Station numbers are indicated in red.

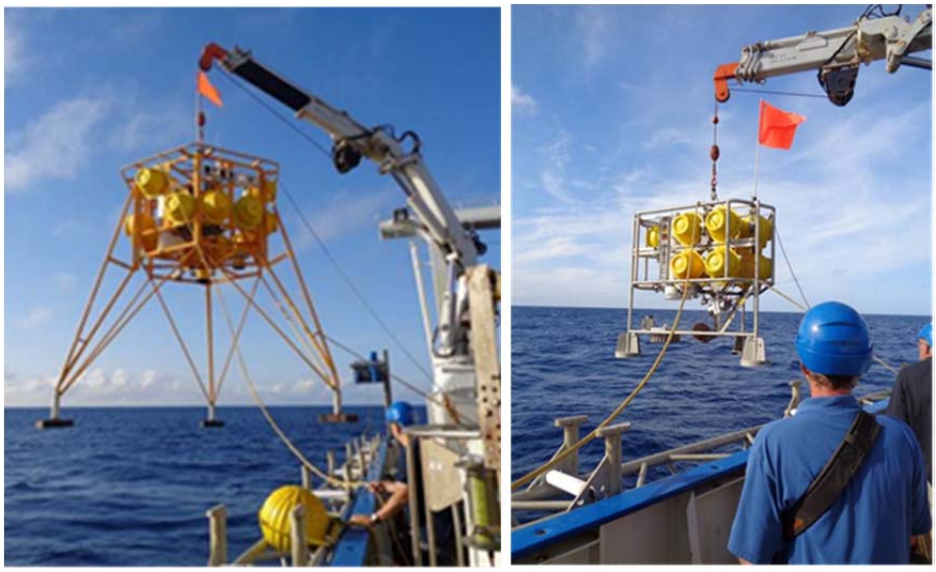

Figure 6.6. Deployments of landers with alu frames and test materials A. BOBO. B. ALBEX lander.

7. Evaluation of the chemical/physical and biological environment – (NIOZ by M.S.S. Lavaleye & G.C.A. Duineveld)

During the cruise to the Rainbow area we collected some data of the environment by direct observations or measurements. However, most data and samples still have to be analysed. Most of this will be done in the 4-year project TREASURE. Below we give a short overview of the data available so far.

PHYSICAL ENVIRONMENT

During an extensive CTD survey of the Rainbow area with 41 stations in an area with a diameter of 40 km the plume of the black smokers of the active vent field was mapped. The plume was easily traceable by our turbidity measurements, and the outcome was that the plume did indeed spread to the NE in the direction of Station 66 (Fig. 7.1), and after passing the seamount at its right, took a turn to the east, and was still traceable at 20 km distance from the vent field. The plume did also spread in the vertical. At 2km north of the vent field it had a vertical diameter of approximately 250 m. At 10 km to the east of the vent field was diluted about 10 times (compared to the 2 km station), and had a vertical diameter of about 500 m. Based on these data the two ALBEX landers were deployed at two different sites.

During the short deployments of the 2 ALBEX (biological) landers data on turbidity, temperature and current were collected during a period of 5 days. One of the landers was positioned at 1962 m depth east of Rainbow (station 57), so outside of the influence of the plume of the black smokers of the Rainbow active vent field. The other ALBEX-lander was deployed at 2210 m depth northeast of the Rainbow active vent field (station 66) in an area under the influence of the plume (Fig. 7.1).

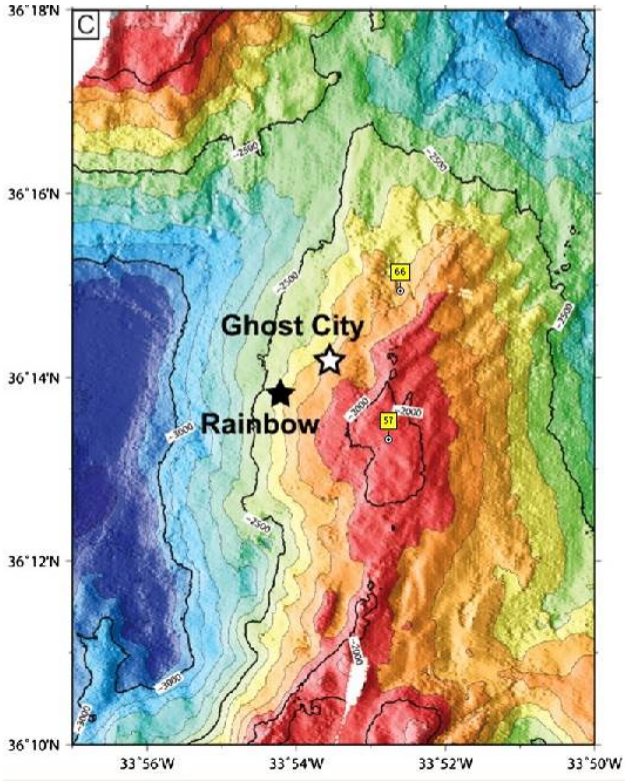

Figure 7.1. Map of the Rainbow area with the positions of the 2 short-term ALBEX lander deployments (yellow squares).

STATION 57 (EAST OF RAINBOW)

The temperature fluctuated between 3.83 and 4.13 ^{0}C (Fig. 7.2). The pattern is quite irregular, but there seem to be some correlation between temperature and the current speed. Current speed varied between 0-17 cm/s (Fig. 7.2). The current speed pattern point to a semidiurnal tidal cycle. This is confirmed by the pattern of the current direction over time (Fig. 7.2), which mainly changes from east to west. Turbidity shows a clear regular pattern too. It is strongly correlated with the current direction. When the current has a more or less easterly direction then the water also has a higher turbidity.

STATION 66 (NORTHEAST OF RAINBOW)

The temperature fluctuated between 3.66 and 3.90 ^{0}C (Fig. 7.3), a fraction colder than at the somewhat shallower sta. 57. The fluctuation are in contrast to sta. 57 very regular, though the relation with the tidal cycle is unclear. Current speed varied between 10.5-15 cm/s (Fig. 7.3), and in contrast to Sta. 57 never reach very low figures. The current speed pattern is quite irregular and a semidiurnal tidal cycle is not clear. The current direction is very stable over time (Fig. 7.3), and only fluctuates between 41 and 48 degrees (NE). Turbidity shows a more or less regular pattern, although less clear than in sta. 57. It is correlated with the temperature, meaning that a high turbidity occurs during periods with a relative high temperature.

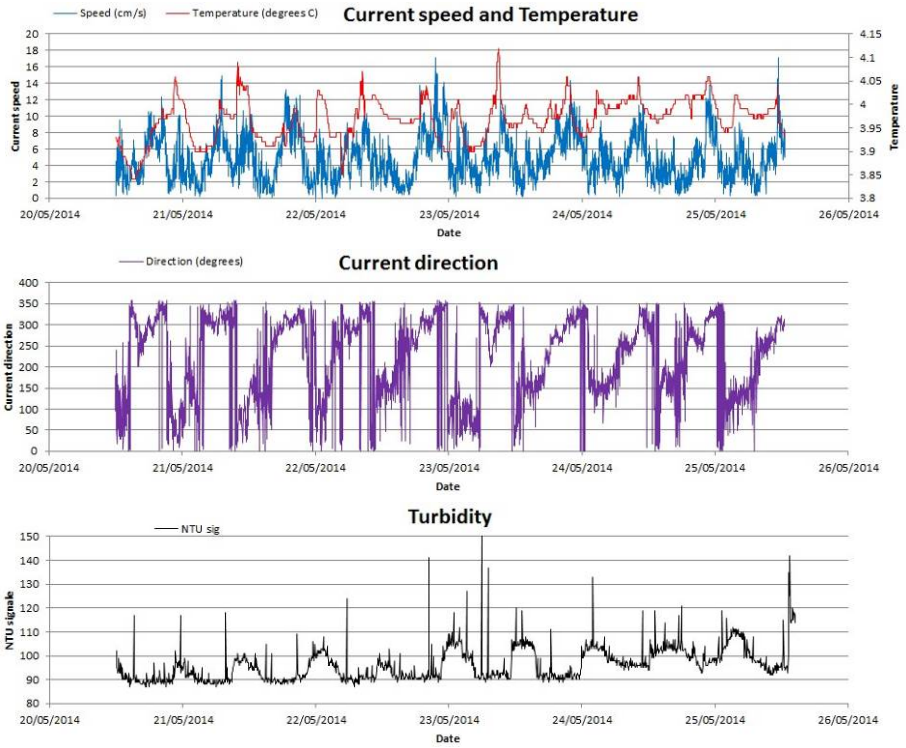

Figure 7.2. Data on near the bottom temperature, current speed, current direction and turbidity during 5 days at station 57 collected by an ALBEX lander.

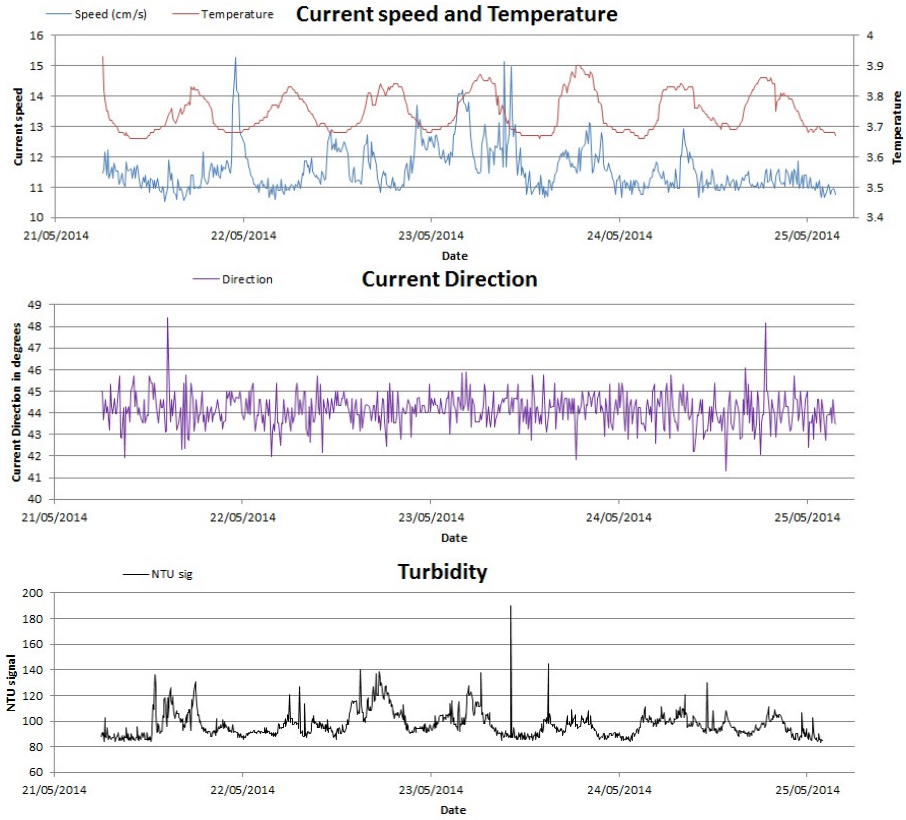

Figure 7.3. Data on near the bottom temperature, current speed, current direction and turbidity during 4 days at station 66 collected by an ALBEX lander.

8. **Sample analysis** (TNO-Endures by C.F. Leon Morales & N. Noel)

ABBREVIATIONS	
Amox	Ammonia-oxidizing bacteria
APB	Acid-producing bacteria
FeOx	Iron-oxidizing bacteria
IRB	Iron-reducing bacteria
MnOx	Manganese (II)-oxidizing bacteria
NiOx	Nitrite-oxidizing bacteria
NiRed	Nitrate-reducing bacteria
SF	Slime-forming bacteria
SOB	Sulfur-oxidizing bacteria
S Ox (MacS)	Acidophilic sulfur-oxidizing bacteria
S Ox (Ti)	Neutrophilic sulfur-oxidizing bacteria
SRB	Sulfate-reducing bacteria
TCC	Total cell counts
VS	Volatile solids

INTRODUCTION

A well informed prediction of possible corrosion processes happening at the exposure site is only possible with both an overview of both chemical and biological processes occurring. In ENDURES report RPT14069b an overview of existent studies at the Rainbow site or as close as possible locations is included. The present report deals with the microbiological analyses of sediments collected from the Rainbow vent field area by the RV Pelagia cruise (64PE388).

Table 8.1. Position and description of boxcore samples from which subsamples for microbiology were taken. Photo's of the samples are shown in Fig. 6.5. Source: NIOZ.

Date	station	result	description	area	deep-cor	Lat	Long	Depth
21-May	**63**	good	soft sediment	N. of Rainbow	y	N 36° 14.77596'	W 33° 52.53042'	2175
23-May	**68**	heavily disturbed	lot of stones in sediment matrix	S. of Rainbow	y	N 36° 13.29462'	W 33° 53.57058'	2046
23-May	**69**	too full	soft sediment	S. of Rainbow	y	N 36° 13.31538'	W 33° 53.53176'	2040
23-May	**70**	good	soft sediment	S. of Rainbow	y	N 36° 13.3446'	W 33° 53.52576'	2033
23-May	**72**	good	soft sediment	S. of Rainbow	y	N 36° 14.99304'	W 33° 52.55136'	2240

MATERIALS AND METHODS

Sample collection and treatment

During cruise 64PE388 5 successful boxcore samples were retrieved from the Rainbow site (see Table 8.1 for positions). Immediately upon arrival of a boxcore sample on deck, a subsample was taken with a sterilized syringe and this was transferred into a steril falcon tube which was stored at 4oC. A total of 5 samples in falcon tubes arrived at ENDURES (Fig. 8.1). Of each sample, 10 g were used from the middle of a sample as indicated in Figure 3. 1/3 of a sample was used for the enrichment cultures; 1/3 was used for microscopy and 1/3 was stored at -20°C for future possible nucleic acid analyses (Fig. 8.2).

Figure 8.1. Samples as they arrived at ENDURES.

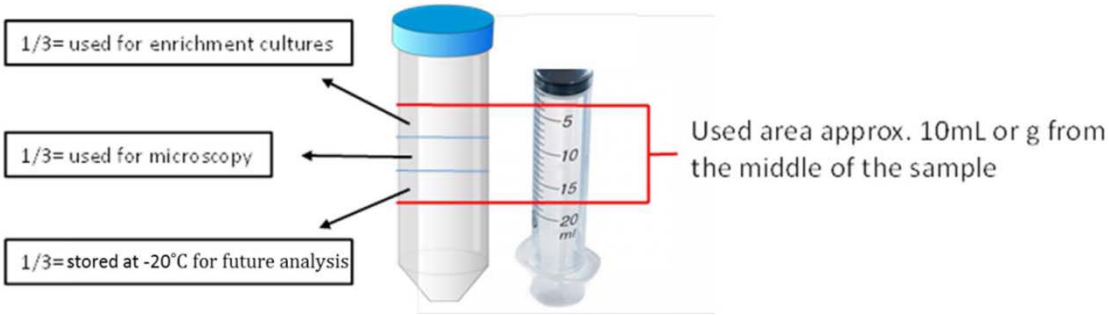

Figure 8.2. Sample treatment scheme for core samples used for microbiological analyses.

For microbial analyses samples were combined in 3 types: (Sample I) including the more coarse sediment including some stones; (Sample II) sediment samples from the South part of the site; and (Sample III) sediment samples from the North part of the site (Fig. 8.3).

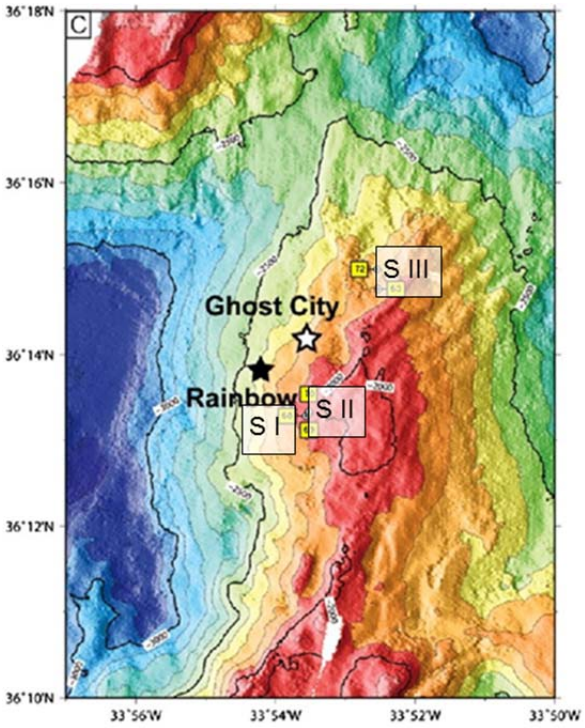

Figure 8.3. Overview of samples origin at Rainbow vent site. Modified from NIOZ.

Volatile solids determination

To give an approximation of the amount of organic matter (volatile solids) present in the solid fraction of the sample, a dry weight determination followed by loss on ignition was performed on approximately 1 g of sample (DIN EN 12880 and DIN EN 12879). For this determination a porcelain evaporating dish was initially rendered free of any organic traces at 550°C for 30 min and left to cool down inside a vacuum desiccator. The dish was then weighted with 1 mg precision (w1). The sample was then put on the evaporating dish, weighted (w2) and left to dry at 105◦C (± 2°C) until apparently dry. After cooling down in the desiccator, the sample together with the evaporating dish were weighted (w3). The dry mass (w3 − w1) was only obtained when w3 remained constant. After obtaining the dry mass, w3, the porcelain dish containing the sample was burned at 550◦C for 60 min. After cooling down, the weight of the dish, w4, was used for the determination of material lost on ignition (w4 − w1). Similarly as for the dry weight determination, the ash content was only considered when w4 remained constant (no more than 2 mg change) after ignition.

Total Cell Counts (TCC)

The total amount of cells in the sample was obtained by the polycarbonate filter method. In short, known volumes of sample were filtered through 0.2 µm pore size, sterile polycarbonate filters with the help of a vacuum pump. The microorganisms accumulated on the top of the filters were made visible by using DNA fluorescent dyes. In this way, after an appropriate volume of sample is filtered through polycarbonate filters, counts of total microorganisms can be made using a fluorescence microscope.

Most Probable Number (MPN)

Presence and activity of MIC related microorganisms can be determined using the Most Probable Number (MPN) method. Samples were directly inoculated and diluted in appropriate growth media, specific for the following types of microorganisms: slime-forming microorganisms (SF) and sulphate-reducing bacteria (SRB). These cultures were incubated aerobically (SF) or anaerobically (SRB) at relevant temperatures for up to 6 weeks. Microbial growth in different dilutions gives a rough estimate of the number and activity of the microorganisms. Growth and especially the speed of growth of microorganisms in selective media are used for judging the likelihood of MIC.

Microscopy (fluorescence)

Microscopic examination of the sediment samples was done by using fluorescence microscopy. For fluorescence microscopy samples were stained with the DNA specific labels SYTO® 9 and propidium iodide. Stained microbial cells are made visible by exciting the DNA/stain with ~490 nm blue light and observing the emitted green or red fluorescence under the microscope at a total magnification of 400X. SYTO® 9, which fluoresces green, penetrates most cellular membranes. In contrast, propidium iodide which fluoresces red, penetrates only compromised (presumably dead) cells. In this way a qualitative determination of the amount of active and inactive microorganisms in a sample can be obtained.

Enrichment cultures

Each sample was dissolved in 40mL, 2.5% NaCl and mixed for 20 min. Inoculation and incubation was done as listed in table1. An inoculum of 0.5mL was used for every medium (4.5mL) to reach a total volume of 5mL. Samples at atmospheric pressure were inoculated in triplicate and incubated at 4°C and 10°C. Samples at in-situ pressure were inoculated once and incubated at 10°C.

Incubation under in-situ pressure: Samples were incubated in a pressure chamber, with a pressure of 200 bar, which resembles pressure conditions at around 2000 m below sea surface. Aerobic samples (2% vol/vol inoculum) were incubated in sterile plastic bags to guarantee gas exchange; anaerobic samples (2% vol/vol inoculum) were incubated in closed serum flasks to keep anaerobic conditions.

Table 8 2. Growth media and conditions used for enrichment cultures

Type of organism	Aerobic/ anaerobic	Pressure atm.	Pressure in-situ*	Temp.	Growth medium	Reference
Neutrophilic sulfur- oxidizers	aerobic	x	x	4, 10°C	Ti	[1] Matin & Rittenberg (1971)
Acidophilic sulfur- oxidizers	aerobic	x		4, 10°C	MacS	Mackintosh (1978)
Ammonia- oxidizers	aerobic	x		4, 10°C	AmOx	Krümmel & Harms (1982)
Nitrite- oxidizers	aerobic	x		4, 10°C	NiOx	Krümmel & Harms (1982)
Manganese (II)- oxidizers	aerobic	x	x	4, 10°C	MnOx	[1] Bromfield (1956); Tyler & Marshall (1967)
Acidophilic iron- oxidizers	aerobic	x	x	4, 10°C	MacFe	Mackintosh (1978)
Slime formers	aerobic	x	x	4, 10°C	SF	DSMZ medium 1
Fungi	aerobic	x		4, 10°C	Sabouraud	Sabouraud (1952)
Sulfate- reducers	anaerobic	x	x	4, 10°C	PostgateE	[1] Postgate (1984)
Iron- reducers	anaerobic	x		4, 10°C	IRB	
Acid- producing bacteria	anaerobic	x		4, 10°C	APB	BD standard medium
Nitrate-reducers	anaerobic	x		4, 10°C	NiRed	Schippers (1994)

*in-situ pressure samples were only incubated at 10°C; [1]= according to but modified

RESULTS

Volatile solids determination

An amount of 1 gram per sample was treated as described above. The results are presented in Table 8.3. Sample III showed the highest amount of volatile solids, which give an indication of higher total organic content in this sample.

Table 8.3. Results of volatile solids determination.

	Sample I	Sample II	Sample III
% moisture	48.3	44.4	49.2
% VS in dry sample	3.1	3.3	3.8

Direct microscopic examination

Samples were observed under the fluorescence microscope in order to assess biofilm formation on the sediment particles. In order to make the microbial cells visible DNA specific stains are used. By using two types of stains, i.e. one with affinity for active cells and the other for non-intact (presumably dead) cells, it is possible to qualitatively determine amount of active cells in a sample (Fig. 8.4).

Sample I:

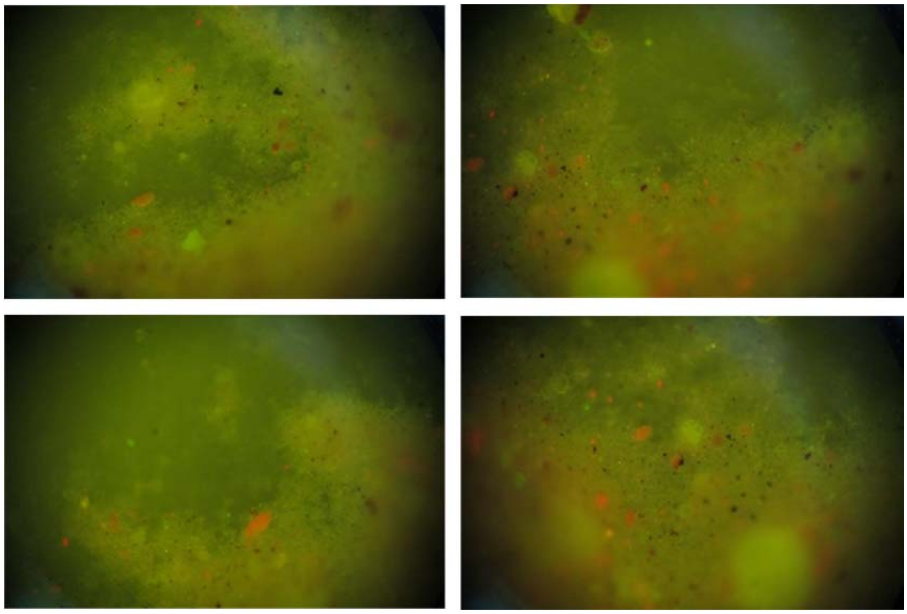

Sample II:

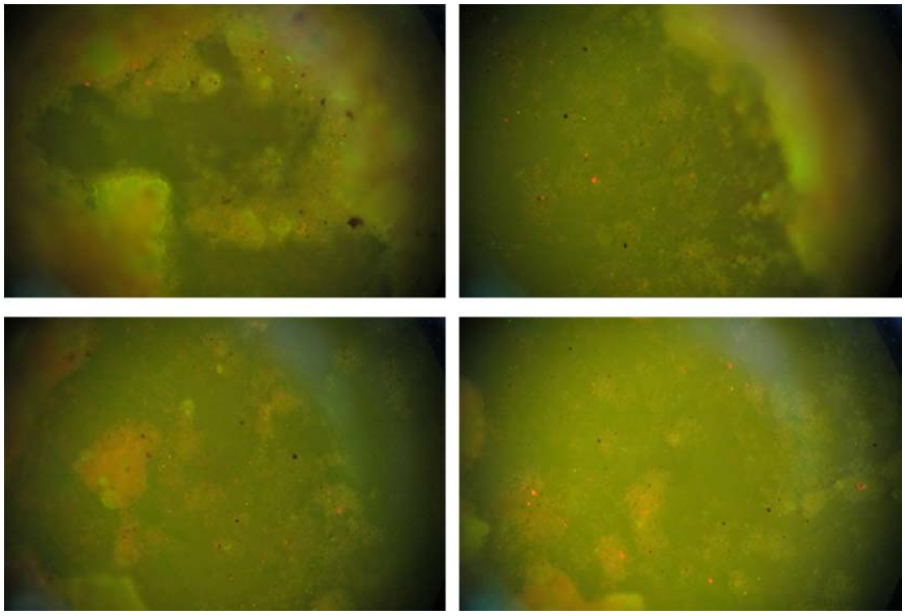

Sample III:

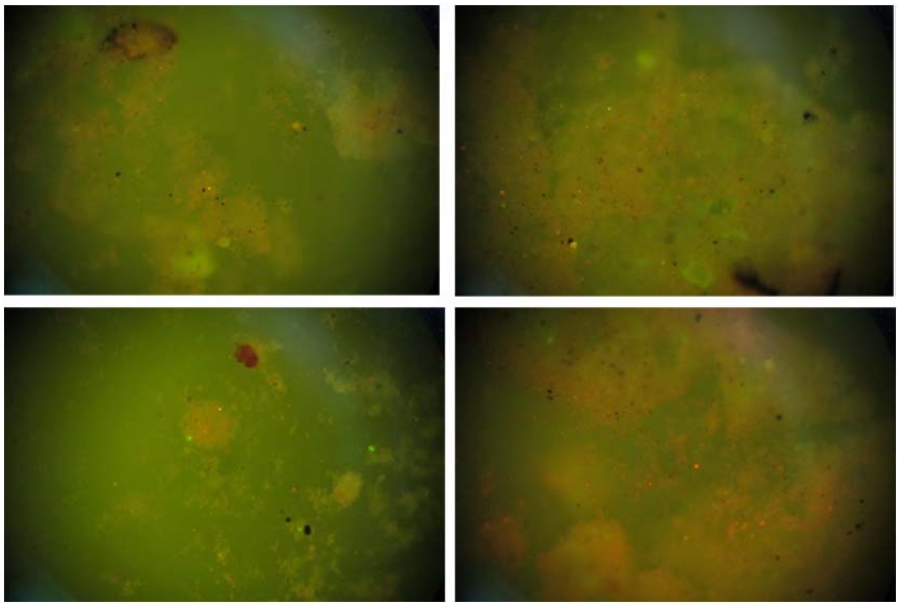

Figure 8.4. Fluorescence micrographs of samples/biofilms. Fuzzy areas are created by out of focus light resulting from the depth of the biofilm. Green areas indicate largely intact organisms while red areas indicate injured or dead cells.

Microbial groups found
Samples were incubated in specific growth media, as described in Section 3. Growth was observed as presented in Table 8.4.

Table 8.4. Results of enrichments obtained at atmospheric pressure and close to in-situ pressure. "+" indicates growth, "-" indicates no growth observed.

Microbial group	Sample I			Sample II			Sample III		
	4 ˚C	10 ˚C	In situ	4 ˚C	10 ˚C	In situ	4 ˚C	10 ˚C	In situ
Fe Ox	+	+	-	+	+	-	-	-	-
S Ox (MacS)	-	-	-	-	-	-	-	-	-
S Ox (Ti)	-	-		-	-		-	-	
fungi	-	-		-	-		-	-	
SRB**	+	+	+*	+	+	+*	+	+	+*
IRB	+	+		+	+		-	-	
APB	+	+		+	+		+	+	
NiOx	-	-		-	-		-	-	
Amox	-	-		-	-		-	-	
NiRed	+	+		+	+		-	-	
SF**	+	+	+	+	+	+	+	+	+
MnOx	+	+	+	+	+	+	+	+	+

*= no blackening observed. **= were also positive for the MPN method.

Total cell counts
Total cell numbers were similar for all tested samples regardless of their origin (Fig. 8.5). However, sample III (originating from the northern part of the site) had slightly less injured or damaged cells. This also coincided with a higher amount of volatile solids present in this sample.

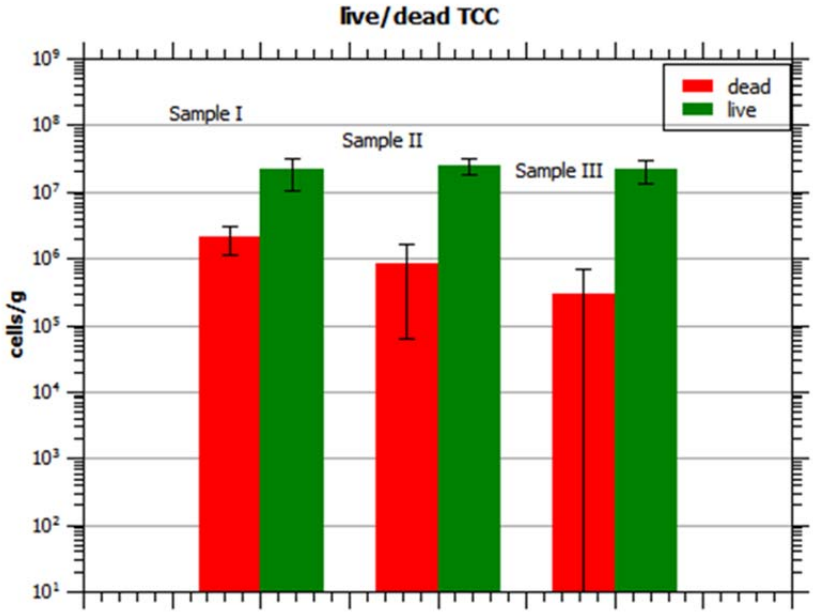

Figure 8.5. Total cell counts (TCC) from Rainbow site sediment samples. Microbial cells were stained with two types of dyes that can discriminate between intact cells (live) and injured or damaged cells (dead). Fluorescence staining detects all microorganisms and does not discriminate corrosion-related microorganisms.

Concluding remarks

- Total amount of microorganisms were comparable among samples and typical of marine sediments.
- Several of the tested microbial metabolisms with relevance to MIC were found on the samples.
- Growth was equally observed at both 4°C and 10°C, which could be expected considering the temperature variability of the site.
- SRB were found but growth took long time to appear. In some incubations no blackening (due to iron sulphide precipitation) was observed. Which implies that other types of anaerobic fermenters were present.
- SOB both neutrophilic and acidophilic were absent. Site is known for relatively low levels of sulphide. Whether this has relationship with the absence of these organisms, needs to be further investigated.
- Acid producing bacteria were present which could have impact in corrosion.
- Both iron oxidizers and reducers were active in the samples. Especially the presence of acidophilic iron oxidizers is interesting since the high levels of ferrous iron (II) typical of the Rainbow site. Many acidophilic iron oxidizers catalyse the oxidation of soluble Fe (II) to non-soluble Fe (III).

Annex 8.1. RECOMMENDED CORE SAMPLING PROTOCOL

Specific details about coring are not included here but only subsampling of microbiological valid samples from cores. Key is to minimize air exposure and introduction of foreign microorganisms. Two options are given accounting for difficulties that might be found on site. Please note that all materials necessary to perform the sub-sampling are provided sterile (microbial-free) and ready to use.

Option 1 - subsampling

Coring process

Note 1: When using plastic liners, if possible core barrels should be steam-cleaned before use and liners should be used every time.

Note 2: Subsamples should be taken as soon as possible after core retrieval. If possible directly after the plastic liner is removed from the metal cylinder and before closing the ends of the plastic liner. Subsampling in the earliest stages of core processing will decrease dramatically chances of contamination.

Note 3: If not immediately subsampled, cores for microbiology should only be opened in a controlled atmosphere: anaerobic chamber, clean laminar flow bench.

- Person performing the sub-coring should first wear provided rubber gloves and then rub hands with a bit of ethanol before doing the procedure.
- Provided sterile plastic syringes, which have been cut (Fig. 8.6A) to form a mini coring system, should be used to obtain sub-cores from the middle of the original cores, as exemplified in Fig. 8.6B.
- Subsamples from intact cores taken in this way should be stored in the provided sterile plastic tubes (Fig. 7.6C), tightly sealed and then stored at 4°C in the dark.

- Ideally samples should be transported between 0-4°C and not take longer than 2 weeks to reach the ENDURES laboratory in Den Helder.

Figure 8.6. Subsampling of typical core for microbiology. All provided sampling material is sterile and ready to use. Sub-cores are taken ideally from the middle of the original core and transferred immediately to sterile plastic tubes (50 mL Falcon tubes) (C). The samples are then stored and transported as described for further analyses.

Option 1 - subsampling

If subsampling is difficult or impossible the only option is to get intact cores. Cores should be sealed air-tight directly after sampling and should be sent refrigerated (0-4°C) as soon as possible. They should reach the lab not later than 2 weeks.

Important note: some microbial growth analyses require microorganisms to be active. For this reason, samples should not be frozen but rather kept refrigerated at 4°C.

Annex 8.2. SUGGESTED SPECIMEN TREATMENT AFTER 1 YEAR EXPOSURE

Representative specimens including various metals have been exposed to the environment at Rainbow vent site. No much information was found in the literature on how to do this but key is to avoid prolonged oxygen exposure as well as humidity that could accelerate corrosion after sample retrieval. The following precautions are reasonable:

- Specimen can be flushed with clean (ideally sterile and oxygen-depleted) fresh water, immediately dried under nitrogen and then put in sterile bags also under nitrogen and seal with heat sealer. Water can be depleted from oxygen by boiling and then cooling down under nitrogen flushing.
- If no heat sealer is available also Whirl Paks (Nasco) could be used and flushed with nitrogen (Royer and Unz 2006).
- Another option could be vacuum sealing.
- Provided the samples are completely dried and without oxygen exposure these can be transported at room temperature to the TNO/ENDURES lab in Den Helder.
- Due to the difficulties on preserving microbiology valid samples from metal specimens, we will attempt to obtain microbial enrichment cultures only from the cores.
- Only if we can have access to two samples of the same sample material then we could attempt to enrich from metal coupons as well but transport should be refrigerated (this can be discussed at a later stage).

9. **Conclusion**

- The switch from Lucky Strike to the Rainbow vent field did not seriously affect the goals of this project

- The Rainbow vent field is a rugged terrain, but some small even areas with a soft sediment bottom were found to successfully deploy the 4 landers with corrosion panels.

- The plume of the black smokers of the Rainbow vent field was easily picked up by the turbidity sensors of the CTD, and therefore could be mapped in the horizontal as well as vertical plane.

- The plume was directed in an NE direction and was still traceable at 20 km distance from the source

- In terms of general corrosion, no critical influence of pressure would be expected and in a similar way as for shallower waters, corrosion would be controlled mainly by oxygen content, salinity and temperature. However under influence of hydrothermal activity, corrosion risk would mean choice of alloys which are not susceptible to hydrogen-induced cracking (HIC), sulphide stress corrosion (SSC) and Microbiologically Influenced corrosion (MIC).

- Other studies (not necessarily close to hydrothermal vent systems) minimize the influence of biological growth on corrosion of tested specimens in the deep sea environment. In the case of the Rainbow system biological growth is expected to play an important role, but this can only be asserted once the exposed specimens are retrieved and analyzed. Because other means of corrosion protection such as CP might be difficult, extra corrosion allowance might be required.

- Main impact for design is the possibility of MIC (combined with general corrosion risk due to low pH and other harsh chemical conditions in vent area, including the presence of various reduced sulphur compounds). Therefore choice of materials should not ignore those that are especially susceptible to microbiologically induced pitting.

Financiële Rapportage
Zie Excel bijlage

Bijzonderheden: none